APPENDIX 1:

USER GUIDE FOR CHARACTERIZING

PARTICULATE MATTER

University of Utah

User Guide for Characterizing Particulate Matter

Evaluation of Several Real-Time Methods

University of Utah
K.E. Kelly, A.F. Sarofim, J.S. Lighty, D.A. Wagner

Desert Research Institute
W.P. Arnott, C.F. Rogers, B. Zielinska

Univeristy of California San Diego
K.A. Prather

Report Documentation Page

Form Approved
OMB No. 0704-0188

1. REPORT DATE	2. REPORT TYPE	3. DATES COVERED
01 OCT 2003	**Final**	**-**

4. TITLE AND SUBTITLE
Characterization of Particulate Emissons: Size Fractionation and Chemical Speciation: User Guide Appendix 1

5a. CONTRACT NUMBER

5b. GRANT NUMBER

5c. PROGRAM ELEMENT NUMBER

6. AUTHOR(S)
Sarofim, Adel F. Lighty, Joann S.

5d. PROJECT NUMBER
CP 1106

5e. TASK NUMBER

5f. WORK UNIT NUMBER

7. PERFORMING ORGANIZATION NAME(S) AND ADDRESS(ES)
University of Utah College of Engineering 1495 East 100 South Salt Lake City, UT 84112

8. PERFORMING ORGANIZATION REPORT NUMBER

9. SPONSORING/MONITORING AGENCY NAME(S) AND ADDRESS(ES)
Strategic Environmental Research & Development Program 901 N Stuart Street, Suite 303 Arlington, VA 22203

10. SPONSOR/MONITOR'S ACRONYM(S)
SERDP

11. SPONSOR/MONITOR'S REPORT NUMBER(S)

12. DISTRIBUTION/AVAILABILITY STATEMENT
Approved for public release, distribution unlimited

13. SUPPLEMENTARY NOTES
The original document contains color images.

14. ABSTRACT
This study developed and validated innovative techniques for characterizing the amount and composition of PM10, PM2.5, and smaller particles for four major classes of DoD emission sources: aircraft ground support vehicles, rocket motors, aircraft, and sandblasting operations. The techniques include the coupling of dilution samplers with advanced measurement techniques for composition and size that provide detailed analyses sufficient to complete a material balance. The size-classified analyses include measurement made with the cascade impactor and aerosol time-of-flight mass spectrometer (ATOFMS). A photoelectric aerosol sensor (PAS) was being evaluated for use in rapidly evaluating field emissions of particle-bound polycyclic aromatic hydrocarbons (PAH). In addition, a photoacoustic spectrometer was investigated for use in measuring soot particle concentrations. The objective was to calibrate and enhance these instruments for DOD use. To this end, the devices are being demonstrated at DoD facilities, and the methodologies developed will be transferred to personnel responsible for monitoring emissions at DoD facilities.

15. SUBJECT TERMS

16. SECURITY CLASSIFICATION OF:			17. LIMITATION OF ABSTRACT	18. NUMBER OF PAGES	19a. NAME OF RESPONSIBLE PERSON
a. REPORT	b. ABSTRACT	c. THIS PAGE			
unclassified	**unclassified**	**unclassified**	**UU**	**109**	

This project was sponsored by the Strategic Environmental Research and Development Partnership, CP-1106 characterization of particulate emissions: size fractionation and chemical composition.

Table of Contents

Table of Contents (continued)

Introduction

This User's Guide is intended to assist environmental or military personnel who work with air quality measurements, regulations, and planning for the Department of Defense. Specifically, it focuses on an evaluation of three newly developed instruments for characterizing particulate matter (PM), general PM sampling recommendations, and background on PM.

What is particulate matter?

PM is material suspended in the air, and it can include soil, road dust, soot, smoke, and liquid droplets. PM can come directly from sources like vehicles, ships, aircraft, unpaved roads, and wood burning. Larger particles, those with a diameter larger than 2.5 μm ($PM_{2.5}$), typically come from unpaved roads and wind-blown dust, but finer particles, those smaller than $PM_{2.5}$, typically come from combustion sources: vehicles, ships, etc. PM is also formed in the air when gases from burning fuels react with sunlight and water vapor (Figure 1-1).

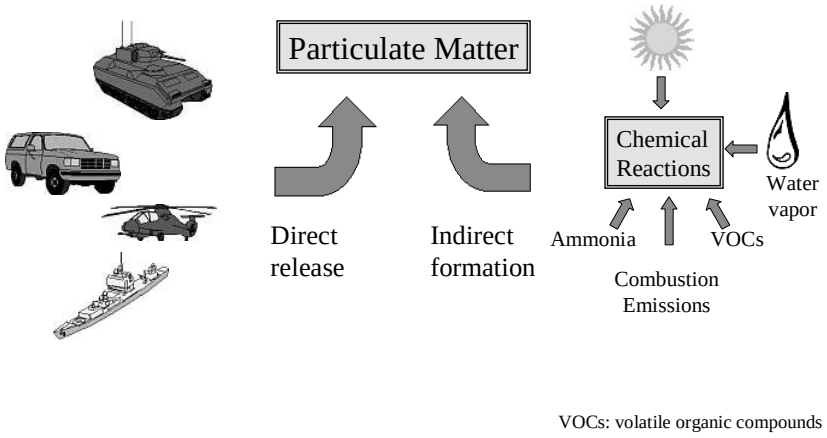

Figure 1-1. Example of the direct release and indirect formation of particulate matter.

PM found in the atmosphere is made up of many compounds including soil, nitrate, sulfate, soot and organic carbon (Figure 1-2). Organic carbon includes products of incomplete combustion, such as polycyclic aromatic hydrocarbons (PAHs) and unburned fuel. The composition of PM can vary dramatically depending on the source or process condition. For example, PM from a gasoline vehicle, diesel vehicle, woodstove, or a coal-fired boiler would have dramatically different composition.

Why is particulate matter important?

Particulate matter can cause serious health effects and impair visibility. Studies over the last ten years have linked PM concentration to increased death rates, an increased incidence of asthma, and adverse cardiac effects (EPA 2000, 2002; Dockery et al. 1993; Morawska and Zhang 2002; Peters et al. 2001). More recent evidence indicates that size, surface area, and composition of PM are important factors in determining the heath effects associated with PM. For example, fine particles are thought to deposit more deeply in the lungs than larger particles (Lighty et al. 2001, Maynard and Mayndard 2002). In addition PM, especially PM from combustion sources, contains polycyclic aromatic hydrocarbons (PAHs), which are reasonably anticipated to be carcinogens (NTP 2003), and elemental carbon, which is linked to adverse cardiac effects (Tolbert et al. 2001).

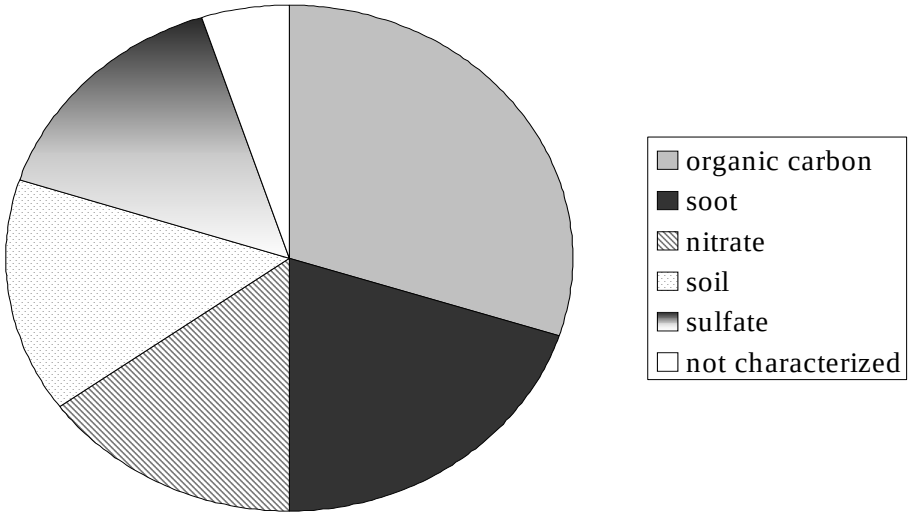

Figure 1-2. Composition of an example atmospheric particle.

PM causes adverse health effects

The EPA directly regulates atmospheric levels of PM_{10}, and it indirectly regulates PM through its visibility programs. New regulations to control $PM_{2.5}$ concentrations have recently been developed. In addition to regulations on the atmospheric PM levels, the EPA, the states, and other agencies also regulate PM emissions from a variety of sources, such as vehicles, power plants, aircraft, and various industries. Finally, the Occupational Safety and Health Administration regulates PM levels in workplaces.

Size and composition of PM are important factors in determining their heath effects

Why characterize PM?

Information about the size and composition of PM in the atmosphere can provide clues about its source. For example, larger particles that contain distinctive compounds, such as iron, silica, potassium, sodium, magnesium and chloride, are likely from wind-blown soil and ocean spray, but smaller particles that contain elemental and organic carbon are likely from a combustion sources. As another sample, PM from a Minuteman rocket motor contains large quantities of aluminum compared to soil particles (Sarofim and Lighty 2003).

PM composition can provide information about its source and its health effects

The size and composition of PM can also provide clues about process performance. For example, an engine operating at idle tends to emit smaller particles than the same engine under load. Engine operating condition also effects the portion of the particle made of organic and elemental carbon. Characterizing PM can also help understand its potential health effects (EPA 2002, HEI 2002). Research in this area is still ongoing (NRC 1988-2001), and the Health Effects Institute is a good resource for health effects information (See the resource list at the end of this section).

How can newly developed instruments help characterize PM?

Traditionally, determining the composition of PM was a time-consuming process. It required collecting and analyzing filters or sets of impactor substrates for composition. Although filter samples can provide detailed information about PM composition and some information about PM size, their analysis can be expensive and time consuming. The analysis methods also require a minimum amount of material, so collecting samples from the atmosphere can take many hours or even days. It is also challenging to collect sufficient PM from clean sources, such as a new gasoline vehicle. In addition, filter samples cannot provide information about process transients, when high PM emissions typically occur.

This guide reviews three newly developed instruments for use in determining PM composition.

- The photoacoustic analyzer measures black carbon, also called elemental carbon, or soot (Section 2).
- The photoelectric aerosol sensor measures particle-bound polycyclic aromatic hydrocarbons (Section 3).
- The aerosol time-of-flight mass spectrometer measures the size and composition of individual particles (Section 4).

These instruments offer several potential benefits over traditional measurements including near real-time results, cost savings, and information about transient conditions.

How do you collect PM samples?

Designing or selecting a system for collecting PM samples can be challenging, and it is important to consider the PM source, the type of measurements you need, and the potential errors associated with the system. Section 5 of this guide discusses several common systems and offers some general guidelines.

Resources

General information about airborne particles:

EPA's PM information page http://www.epa.gov/oar/oaqps/regusmog/infpart.html

Hinds W.C. *Aerosol Technology*, 2nd edition, John Wiley & Sons: New York, **1999**.

Kouimtzis T. (ed.) *Airborne Particulate Matter***,** Springer Verlag: Heidelberg **1995**.

Maynard R.L., C.V. Howard, *Particulate Matter: Properties and Effects Upon Health*, Oxford: Bios Scientific, **1999**.

Wilson R., D. Spengler (eds). *Particles in Our Air: Concentrations and Health Effects*, Harvard University Press: Cambridge MA, **1996**.

Health effects of particles: Health Effects Institute http://www.healtheffects.org

Information about the User's Guide: Kerry Kelly kelly@eng.utah.edu

References

EPA, *PM-How Particulate Matter Affects the Way We Live & Breathe*, Office of Air Quality Planning & Standards, Washington DC, **2000**.

EPA, *Health Assessment Document for Diesel Exhaust*, EPA 600/8-90/057F. National Center for Environmental Assessment, Office of Research and Development, Washington DC, **2002**.

Dockery, D.W., A.C. Pope, X. Xiping, J.D. Spengler, J.H. Ware, M.E. Fay, B.G. Ferris, F.E. Speizer, An Association between Air Pollution and Mortality in Six U.S. Cities; *New Engl. J. Med.* **1993**, 329 (24) 1753-1759.

HEI (Health Effects Institute) Understanding the Health Effects of Components of the Particulate Matter Mix: Progress and Next Steps, *HEI Perspectives*, April **2002**.

Lighty, J.S., J.M. Veranth, A.F. Sarofim, Combustion Aerosols: Factors Governing their Size and Composition and Implications to Human Health. Critical Review; *J. Air & Waste Man. Assoc.* 50 **2000**, 50, 1565-1618.

Maynard A.D., R.L. Maynard, A Derived Association between Ambient Aerosol Surface Area and Excess Mortality using Historic Time Series Data, *Atmos. Environ*. 36 **2002**, 5561-5567.

Morawska L., J. Zhang Combustion Sources of Particles 1. Health Relevance and Source Signatures, *Chemosphere* 49 (2002) 1045-1058.

National Research Council (NRC), *Research Priorities for Airborne Particulate Matter*, volumes I – III, **1998, 1999, 2001** Washington D.C.: National Academy Press, http://www.nas.edu/nrc/

National Toxicology Program, *10th Report on Carcinogens*, U.S. Department of Health and Human Services, National Toxicology program, **2003**, http://ehis.niehs.nih.gov/roc

Peters A.; D. Dockery, J.E. Muller, M.A. Mittleman M.A. Increased Particulate Air Pollution and the Triggering of Myocardial Infarction; *Circulation*, **2001**, 2810-2815.

Sarofim A.F., J.S. Lighty; Characterization of Particulate Emissions: Size Fractionation and Chemical Speciation, Final Report, Strategic Environmental Research and Development Program, **2003**.

Tolbert P.E., M. Klein, K.B. Metzger, J. Peel, W.D. Flanders, K. Todd, J.A. Mulholland, P.B. Ryan, H. Frumkin Interim Results of the Study of Particulates and Health in Atlanta (SOPHIA), *J. Exposure Analy. and Env. Epid.* 10 **2000**, 446-460.

Photoacoustic Analyzer

for the measurement of soot

The photoacoustic analyzer (PA) measures soot concentration, also called black carbon or elemental carbon, in real time. The PA actually measures light absorption, which is closely correlated to soot concentration. It offers several advantages over traditional filter measurements of soot including rapid turnaround of results, study of transient conditions, large dynamic range, and

The PA measures soot concentration in real time

What is soot?

Soot is linked to health effects

Soot comes from the combustion of jet fuel, gasoline, diesel and other fuels, and it makes up a large fraction of particulate matter in the atmosphere. Soot has been linked to adverse health effects including dysrhythmia and cardiovascular disease (Tolbert et al. 2000), and it is a significant component of diesel exhaust particulates, which are reasonably anticipated to be carcinogenic (National Toxicology Program 2003). Soot also contributes to global warming and impaired visibility (haze).

When discussing soot, it is useful to understand the terms elemental carbon (EC), soot, and black carbon (BC). If you collect particulate matter on a filter, elemental carbon is the material that remains after heating the filter to 700°C, and soot is the material remaining on a filter after extracting it with a solvent. Black carbon is the part of particulate matter that absorbs light. The PA actually measures black carbon, but it is closely correlated to elemental carbon and soot concentration. For simplicity, we've used the term soot throughout the guide.

In general, soot isn't regulated directly, but it is a significant component of particulate matter, especially particulate matter smaller than 2.5 μm in diameter ($PM_{2.5}$). However, soot is regulated indirectly through standards for particulate matter, opacity, smoke, and visibility. As evidence for the health effects of particulate matter grows, regulations on particulate matter are becoming increasingly stringent. In addition, increasing emphasis is being placed on fine particulate matter. This will likely result in requirements for reduced soot emissions from diesel and aircraft engines.

Soot is a major component of $PM_{2.5}$

How does it work?

The PA rapidly measures light absorption as particles flow through the instrument, without the need to collect particles on a filter. The light absorption correlates to soot concentration. The PA also has a large dynamic range (130 dB), making it suitable for use on a wide range of exhaust and ambient samples. Specifically, the instrument measures light absorption at a laser wavelength of 1047 nm. Soot absorbs very strongly at this wavelength, in contrast to other types of particles and gases. Sample air is pulled continuously through an acoustical waveguide, and the laser also passes through the waveguide (Figure 2-1). The laser power is modulated at the resonance frequency of the waveguide. Now when soot absorbs light, it is heated. This heat transfers very rapidly to the surrounding air, in a time that is much shorter than the period of the laser-beam modulation, so all of the heat from light absorption comes out of the particles during each acoustic cycle. Upon receiving heat, the surrounding air expands, generating a pressure disturbance (i.e. an acoustical signal) that is measured with a microphone attached to the waveguide. Since soot absorbs light throughout the entire particle volume, the light absorption measurement is also a measure of soot mass concentration. This is the reason that light absorption can be used as a measure of black carbon mass concentration.

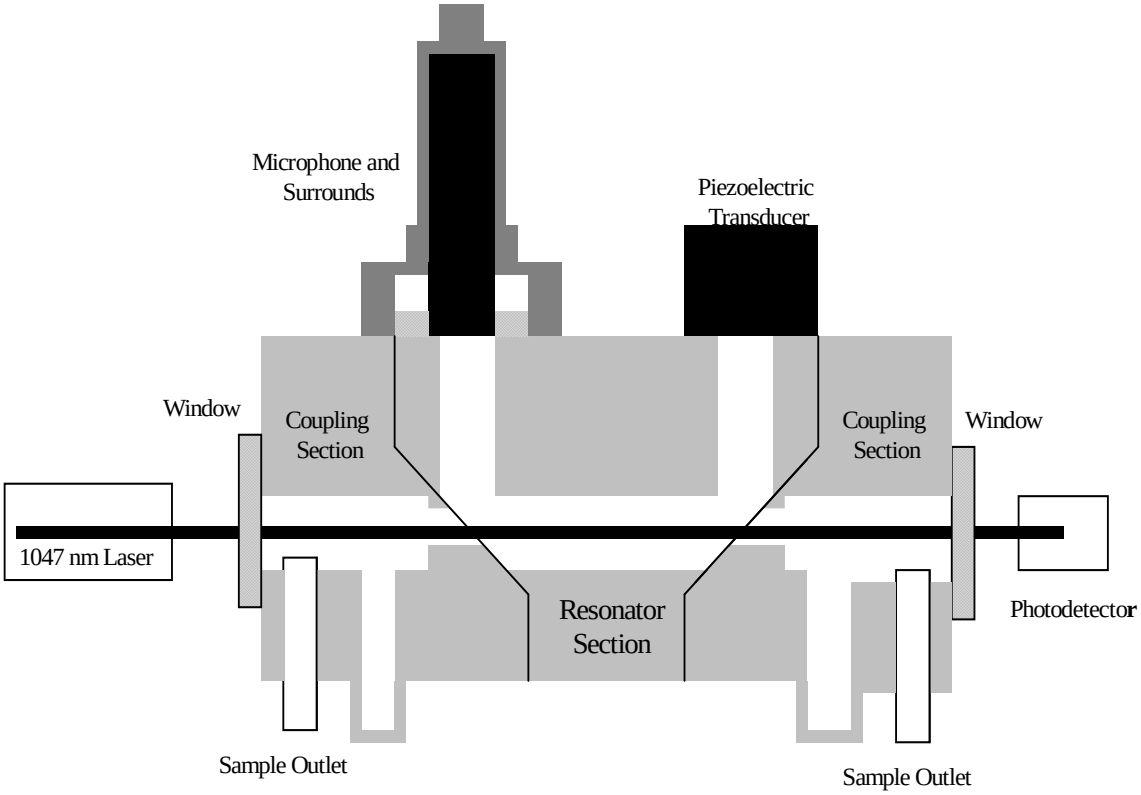

Figure 2-1. Schematic of the photoacoustic analyzer.

When can you use the photoacoustic analyzer?

The PA can measure soot from a variety of emission sources and ambient air. It is portable and suitable for field testing. However, there are a few practical considerations for using the PA:

- The PA operates best between temperature ranges of 40°F to 100°F.
- Particle concentrations should range from 50 ng/m^3 to 100 mg/m^3.
- The relative humidity of a sample should not exceed 80%.
- The PA must remain dry and protected from the elements.

The PA has been successfully demonstrated on emissions from gasoline and diesel vehicles, jet aircraft, brick kilns, and domestic trash burning. Figure 2-2 shows an example of how well the results from the PA correspond to filter measurements of elemental carbon (not organic carbon) for a variety of aircraft ground support equipment. Organic carbon is the portion of particulate matter that volatilizes when heating a filter from 300°C to 700°C.

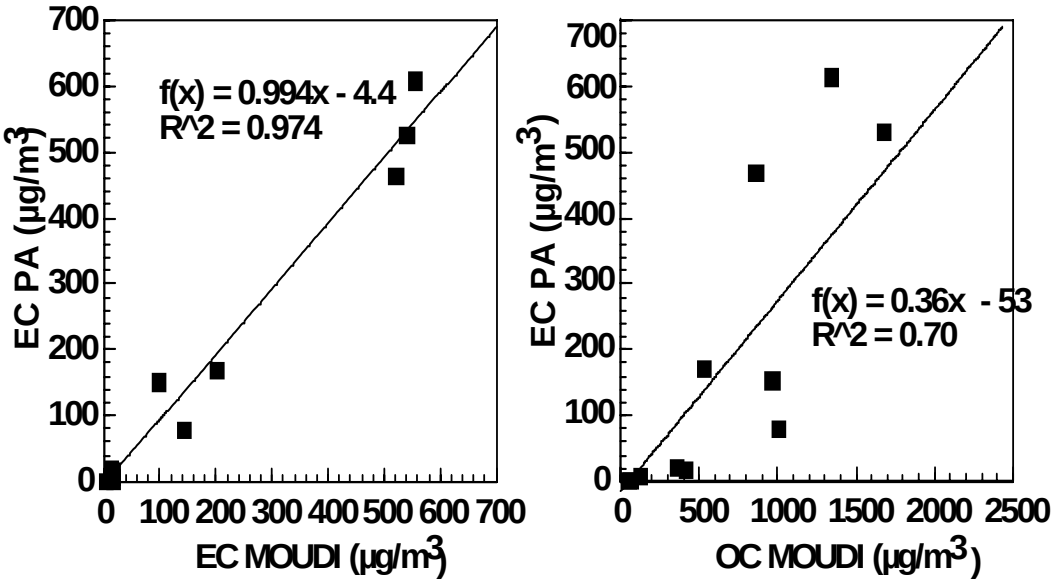

Figure 2-2. Comparison of PA results with filter measurements of EC and organic carbon OC.

One of the main benefits of the PA is its ability to provide information on transient conditions, as in Figure 2-3. It shows how soot concentration varies with engine condition for a diesel Dodge Bobtail (Hill Air Force Base, 2000).

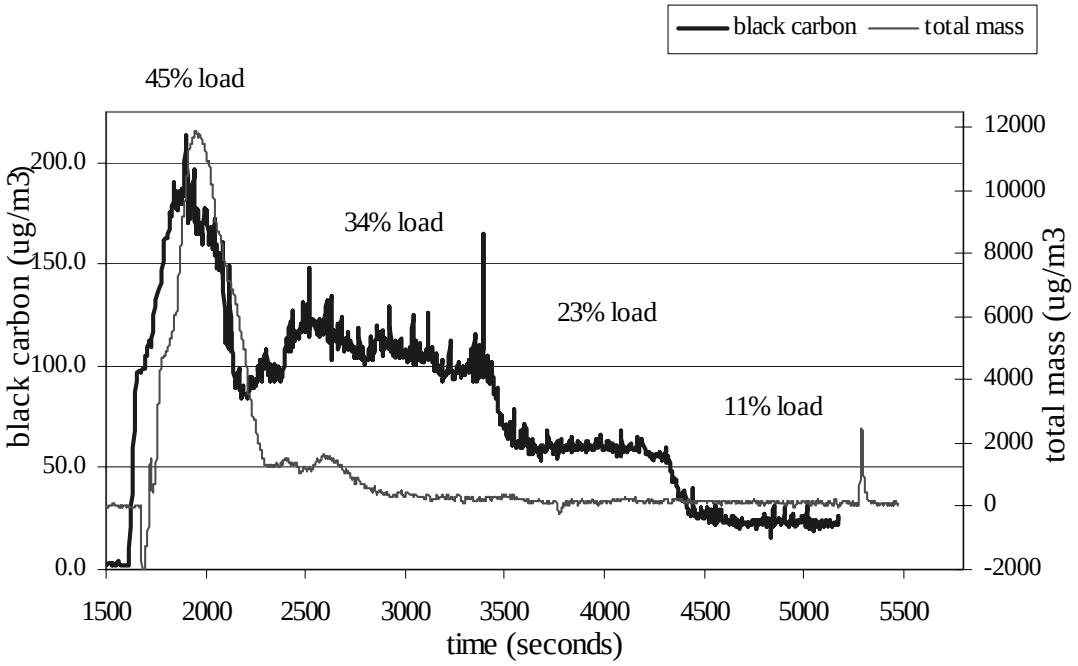

Figure 2-3. PA signal versus engine load.

Cost comparison

Currently, the purchase price of PA assembled from premium components is approximately $36,000, including a computer. However, it is expected to decrease in the future. Analyzing filters for elemental carbon is relatively inexpensive. If you collected a set of cascade impactor filters, it would cost approximately $550 to analyze a set of nine filters. One common system for collecting filter samples is a Micro Orifice Uniform Deposit Impactor (MOUDI), and it costs approximately $12,000. The MOUDI contains eight or ten stages, with cut points ranging from 10 µm to 56 nm. Other impactors are available, but when measuring soot remember that much of it is associated with particles less than 1 µm in diameter. So, care must be taken to ensure that particulate matter is collected in the correct size range. A qualified technician could operate the photoacoustic analyzer or a system to collect filter samples. Because the PA can produce measurements more rapidly, it offers the potential for some labor savings.

As a rule of thumb, if you are interested in collecting a few samples, filter samples are likely to be more cost effective. However, if you need to make numerous measurements or require information on transient conditions, the PA would be more cost effective and relevant.

Comarison of the PA with other methods

The PA provides results more rapidly than filters

There are some differences in how soot, elemental carbon, and black carbon are measured. Elemental carbon is measured as the mass of carbon that evolves on ramping an exposed quartz filter sample form a lower to upper temperature range, typically 500°C to 700°C. In practice, the most reproducible elemental carbon concentration is when 47-mm filters are loaded with 1 mg of material. Filters are exposed, shipped to the laboratory, put in the analysis queue, and eventually analyzed, perhaps months after they were exposed, so the data acquisition rate is often slow. The dynamic range is limited by the need to obtain a loading of about 1 mg/sample on the filter. On the other hand, if you are interested in the size-segregated distribution of elemental carbon, cascade impactors, such as a MOUDI, are more appropriate.

Black carbon is measured by light absorption, and this correlates to soot concentration. The absorption efficiency of soot is much larger than the efficiency of other atmospheric aerosols. Soot aerosols are small enough that the light is absorbed throughout the aerosol volume, so that aerosol light absorption is proportional to the mass concentration of light-absorbing aerosols. The proportionality between aerosol light absorption and soot mass concentration is typically obtained from the linear rgression coefficient against elemental carbon. In this sense, soot should be equivalent to elemental carbon in source-profile measurements.

Light absorption measurements are commonly made by filter-based methods in instruments such as aethalometers (Hansen et al. 1984) and particle soot absorption photometers (PSAP). In these methods, a quartz filter is exposed to aerosol, and the attenuation of light through the filter is monitored over time. The filter is a multiple scattering substrate so that the reduction in the transmitted light is proportional to the aerosol absorption cross section. The PSAP calibration requires simultaneous measurement of aerosol scattering coefficient with a nephelometer because a fraction of scattering is subtracted from the apparent light absorption from the filter attenuation (Bond et al. 1999). For very black aerosols, such as those from diesel engines or coal combustors, the multiple scattering character of the filter reduces with aerosol load. Consequently, the reported black carbon concentration can be incorrect by a factor of two, depending on the time history of filter loading. These filter-based methods suffer from low dynamic range because the black carbon concentration is proportional to filter attenuation only

for light filter loads. This limitation reduces the effectiveness of the filter method for source profile measurements of high emitters, as filter changes are needed often. Secondary dilution can extend the upper limit, although quantification of the dilution ratio increases measurement errors. Filter-based measurements perform best with low concentrations of black carbon, such as in ambient applications. The practical flow rates for these instruments range from 1 to 6 l/min , and the flow rate must be accurately determined to quantify filter exposure during a particular time interval. Rapid changes in the relative humidity (over seconds to many minutes) can cause unsatisfactory measurements by these methods.

Filter-based instruments work best for low soot concentrations

The PA also measures aerosol light absorption and can be calibrated to read soot concentration (Arnott et al. 1999, 2000). The aerosol light absorption measurement can be verified independently with measurements of light-absorbing gases, such as NO_2 at known concentrations and for visible wavelengths. Aerosol light absorption is measured in situ, no filters are needed, and flow rates are only important to ensure that aerosols are not deposited in the instrument or sample lines before they are measured. Since the PA's microphones have such a wide dynamic range, the black carbon measurements have the same dynamic range, e.g. a factor of 10^6. The PA can equally be used in pristine ambient locations or in source profile measurements for high emitters. There are no filter artifacts. Relative humidity influence is likely not important when it is below 80%.

The PA can quantify a large range of soot concentrations and is less sensitive to humidity

Vision for use

DoD users should look to the PA for all of their black carbon mass concentration needs. It is useful in doing ambient measurements at fixed locations such as in air quality measurements at military bases. It is useful in profiling sources at these bases, particularly when dynamometers and constant-volume samplers are used. It is also useful in instrumented vehicles to measure black carbon issuing from the vehicle it is on, or as a function of time and space.

Resources

Website for the photoacoustic analyzer: http://photoacoustic.dri.edu

For more information about the photoacoustic analyzer, Dr. Pat Arnott: pat@dri.edu

For general information or information about this User's Guide, Kerry Kelly: kelly@eng.utah.edu

References

Arnott W.P., H. Moosmuller, J.W. Walker, Nitrogen-Dioxide and Kerosene-Flame Soot Calibration of Photoacoustic Instruments for Measurement of Light Absorption by Aerosols. *Rev. Sci. Instrum.* 71 **2000** 4545-4552.

Arnott W. P., H. Moosmüller, C. F. Rogers, T. Jin, R. Bruch, Photoacoustic spectrometer for measuring light absorption by aerosols: Instrument description. *Atmospheric Environment* 33 **1999** 2845-2852.

Bond T.C., T L. Anderson, D. Campbell, Calibration and Intercomparison of Filter-Based Measurements of Visible Light Absorption by Aerosols. *Aerosol Science and Technology* 30(6) **1999** 582-600.

Hansen, A.D.A., H. Rosen, T. Novakov (1984). The Aethalometer - An Instrument for the Real-Time Measurement of Optical Absorption by Aerosol Particles. *Science of the Total Environment* 36 **1999** 191-196.

NTP (National Toxicology Program 10th Report on Carcinogens, U.S. Department of Health and Human Services, National Toxicology Program, **2003**, http://ehis.niehs.nih.gov/roc/

Tolbert P.E., M. Klein, K.B. Metzger, J. Peel, W.D. Flanders, K. Todd, J.A. Mulholland, P.B. Ryan, H. Frumkin Interim Results of the Study of Particulates and Health in Atlanta (SOPHIA), *J. Exposure Analy. and Env. Epid.*10 **2000** 446-460.

Photoelectric Aerosol Sensor

for measuring particle-bound polycyclic aromatic hydrocarbon concentration

The photoelectric aerosol sensor (PAS) qualitatively measures the concentration of particle-bound polycyclic aromatic hydrocarbons (PAHs). It gives a relative measure of particle-bound PAH concentration or, with appropriate calibration, a more accurate measure of PAHs. The PAS may provide a qualitative measure of total PAH concentrations more rapidly and cost effectively than traditional measurements, such as filter extraction and subsequent GC/MS analysis. However, the PAS cannot provide concentrations of individual PAHs, and developing a calibration curve for each instrument and source can be expensive and time consuming.

PAS measures particle-bound PAHs

What are PAHs?

PAHs have negative health effects

PAHs are a complex group of hundreds of chemicals that are formed during the incomplete burning of fuels, such as oil, wood, gasoline, diesel and jet fuel, and garbage. They are commonly found in vehicle exhaust and cigarette and wood smoke. Figure 3-1 gives the structure of some PAHs. PAHs as a group are reasonably anticipated to be carcinogenic (NTP 2003), and a few individual PAHs, such as benz[a]anthracene and benzo[a]pyrene, are probably carcinogenic (IARC 2003).

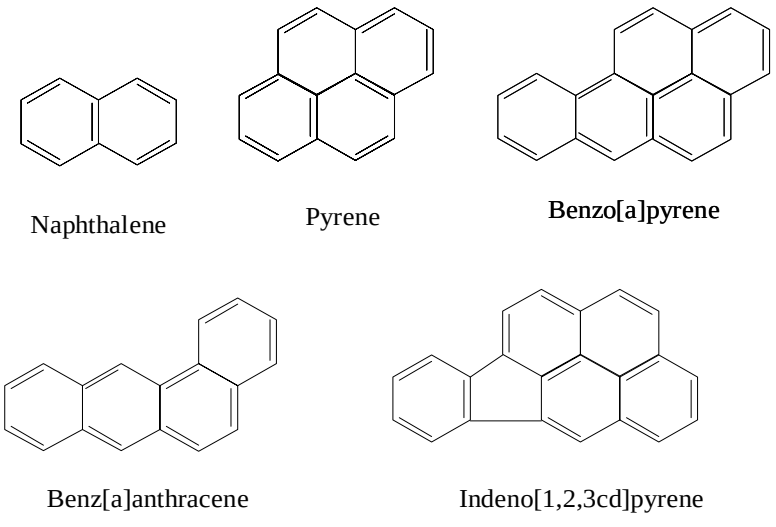

Figure 3-1. Example structure of a few PAHs.

In the atmosphere or in exhaust from a combustion source, PAHs can be found on particles or as a vapor. Heavier molecular weight (MW) PAHs tend to be found on particles, whereas lighter MW PAHs are more typically found as vapors. The phase of the PAHs will also depend on their source and its operating condition. For example, diesel exhaust tends to contain more particle-bound PAHs at higher engine load than at idle conditions.

A few PAHs are regulated directly in the United States, and other countries regulate individual PAHs or classes of PAHs. The EPA regulates emissions of one PAH, naphthalene, as a hazardous air pollutant, and seven PAHs are included on EPA's list of urban air toxics, which may be regulated in the future. Particle-bound PAHs are regulated indirectly through standards for particulate matter, opacity, smoke, and visibility. Typically, PAHs make up a small fraction of particle mass.

PAHs can be found in vapor or on particles

How does it work?

Figure 3-2 shows a schematic of the PAS, and additional instrument details can be found in EPA (1997) and Burtscher (1992). Briefly, samples flow continuously into the PAS and through the eximer-lamp ionization region, where particle-bound PAH molecules are ionized and loose an electron. The photon energy of the lamp is chosen so that gas-phase molecules are not ionized. The negatively charged particles collect on a filter where charge is measured with an electrometer. The charge is integrated over time to give the photoelectric current (in femto- or picoamps). This current should be proportional to the PAH loading on a particle. Three versions of the PAS are available commercially, but they all have similar operating principles.

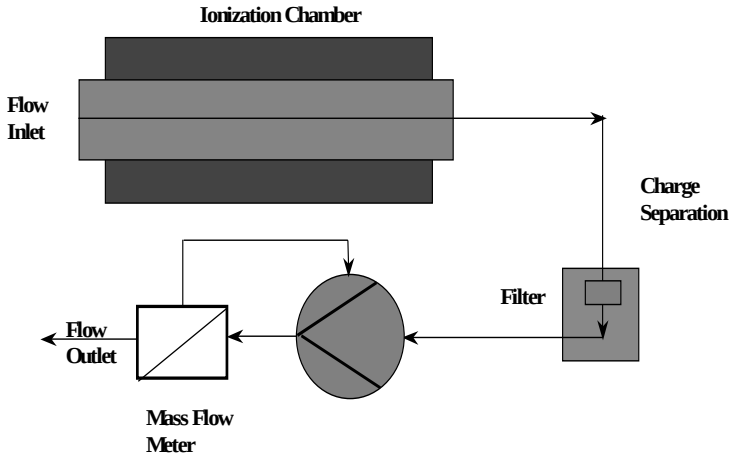

Figure 3-2. Schematic of the PAS.

For a more accurate measure of PAHs, calibrate each PAS for each source type

The PAS was originally calibrated to fifteen individual PAHs (called the Siegmann sum) from several sources, with a universal conversion factor of 1-3 $\mu g/m^3$ $picoamp^{-1}$ (Wilson and Barbour 1994, Wilson et al. 1991, EPA 1999). Because PAHs are such a complex mix of vapor and particle-phase compounds, the PAS responds differently to each type of source, and calibration factors can vary widely (Figures 3-3 and 3-4). Without an appropriate calibration curve, the PAS will only give you a relative measure of particle-bound PAH levels. Independent comparisons of the PAS and filter measurements are limited (Chuang et al. 1999, Chetwittayachan et al. 2002, Tang et al. 2001, Arnott et al. in progress), and the results are contradictory. Figures 3-3 and 3-4 compare PAS results with filter measurements for military vehicles and aircraft, and they show how the PAS response varies for different sources. The PAS results correlate reasonably well with filter measurements for military vehicles ($R^2 = 0.762$) and better for military aircraft ($R^2=0.99$), but the aircraft correlation is heavily weighted by one data point. The response of each PAS instrument varies for each source type, so a calibration curve for each instrument should be developed for each source. For vehicle and aircraft emissions, it is also interesting to note that the PAS correlates well with soot concentration (Baltensperger et al. 2001, Matter et al. 1999, Arnott et al. in progress).

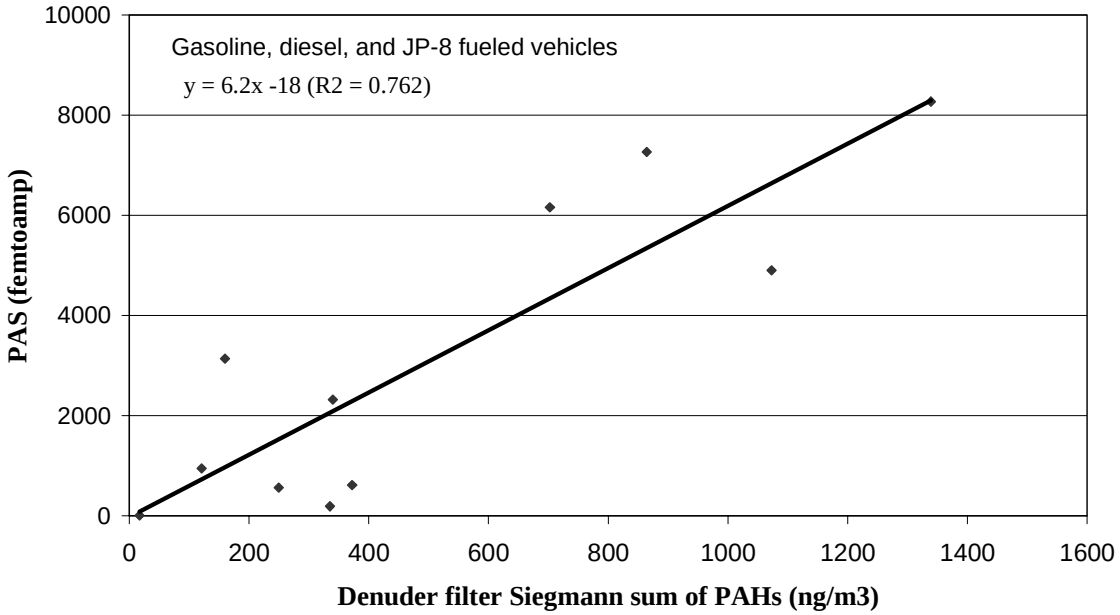

Figure 3-3. Correlation of PAS readings with denuder filter measurements of particle-bound PAHs for several vehicles.

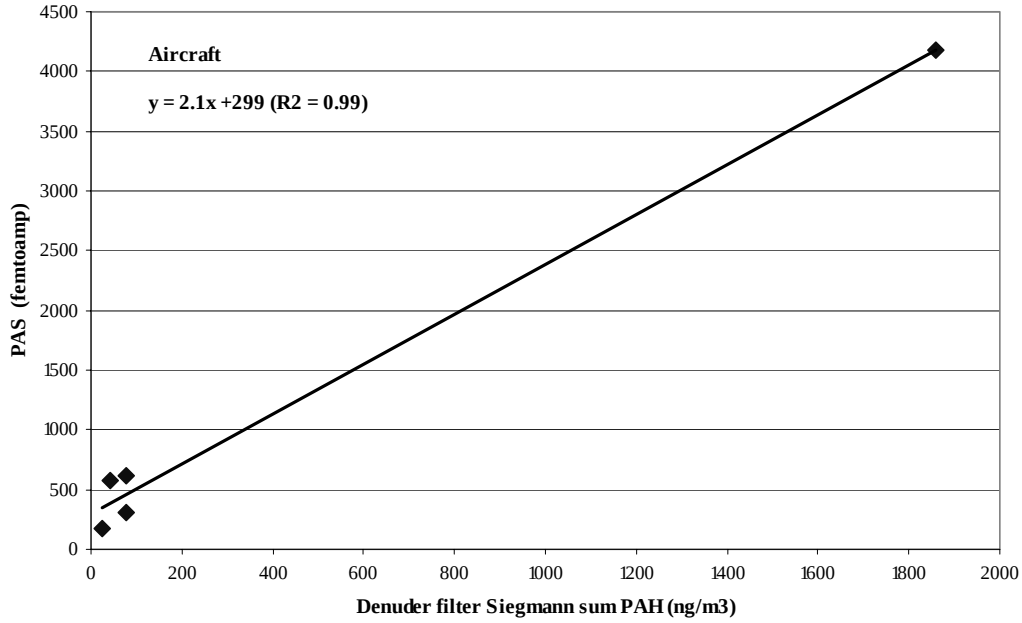

Figure 3-4. Correlation of PAS readings with denuder filter measurements of particle-bound PAHs for aircraft.

When can you use the photoelectric aerosol sensor?

PAS results correlate somewhat with filter measurements

The PAS can qualitatively measure PAH emissions from a variety of emission sources and ambient air. For source sampling, there are a few practical considerations:

- Maintain PAS readings below 50 picoamps. Exposing the PAS to high levels of water vapor or source emissions, such as diesel exhaust, will cause erratic results. Measurements of anything other that ambient air requires dilution with dry, particle free air.
- Keep the PAS inlet temperature constant because PAS results vary with inlet temperature. Studies at the University of Utah found a temperature of approximately 250-300°F to be reduce erratic negative signals. The PAS manufacturers sell a dilution/heated inlet system. Alternatively, you can wrap the inlet line with heating tape.

- The instrument itself should operate at temperatures between 0°F and 105°F.
- Depending on the source, the PAS can detect a minimum PAH concentration of 10 ng/m^3.
- The PAS must remain dry and protected from the elements.

Cost comparison

Chemical analysis of PAHs from filter samples is expensive. For example, analyzing nine stages of a cascade impactor for PAHs costs approximately $4,700 and analyzing a denuder/filter system costs approximately $1,500 (if the three components are analyzed separately). These costs do not include the labor costs associated with collecting the samples or the costs of the sampling devices. One type of cascade impactor, a micro-orifice uniform deposit impactor (MOUDI), costs approximately $12,000 for the entire complete setup and a denuder/filter system costs approximately $2,000 – 4,000 (depending on configuration). Furthermore, chemical analyses for PAHs are time consuming; it typically takes several months to receive the analytical results. Alternatively, the PAS collects data in real time, and the data can be downloaded and analyzed in the matter of days. The PAS 2000 costs approximately $15,000 (2003 price).

Comparison of the PAS with other methods

There are two basic methods for measuring particle-bound PAHs. The first involves collecting samples on a filter followed by chemical analysis, and the other is the PAS. Filter samples are commonly collected on cascade impactors, such as MOUDIs, or on a denuder/filter system. The MOUDI contains eight to ten stages plus an after filter, and each stage contains a filter. A denuder/filter system contains three parts, a resin-coated denuder that absorbs vapor-phase PAHs, a filter that collects particles, and a cartridge to collect excess particles and vapor from the filter and denuder. The next step in chemical analysis is extracting the filters or denuder/filter components with a solvent, such as hexane. The extract may be concentrated to improve the detection of low-concentration PAHs, and impurities may be removed. Next, the extract is analyzed by an advanced analytical method, such as gas chromatography/mass spectrometry. The entire process of PAH analysis is challenging because of the low concentrations of PAHs, the potential interference from the complex mixtures of chemicals in which PAHs are found, and the reaction of compounds during sampling and storage.

PAH analysis is challenging

Traditional filter measurements and denuder/filter systems provide some information that cannot be obtained with the PAS. For example, the traditional analyses measure concentrations of individual PAHs, instead of the total particle-bound PAH content as measured by the PAS. In addition, the denuder/filter system provides information on vapor- and particle-

phase concentrations of individual PAHs. Finally, substrates collected on a MOUDI or other cascade impactor can give information on the size of particles on which PAHs are found.

Chemical analysis provides more information

A filter or denuder/filter system requires a minimum amount of material for analysis, but excessive amounts of sample may cause artifacts. If a filter is properly prepared, a trained graduate student or technician can collect a filter or impactor sample. However, it is difficult to determine if there is sufficient sample for PAH analysis before the sampling is complete. After sampling is complete, a small section of the filter can be analyzed for organic carbon content, which provides an indication of the PAH loading. A further complication for cascade impactors, such as a MOUDI, is that mass loading will vary by impactor stage. Operation of the denuder/filter system is delicate and requires an experienced scientist. For example, an individual must ensure that the flow is sufficiently high to prevent very small particles from depositing on the denuder portion. However, if one overloads the denuder, the flow will drop, causing particle deposition and erroneous results. For ambient samples, collecting sufficient material may require several days of sampling, and for source samples it may require from tens of minutes to hours.

The PAS is relatively easy to operate, and it provides results rapidly. However, it is not as accurate as the chemical analysis methods, and it provides less detailed information. A technician or student could operate the PAS. The PAS can measure a large range of PAH concentrations, and it is sensitive enough to detect ambient levels of PAHs down to 10 ng/m^3. With dilution the PAS can measure emissions from combustion sources, such as diesel engines. However, care must be taken not to expose the PAS directly to undiluted exhaust from a source like a diesel engine, which will cause erratic signals. Because the PAS records PAH concentrations rapidly (at intervals less than 10 seconds), it is particularly useful for studying transient conditions, such as process start up or engine acceleration. On the other hand, filter analyses require sufficient time for material to deposit on the substrates, and these analyses are not sensitive enough to provide information on transient conditions. The PAS does have a few disadvantages: is not as accurate as the chemical analysis methods, and each instrument should be calibrated for each source type, which is expensive and time consuming. Furthermore, the PAS provides the total concentration of particle-bound PAHs; it cannot provide the concentrations of individual PAHs or information about vapor-phase PAHs.

The PAS provides rapid results

PAH detection and analysis is challenging, and there are significant tradeoffs between chemical analysis methods and the PAS. Chemical analysis provides accurate concentrations of individual PAHs. They can provide the size of particles on which PAHs are associated and which PAHs are found in vapor and particle phases. However, chemical analysis methods are expensive, time consuming, and subject to artifacts. The PAS rapidly provides a relative measure of total PAH concentrations and can provide information on transient conditions. However, more accurate results could be obtained by calibrating each PAS for each source.

Chemical analysis is more accurate and provides more data but is more expensive and time consuming

Vision for use

The PAS is a good choice when a relative measure of particle-bound PAHs is desired or when transient conditions are studied. For example, it would be useful for the preliminary evaluation of a control device, for screening sources for further analysis, or for studying transient conditions. The PAS is a relatively new instrument, and with additional study and independent calibration it may produce more valuable results. Chemical analysis methods are a good choice if you want quantitative PAH concentrations, accurate concentrations of individual PAHs, or information about the phase distribution of PAHs.

Resources

Website for the photoelectric aerosol sensor:
http://www.ecochem.biz/PAH/PAS2000.htm

For general information or information about this User's Guide, Kerry Kelly:
kelly@eng.utah.edu

References

Arnott et al., Evaluation of 1047 nm Photoacoustic Instruments and Photoelectric Aerosol Sensors in Source-Sampling of Black Carbon Aerosol and Particle-Bound PAH's from Gasoline and Diesel Powered Vehicles, *in progress*.

Baltensperger, U. E. Weingartner, H. Burtscher, J. Keskienen, Dynamic Mass and Surface Area Measurements. In: P.A. Baron and K. Willeke (eds.) *Aerosol Measurement* **2001** New York:Wiley, pp. 387-418.

Burtscher, H. Measurement and Characteristics of Combustion Aerosols with Special Consideration of Photoelectric Charging and Charging by Flame Ions; *J. Aerosol Sci.* **1992**, *23* (6) 549-595.

Chetwittayachan T., D. Shimazaki, K. Yamamoto, A comparison of temporal variation of particle-bound polycyclic aromatic hydrocarbons (pPAHs) concentration in different urban environments: Tokyo, Japan, and Bangkok, Thailand, *Atmos. Environ*. 36 **2002** 2027-2037.

Chuang, J.C, P.J. Callahan, C.W. Lyu, N.K. Wilson, Polycyclic aromatic hydrocarbon exposures of children in low-income families, *J. Exposure Analysis and Environ. Epid.* 2 **1999** 85-98.

EPA. *Field and Laboratory Analyses of a Real-Time PAH Analyzer*, EPA/600/R-97/034; EPA Office of Research and Development, **1997**.

International Agency for Research on Cancer, *IARC Monographs*, **2003**, vol. 1-82 http://monographs.iarc.fr/monoeval/crthall.html

Matter U., H.C. Siegmann, H. Burtscher, Dynamic Field Measurements of Submicron Particles from Diesel Engines, *Environ. Sci. Technol.* 33 **1999** 1946-1952.

National Toxicology Program, *10th Report on Carcinogens*, U.S. Department of Health and Human Services, National Toxicology program **2003**, http://ehis.niehs.nih.gov/roc

Tang, S., R. Johnson, T. Lanni, W. Webster, T. Tagliaferro, H. Munn, C. Barnes, D. Barnes, K. Newkirck, D. Rivenburgh, D. Guerrieri, *Monitoring of PM-bound polycyclic aromatic hydrocarbons from diesel vehicles by photoelectric aerosol sensor (PAS)*, Automotive Emissions Laboratory, New York Department of Environmental Conservation, March 22, **2001**.

Wilson N.K., Barbour, R,K., Evaluation of a real-time monitor for fine particle-bound PAH in air, *Polycyclic Aromatic Compounds* 5 **1994** 167-174.

Wilson N.K., Chuang, J.C., MR. Sampling polycyclic aromatic hydrocarbons and related semivolatile organic compounds in indoor air. *Indoor Air* 4 **1991** 513-512.

Aerosol Time-of-Flight Mass Spectrometer

for measuring individual particle size and composition

The aerosol time-of-flight mass spectrometer (ATOFMS) determines size and composition of single particles in near real-time. It is available commercially from TSI Inc. (Model 3800). The ATOFMS is a powerful tool because it provides associations between compounds within single particles, and this information can be used to identify a particle's source. The ATOFMS also provides PM composition for transient conditions, when bulk techniques, such as filters, cannot.

The ATOFMS determines a particle's size and composition

Why is understanding the size and composition of individual particles useful?

Studies over the last ten years have linked particulate matter (PM) concentration to adverse health effects, and more recent evidence indicates that size, surface area, and composition of PM are important factors in determining the heath effects associated with PM. For example, certain metals found in PM, such as iron, nickel and vanadium have been linked to adverse effects on the lung. The composition of individual particles can also provide insight into particle formation and chemistry, and it can help identify the source of a particle by its chemical composition, i.e., fingerprint. For example, it can provide fingerprints for specific sources, such as explosives, diesel engines, and biological aerosols.

A particle's size and composition can provide clues about its source and health effects

How does it work?

Figure 4-1 shows a schematic of the ATOFMS. The ATOFMS consists of three regions:

- Particle sampling region
- Particle sizing region
- Mass spectrometry region

In the commercially available ATOFMS, particles are introduced into the particle-sampling region under atmospheric pressure through a converging nozzle where they are accelerated according to their aerodynamic size. Smaller particles reach a higher terminal velocity than larger particles. The accelerated particle next enters the particle sizing region, where particle velocity is measured by recording the transit time for the particle to pass between two continuous-wave laser beams

positioned a fix distance apart. Particle size is then determined by comparing the velocity of the particle to a calibration curve, which is obtained using particles of known size. Finally, the particle reaches the mass spectrometry region. Using the known speed of the particle, a Nd:YAG laser at 266 nm is fired at the exact time the particle reaches the center of the ion source in the mass spectrometer. This laser pulse desorbs and ionizes the compounds making up the particle. The ions formed in this process are analyzed by a bipolar time-of-flight mass spectrometer. The resulting mass spectra are then used to determine the chemical composition of the particle.

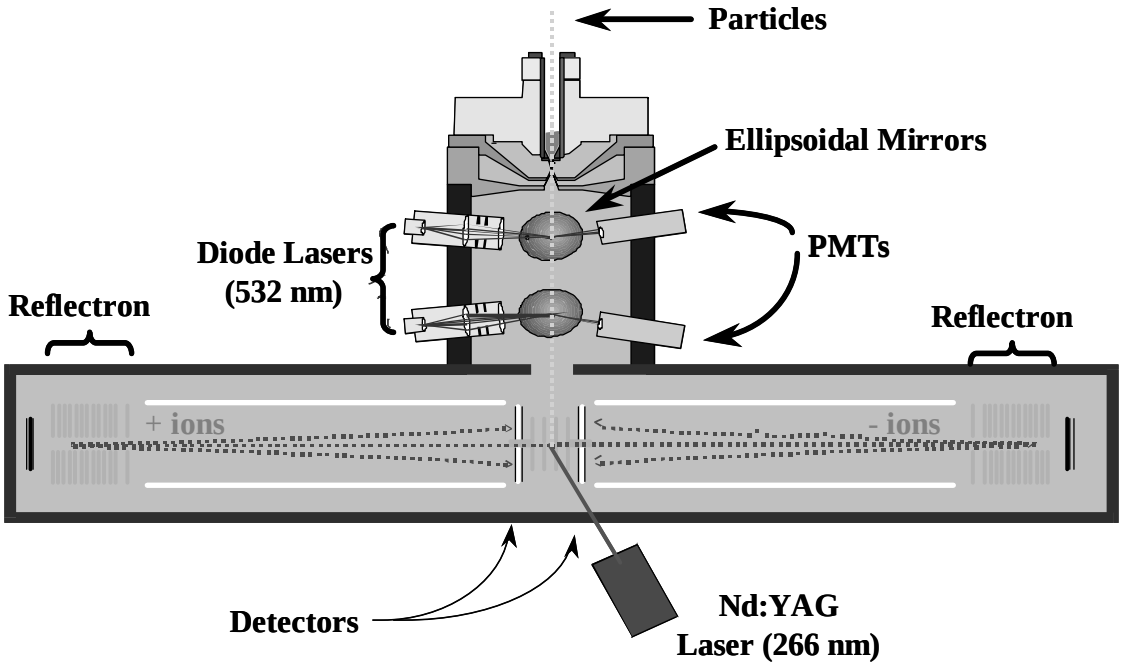

Figure 4-1. Schematic of the ATOFMS.

The operation of the ATOFMS is based on two established methods:

- Aerodynamic particle sizing
- Time-of-Flight Mass Spectrometry (TOFMS)

What is aerodynamic sizing?

Aerodynamic particle sizing is based on the inertia of particles. When a gas expands, it is accelerated. Particles suspended in the gas are also accelerated, but the extent of the acceleration depends on their aerodynamic diameter. The aerodynamic diameter is defined as the diameter of a unit density (density = 1 g/cm^3) sphere that has the same settling velocity as the particle (TSI, 2002). Not only the physical diameter but also the shape and density of the particle are taken into account. The smaller a particle, the higher the acceleration and therefore the terminal velocity it reaches. This velocity can be determined by measuring the time it takes the particle to travel a known distance. Usually this transit time is measured using a split laser beam or with beams from two lasers (which is used in the 3800 ATOFMS). The scattered light is collected with a detector and the signals are used to start and stop a clock registering the transit time. Transforming the transit time into size is done by calibrating the instrument with a number of particles of known size to create a calibration curve. This calibration curve is then used to determine the size of the unknown sample (TSI, 2002).

What is time-of-flight mass spectrometry?

There are many types of mass spectrometry (MS). A common component of all MS systems is that ions are separated based on their mass-to-charge ratio (*m/z*). The first mass spectrometry instruments used a magnetic field to separate ions. Later instruments used magnetic and electric fields. Other common methods include those that use quadrupole mass filter, quadrupole ion traps, ion traps in static magnetic fields (Fourier transform mass spectrometry), and time-of-flight (TOF-MS) measurements. Each method has its advantages and disadvantages depending on the application. FTMS, for example, can provide extremely high mass resolution. Quadrupole and quadrupole ion trap instruments can be very small. TOF instruments offer the advantage of not being a scanning method, that is, you get a complete spectrum for each ionization event. As the name suggests, TOFMS accelerates ions to a specific kinetic energy and measures the ions' time-of-flight between a distinct starting point (often the ionization event) and the arrival at the detector. The ions arrival times are correlated with their mass-to-charge ratios, with smaller m/z ions arriving before larger m/z ions. Upon calibration of the mass spectrometer, the measured ion transit times can be converted to the corresponding mass-to-charge ratios, which are related to the chemical components in the original particles. The most common start event is the pulse of the desorption/ionization (D/I) laser. This event starts the data logging; the ion current from the detector is recorded over time and creates the mass spectrum. Ions created in the ion source are accelerated into the flight tube by a potential that is usually created by two source plates. As all ions have the same energy, the potential where they were formed, the acceleration (and therefore the velocity they reach at the end of the ion source) depends only on their mass-to-charge ratio:

$$eV = \frac{mv^2}{2z}$$

$$v = \sqrt{\frac{2zeV}{m}}$$

where: eV is the potential energy of the ion,
m/z is the mass-to-charge ratio,
and v is velocity.

This equation shows that ions with a small m/z are accelerated to a higher terminal velocity than ions with a large m/z. After the initial acceleration step, the ions enter the flight tube, also known as the field free region or drift region. This part of the mass spectrometer is held at a constant potential (hence the name *field free region*) and the ions drift at the velocity they achieved from their acceleration in the ion source (*drift region*). During this time, ions separate based on their velocity and therefore their m/z. At the end of the flight tube, they hit a detector and create an ion current that is measured and recorded to create the mass spectrum.

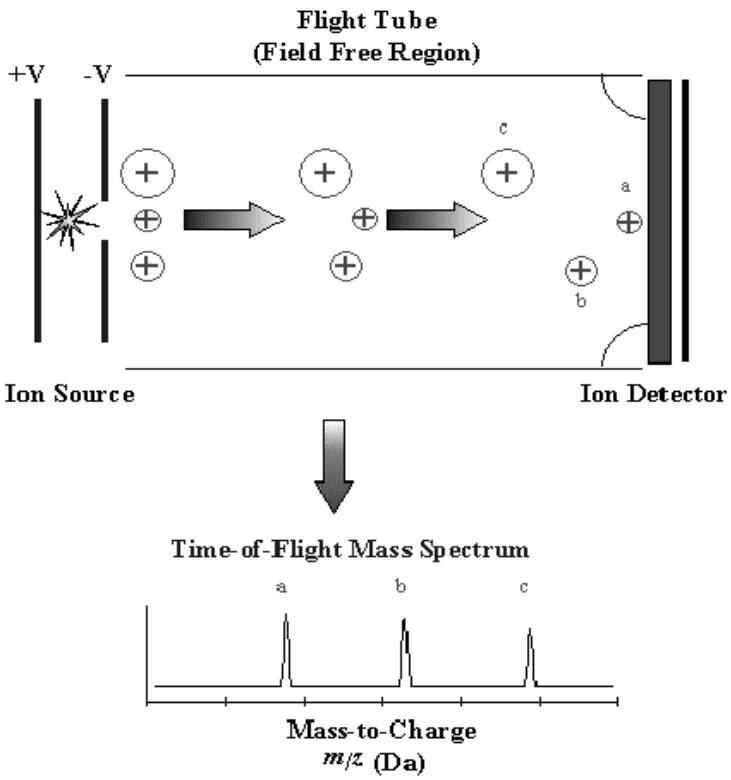

Figure 4-2. Time-of-flight mass spectrometry principles.

During the desorption/ionization event, ions can obtain additional kinetic energy from the explosion during desorption. Some ions travel in the direction they are accelerated in, while other ions travel in the opposite direction. This leads to a spread in energy for ions with the same *m/z*. As a result of this, ions with the same *m/z* end up with different velocities, which results in peak broadening due to different arrival times at the detector (low mass resolution). One way to correct this resolution issue is to use a reflectron or ion-mirror. The reflectron consists of a number of parallel, concentric electrodes to which a potential ramp is applied. The most common type of reflectron is the linear reflectron, which shows a linear potential increase. As the ions enter the reflectron, they slow down, stop, turn around, and are accelerated out of the reflectron again. Ions with higher energies penetrate the reflectron more deeply than ions with a smaller energies. Faster ions (high energy ions) therefore travel deeper into the reflectron than slower ions *of the same m/z* and spend more time in the reflectron. With the voltages set correctly, all ions of the same *m/z* are focused at the same arrival time on the detector surface (see Figure 4-3).

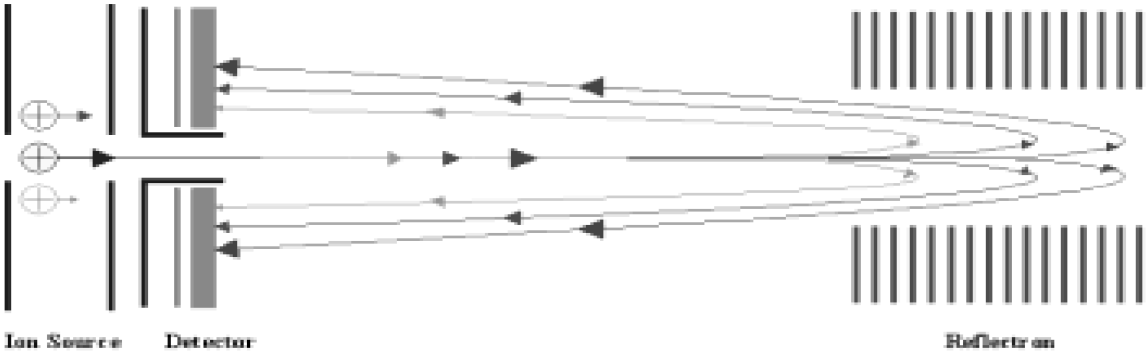

Figure 4-3. The reflectron focuses ions with different velocities/energies in time onto the detector.

When can you use the ATOFMS?

The ATOFMS has a few practical considerations:

- The commercially available version of the ATOFMS detects PM in the size ranging from 300 nm to 3 μm. It is possible to modify the ATOFMS with an aerodynamic lens to detect smaller sized particles, as small as 50 nm.
- The ATOFMS is mobile and frequently operates in the field. However after moving, the instrument's lasers may need alignment. In addition, it weighs approximately 800 lbs.
- For power, the ATOFMS requires 20 A of 220-240 VAC and 20 A of 110-120 VAC.
- The instrument itself should operate at temperatures between 50°F and 95°F.
- The ATOFMS must remain dry and protected from the elements.

Cost comparison

The ATOFMS is relatively expensive compared to an individual bulk sample. It currently costs $360,000. However, it can provide information that is not available through any other methods. Costs for the analysis of bulk samples (i.e., filters) range from a few dollars to a few thousand dollars per filter. If you are collecting and analyzing many bulk samples, the analysis costs can quickly run into the range of the ATOFMS's price. For the ATOFMS, a trained scientist must collect the samples and interpret the results. By comparison, bulk samples can be collected by a technician and sent away for analysis.

The ATOFMS is more expensive than bulk samples, but it can provide more data

Comparison of the ATOFMS with other methods

There are two basic methods for measuring particle size and concentration. The first involves single-particle mass spectrometry and the other involves collecting bulk samples on a set of cascade impactors or filters followed by chemical analysis.

Single-particle mass spectrometry

A number of mass spectrometer designs have been developed for aerosol analysis in the past decade. The other alternative single-particle methods (i.e. PALMS, RSMS) either provide limited size information or must step through discrete particle sizes. The ATOFMS is the only commercially available single particle MS and the system offers the highest size resolution and real-time analysis of particle size and composition across a range of sizes from 50 nm up to 7-8 μm. A complementary alternative to single particle mass spectrometry is aerosol mass spectrometry (AMS), a system developed by Aerodyne, which collects the average composition of an ensemble of many particles. This technique can be more quantitative than single-particle instruments but does not provide any information on the chemical associations within individual particles (or mixing state).

Single-particle mass spectrometry is the only method to provide the composition of single particles, and the ATOFMS was the first commercially available instrument. When comparing ATOFMS to bulk methods, the advantages and disadvantages are similar to other single-particle mass spectrometry methods.

The key advantage is that ATOFMS can be used to determine associations between species within individual particles. These associations can be linked with sources, making source apportionment much more straightforward than bulk measurements, which scramble the chemical information from multiple sources collected over some long sampling interval.

Also, the associations are key to understanding the health effects of these particles, as well as their optical properties, which are important in climate change issues. It is impossible to get these associations with bulk techniques, which mix the chemical signatures of thousands of particles together. Furthermore, the ATOFMS can acquire information on much shorter timescales than bulk measurements, which must sample for many hours in order to collect enough material for analysis, precluding the observation of short-term changes in PM composition.

Experience is needed to operate the ATOFMS and interpret its results

The key disadvantage of the ATOFMS is its cost and the learning curve required to interpret the spectra. However, the commercial system is now being successfully used by a broader set of users, and more information is becoming available on particle types and analysis methods. The commercial ATOFMS is the only available method that can continuously measure single particle size and composition. New ATOFMS systems are currently being designed which will reduce the size, weight, and power requirements and the overall cost of the system. This will make them more widely available.

Bulk samples

Bulk PM samples are commonly collected on cascade impactors, such as a micro-orifice uniform deposit impactors (MOUDIs) or Andersen impactors. The impactors contain eight to ten stages plus an after filter, and each stage contains a filter. Depending on the analysis method, the next step may be extracting the filters a solvent, such as hexane. The extract can be concentrated to improve the detection of low-concentration compounds, and impurities may be removed. Next, the extract or the filter is analyzed by an advanced analytical method, such as gas chromatography, mass spectrometry, x-ray fluorescence, or instrumental neutron activation analysis. Some compounds are present in low concentrations, so analysis can be challenging. Furthermore, evaporation, condensation, and reaction of compounds during sampling, extraction, and storage can also cause artifacts.

Chemical analysis of filter samples for some compounds is challenging

Cascade impactor samples provide PM within a certain size range, such as 0.05 μm to 0.1 μm, so the PM sizing is not as precise as the ATOFMS. Furthermore, a filter requires a minimum amount of material for analysis; depending on the source, sample collection may take hours or even days, so any transient differences in PM composition will be lost in the bulk sample. It is also difficult to determine if there is sufficient sample for analysis before the sampling is complete. A further complication for cascade impactors is that material loading will vary by impactor stage.

The key advantage of a filter/impactor samples is that they are less expensive than ATOFMS measurements or other single-particle mass spectrometry methods. Furthermore, a trained technician can collect samples instead of an experienced scientist. However, these bulk measurements lack the ability to provide rapid results, information about transient conditions, and associations between species in individual particles.

Bulk samples cannot provide data on transient conditions

Vision for Use

The most obvious applications for DoD users would be source apportionment (as demonstrated in SERDP project CP1106) and detection of signature compounds, including biowarfare detection. Biological particles can easily be discriminated from other atmospheric particles on a continuous basis. These instruments conceivably could detect individual bacteria and discriminate between them and particles from other sources. ATOFMS could acquire this information continuously so the particles of concern could be detected instantaneously for early warning. This has serious defense ramifications.

Resources

For more information about time-of-flight mass spectrometry:

Cotter, R.J. The new time-of-flight mass spectrometry. *Analy. Chem.*71(13) **1999** 445A-451A.

Cotter, R. J. Time-of-flight mass spectrometry, instrumentation and applications in biological research. *J. Liq. Chrom. & Rel. Technol*. 21(6) **1998** 903-914.

Mamyrin, B.A., V.I. Karataev, D.V. Shmikk, V.A. Zagulin, *Sov. Phys. JETP* **1973** pp. 37, 45.

For additional information about the ATOFMS:

ATOFMS Web site *http://www.tsi.com/particle/products/massspec/3800.shtml*

Galli, M., S.A. Guazzotti, K.A. Prather, Improved Lower Particle Size Limit for Aerosol Time-of-Flight Mass Spectrometry. *Aerosol Sci. & Technol.* 34(4) **2001** 381-385.

Gross, D.S., M.E. Galli, P.J. Silva, S.H. Wood, D.Y. Liu, K.A. Prather, Single Particle Characterization of Automobile and Diesel Truck Emissions in the Caldecott Tunnel. *Aerosol Sci. & Technol.* 32(2) **2000** 152-163.

Middlebrook, A.M.; D.M. Murphy, S.H. Lee, et al. A Comparison of Particle Mass Spectrometers during the 1999 Atlanta Supersite Project. *J. Geophys. Res*. [Atmospheres] **2003** 108(D7).

Noble, C.A, K.A. Prather, Real-Time Single Particle Mass spectrometry: A Historical Review of a Quarter Century of the Chemical Analysis of Aerosols. *Mass Spec. Rev.* 19(4) **2000** 248-274.

Noble, C.A., K.A. Prather, Aerosol Time-of-Flight Mass Spectrometry. *Analy. Chem. Aerosols* **1999** 353-376.

Suess D.T., K.A. Prather, Mass Spectrometry of Aerosols, *Chem. Rev.* 99 **1999** 3007-3035.

Wexler, A., K.A. Prather, Introduction: Online Single Particle Analysis. *Aerosol Sci.& Technol.* **2000** 33(1-2) 1-2.

ATOFMS Applications:

Guazzotti, S. A., J.R. Whiteaker, D. Suess, K.R. Coffee, K.A. Prather, Real-Time Measurements of the Chemical Composition of Size-Resolved Particles during a Santa Ana Wind Episode, California USA. *Atmos. Environ.* 35(19) **2001** 3229-3240.

Liu, D.Y., D. Rutherford, M. Kinsey, K.A. Prather, Real-Time Monitoring of Pyrotechnically Derived Aerosol Particles in the Troposphere. *Analy. Chem.* **1997** 69(10), 1808-1814.

Liu, D.Y., R.J. Wenzel, K.A. Prather, Aerosol Time-of-Flight Mass Spectrometry during the Atlanta Supersite Experiment: 1. Measurements. *J. Geophys. Res.* [Atmospheres] **2003** 108(D7).

Prather, K., C. Noble, D. Liu, P.J. Silva, Single Particle Analysis of Transient Variations occurring in Atmospheric Aerosols. *J. Aerosol Sci.* **1998** 29(Suppl. 1, Pt. 2), S1185-S1186.

Silva, P.J, R.A. Carlin, K.A. Prather, Single Particle Analysis of Suspended Soil Dust from Southern California. *Atmos. Environ.* 34(11) **2000** 1811-1820.

Suess, D.T., K.A. Prather, Reproducibility of Single Pparticle Chemical Composition during a Heavy Duty Diesel Truck Dynamometer Study. *Aerosol Sci. & Technol.* 36(12) **2002** 1139-1141.

Wenzel, R.J., D.Y. Liu, E.S. Edgerton, K.A. Prather, Aerosol Time-of-Flight Mass Spectrometry during the Atlanta Supersite Experiment: 2. Scaling Procedures. *J. Geophys. Res.* [Atmospheres] **2003** 108(D7).

Whiteaker, J.R., K.A. Prather, K.A. Detection of Pesticide Residues on Individual Particles. *Analy. Chem.*75(1) **2003** 49-56.

For general information or information about this User's Guide, Kerry Kelly:
kelly@eng.utah.edu

References

Hinds, W.C. *Aerosol Technology*, 1 ed.; John Wiley & Sons: New York **1982**.

TSI, *Model 3800 Aerosol Time-of-Flight Mass Spectrometer Instruction Manual*, P/N 1930036. TSI Incorporated **2002**.

Dilution and Sampling

Design and selection of a dilution/sampling system is one of the most challenging problems associated with characterizing particulate matter (PM). This section highlights some important things to consider when selecting a dilution/sampling system, and it is divided into:

- Sample types
- Types of measurements
- Effects of dilution systems
- Dilution gas
- General recommendations for dilution/sampling systems
- Common systems
- Rules of thumb

What type of samples will you be collecting, ambient or source?

Sample types

If you are collecting a PM sample, the first question to ask is whether you'll be collecting a source sample or an ambient sample. For sources, your sample intake will be located directly in the exhaust, i.e., in the tailpipe of a vehicle. For ambient samples, your intake is located out of the direct exhaust of any sources. Typically, ambient samples experience much lower levels of PM than source sampling. This guide focuses on source sampling. For guidance on ambient sampling see the list of resources at the end of this section.

For source sampling, the instruments discussed in this guide (and most particle instruments) require dilution in order operate within their required ranges. Dilution with dry gas also may approximate the processes that occur naturally after exhaust particles and gases mix with ambient air. It also reduces the humidity of the sample gas and water condensation in the sample lines.

Figure 5-1 illustrates a generic dilution system. In most systems, exhaust from a source is pulled into a chamber, where it mixes with dry, clean dilution air; this mixture then flows into a sampling chamber, where particle instruments are located.

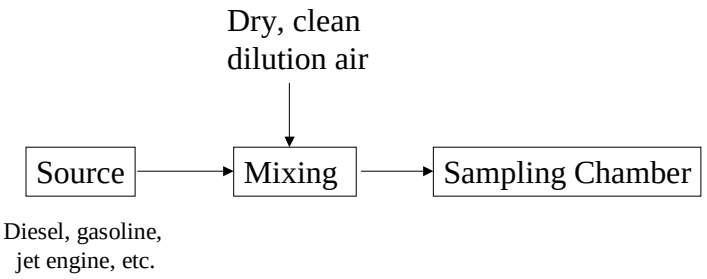

Figure 5-1. Generic dilution and sampling system.

Types of measurements

Currently, particle mass is a regulated pollutant, but interest is growing in particle number and composition. Your design and selection of a dilution/sampling system will depend on what you'd like to measure.

Do you want to measure PM mass, number, or composition?

Extensive research on the effects of dilution systems on PM shows that dilution/sampling systems typically affect particle counts for particles less than 50 nm in diameter (Maricq et al. 2001; Abdul-Khalek et al. 1999; Kittelson et al. 1999, 2000, 2002; Shi and Harrison 1999). There are two main effects. Rapid cooling can cause nucleation of droplets of sulfuric acid or hydrocarbons. These are usually in the size range of 1 nm and produce an artificially large number count. Alternatively if large numbers of particles exist in the nucleation size range, they will agglomerate with larger particles if the dilution rate is not fast enough and the number count will be artificially low. If the systems are clean and operated properly, they have little effect on particle mass or bulk composition. In other words, if you are only concerned about particle mass, selection of the dilution system is not as important as if you were concerned about particle number.

Dilution systems have the biggest effect on

Effects of the dilution systems

Recent studies have shown how dilution conditions can affect particle number concentrations, particularly for very small particles (Maricq et al. 2001; Shi and Harrison 1999; Kittelson et al. 1999, 2000; Abdul-Kahlek et al. 1999). Specifically, dilution ratio, temperature, humidity, residence time, and system configuration can dramatically affect the formation of nanoparticles, particles less than 50 nm in diameter (definition from Baumgard and Johnson 1996). However, these factors tend to have little effect on particle mass.

Humidity

As humidity of dilution air increases, the number of nanoparticles increases (Abdul-Khalek et al. 1999). Dilution air should be dry to limit this effect.

Temperature

As temperature increases, the number of nanoparticles decreases (Abdul-Khalek et al. 1999; Kittelson 2000). Ensure that the temperature is recorded.

Residence time in the dilution/sampling chamber

The effects of residence time depend upon other factors such as dilution temperature, dilution ratio, and relative humidity. If these factors are held constant, as residence time increases particle counts increase (Abdul-Khalek et al. 1999). It is possible that additional residence time allows particles that are too small to detect to grow to a detectible size (Brockhorn 1994; Gulder, 2000). Another important process in particle growth is coagulation – small particles collide and stick to each other or stick to larger particles. This causes the number of smaller particles to decrease and the number of larger particles to increase. Figure 5-2 illustrates the effect of coagulation on a particle size distribution in a bag sample. For both processes, growth of nanoparticles to a detectible size and the loss of nanoparticles through coagulation, could affect the particle number. These factors would not affect particle mass, only particle count. The Hildemann dilution system and the constant-volume dilution system have a greater residence time than eductor systems, and the bag sampling system has the longest residence time.

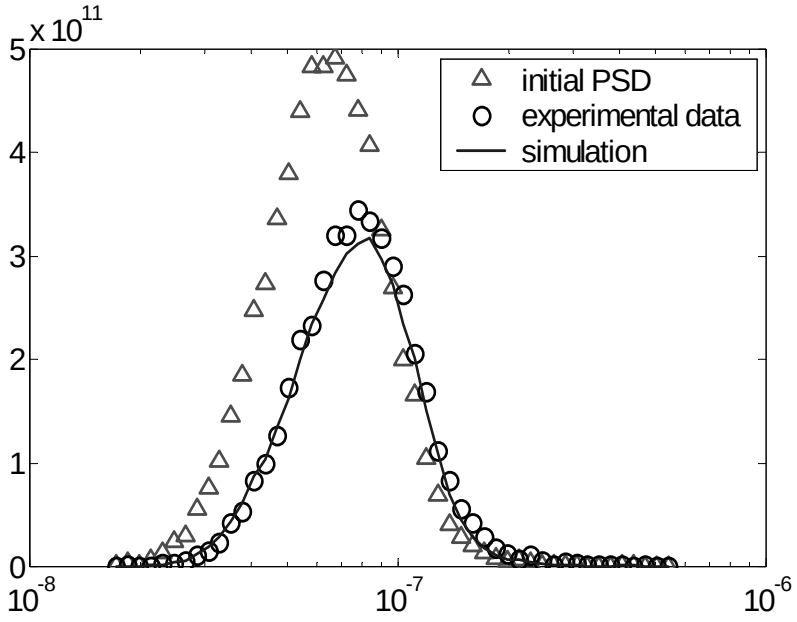

Figure 5-2. Particle size distributions in a Tedlar bag at 0.44hr and 1.24 hr, demonstrating the effect of coagulation (Jiang et al., 2002).

Dilution system configuration

PM can adhere to sampling lines, sampling chambers, and sampling bags. Maricq et al. (2001) found that transfer hoses can act as storage reservoirs for particles. This is because particles in warm exhaust gas are attracted to cold sample lines, where they can outgas at a later time. Therefore, sample lines should be as warm as or slightly warmer than the exhaust sample to prevent particles from sticking to the sample lines. In addition, sample lines should be as short as possible and replaced or cleaned often. The surface area in a sampling system should also be limited to reduce PM wall losses.

Dilution gas

Typically dilution is performed using compressed air. The compressed air or other dilution gas should be dry, particle free, and free of other contaminants, such as oil. This is accomplished by a series of traps and filters. A common compressed air clean up system includes: a spin-down water filter with a sintered nylon 20-40 μm filter element, a 0.3 μm borosilicate coalescing filter, an activated charcoal filter, and two HEPA filters. Prior to testing, it's a good idea to test the dilution air to ensure that it is clean and particle free with an optical particle counter, a scanning mobility particle sizer, or another particle measurement instrument.

General recommendations for dilution/sampling systems

Design your dilution/sampling system to limit particle deposition and re-entrainment by:

- Diluting your sample as close to the source as possible.
- Making your sample lines as short as possible and avoiding bends and sharp turns in the lines.
- Matching the temperature in your sample line to the exhaust temperature and matching your diluted exhaust temperature closely to the sampling chamber temperature.
- Replacing or cleaning your sample inlet line often.
- Frequently cleaning your sampling chamber.
- Avoiding plastic or rubber components that could collect or outgas material into the sampling system.

Control and understand your sampling conditions by:

- Carefully measuring and recording your sample and dilution flows.
- Measuring and recording the temperature of your undiluted sample, and the temperature and relative humidity of the diluted sample.
- Using clean, dry, particle free air to dilute samples.

If you want to compare your results to previous studies:

- Ensure that you use the same sampling/dilution conditions, or duplicate the sampling/ dilution conditions as close as possible.

Common systems

We'll discuss four common types of dilution systems: an eductor system, a Hildemann system with an aging chamber, a constant-volume dilution sampler, and a bag sampling system. Other types of dilution/sampling systems exist, but these four systems are the most common. They also contain important aspects of most dilution systems.

Eductor sampling system

The eductor dilution/sampling system provides rapid mixing of the exhaust sample and dilution air (Figure 5-3). An eductor sampling system consists of an eductor, with a critical orifice located on the suction inlet, and an expansion/sampling chamber where individual instrument pull samples at atmospheric pressure. The eductor (also known as an ejector) operates by introducing pressurized (motive) air into a diverging nozzle system, where the motive air rapidly expands, creating a local region of low pressure that draws the sample into the eductor. The critical orifice is a precisely machined hole, located on the suction side of the eductor, through which the sample flow is regulated. The sample flow rate through the critical orifice increases with increasing motive airflow up to the point at which the pressure upstream of the critical orifice is twice that of the pressure downstream. At this point, the velocity of the sample through the critical orifice is choked and will not increase, regardless of any further increase in the motive airflow. In this system the particulate matter spends a short time between dilution and sampling, typically on the order of seconds.

Eductor systems rapidly dilute a sample

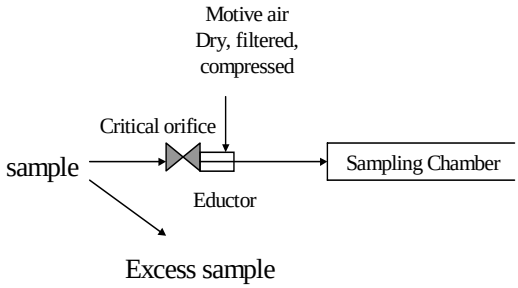

Figure 5-3. Eductor dilution system.

Advantages

1. Small, transportable, and relatively easy to set up.
2. Number counts from this type of system agree well with wind tunnel results (Maricq et al., 2001).
3. It is simpler to operate than some other systems.
4. It is relatively inexpensive to construct.

Disadvantages

1. Flows must be measured accurately.
2. The critical orifice can get clogged, so the pressure drop must be monitored continually.

Hildemann Dilution Sampler

The Hildemann system has a residence chamber

The dilution tunnel/residence chamber was originally developed by Hildemann et al. (1991) to characterize the organic components of particles at very low concentrations. The key property of this system is that particles spend a relatively long time between dilution and sampling, typically from tens of seconds to minutes, and this was designed to approximate atmospheric processes (Figure 5-4). In this sampling system, a portion of the exhaust from the source flows into a heated line and venturi flow meter. It then mixes with dilution air and flows into a residence chamber. Typical residence times range from tens of seconds to several minutes.

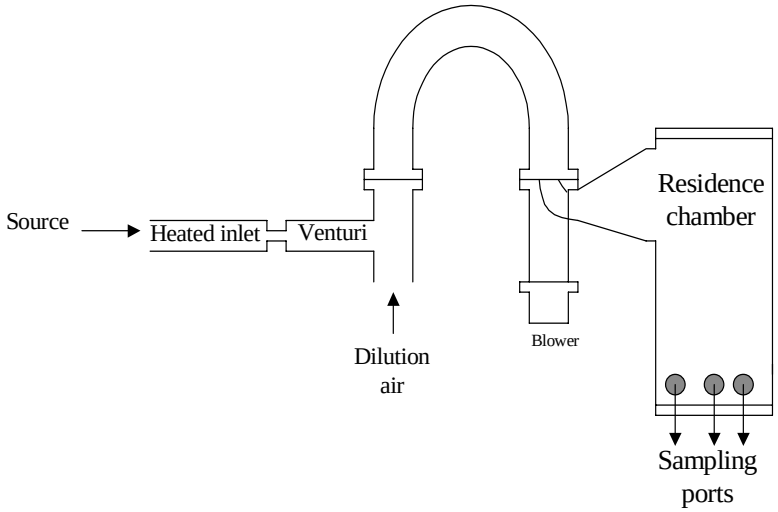

Figure 5-4. Hildemann dilution system.

Advantages

1. It provides a large volumetric flow, which is necessary for some analyses.
2. It permits complete mixing and cooling of the sample to ambient temperature.
3. The residence chamber allows particles, exhaust gas, and dilution air to reach equilibrium.

Disadvantages

1. It is large and not very portable.
2. It is time consuming to clean.
3. The long residence time can lead to the loss of nanoparticles, which coagulate to form larger particles. This would not affect particle mass but could affect particle number count.
4. The long residence time can also cause particles that are too small to detect to grow to a detectible size.
5. The system is moderately complex and must be monitored to ensure constant flows and prevent leaks.
6. It is moderately expensive to construct.

Constant-volume sampler

Constant-volume samplers are typically found in vehicle certification laboratories, and this type of sampler is required to certify vehicle emissions according to EPA regulations. These samplers provide a constant total volume of sample plus diluted air (Figure 5-5). All of the exhaust flows into the sampler. Because the quantity of exhaust emitted by a source, such as a vehicle, changes with setting (i.e., engine speed or load), the dilution rate also changes to provided a constant volume. If you need certification testing, it is best to go to an established vehicle certification laboratory.

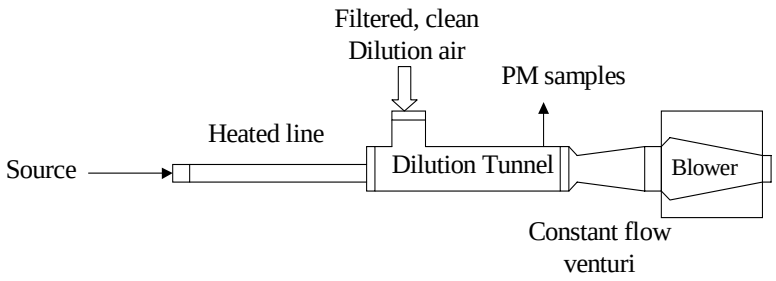

Figure 5-5. Constant-volume dilution sampler.

Advantages

A constant-volume sampler is used for vehicle certification

1. The total exhaust flow rate does not need to be measured.
2. This is the EPA certification method.
3. It easily generates emission rates for vehicles in terms of particulate matter per mile.

Disadvantages

1. This system is not very portable.
2. A different sized system is required for dramatically different sources (i.e., a passenger vehicle versus a heavy-duty diesel truck).
3. It must be operated by experienced personnel.
4. The heated line can act as a reservoir for particles.

Bag sampling system

A bag sampling system can be used to capture a known volume of sample, and the contents of the bag can then be analyzed at another time and location. This type of system is particularly useful when it is not possible to place instruments close to a source or when a source produces erratic emissions. However, a bag sampling system can cause static losses of PM to the bag's walls and changes in the particle size distribution due to coagulation. Coagulation leads to the loss of smaller particles and the growth of larger particles. Analyzing samples as rapidly as possible can reduce artifacts associated with bag sampling.

Figure 5-6 illustrates an example bag-sampling system, and these systems can be purchased commercially. A stainless steel, airtight container is fitted with a sampling bag through a clamp-down lid. A twist valve is affixed to the inlet of the sampling bag, and an actuated ball valve is placed in line with the sample inlet. A vacuum pump evacuates the space between the stainless steel container and the sampling bag. Upon opening the ball valve on the sample inlet, sample is drawn into the bag until the pressure in the bag is the same as that between the stainless steel container and the sampling bag. Once the bag is filled, the sample ball valve and twist valve are closed. After detaching the sample bag from the stainless steel container, the twist valve inlet can be connected directly to an analyzer sample inlet or to a dilution system for further analysis.

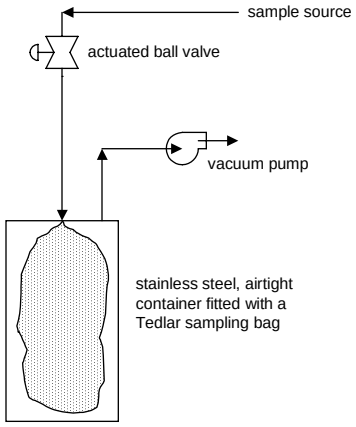

Figure 5-6. Bag sampling system.

Advantages

1. The system is small, robust, transportable, and relatively easy to set up.
2. It is relatively inexpensive to construct or purchase.
3. It provides an uniform sample, which may be necessary for some instruments.

A bag-sampler is good when instruments cannot be placed near a source

Disadvantages

1. This system can cause changes in the particle mass and size distribution. These changes are not well quantified and can include static particle losses and changes to the particle size distributions. Bags should be analyzed as rapidly as possible.
2. The dilution ratio may be difficult to determine. If you collect emissions downwind from a source, the sample will be diluted by ambient air. For combustion sources, the dilution ratio can be estimated with CO and CO_2 concentrations, but for other sources, i.e., sand blasting, the dilution ratio may be difficult to determine.
3. It will provide an aggregate sample, so variations in PM concentration or composition that occurred during the sampling interval will be lost.

A bag sampling system can cause particle loss and changes in the particle size distribution

Rules of thumb for selecting a dilution/sampling system

To summarize, we've provided some general guidelines for selecting a dilution/sampling system:

If you only want to measure particle mass from a source:

- For general use, select an eductor system.
- For vehicle certification, select a laboratory with a constant-volume sampling system.

If you want to measure particle number concentration:

- Select an eductor system.

If you want to measure particle composition:

- Select an eductor system or a Hildemann system, depending on the volume of sample required.

If you want the least expensive system:

- Select an eductor system.

If you cannot place instruments or a sampling/dilution system near a source:

- Select a bag sampling system and analyze the samples as quickly as possible.

Resources

For general information or information about this User's Guide, Kerry Kelly: kelly@eng.utah.edu

EPA's PM2.5 Monitoring Information: http://www.epa.gov/ttn/amtic/amticpm.html

EPA's Supersite Program: http://www.epa.gov/ttn/amtic/supersites.html

EPA's PM Method: http://www.epa.gov/ttn/amtic/pm.html

References

Abdul-Khalek, I.S.; D.B. Kittelson, F. Brear, The Influence of Dilution Conditions on Diesel Exhaust Particle Size Distribution Measurements, Paper 98011142, Society of Automotive Engineers, Warrendale, PA, **1999**.

Baumgard, K.J., J.H. Johnson, The Effect of Fuel and Engine Design on Diesel Exhaust Particle Size Distributions, Paper 960131, SAE International, Warrendale, PA, **1996**.

Brockhorn, H. Soot Formation in Combustion, Mechanisms, and Models, Springer Series in Chemical Physics, Springer-Verlag: Berlin **1994**, vol. 59.

Gulder, O.L. Soot Particulate Formation in Combustion, *Trans. Can. Soc. Mech.* Eng. 1999, 23, 225-240.

Hildemann, L.M., G.R. Markowski, G. Cass, Chemical Composition of Emissions from Urban Sources of Fine Organic Aerosol, *Environ. Sci. Technol*. 25 **1991**744-759.

Jiang, P., J.S. Lighty, AF. Sarofim, E.G. Eddings, 2002, Coagulation Simulation and Inference of Initial Particle Size Distributions, *Annual Meeting, American Association for Aerosol Research*.

Kittelson, D, Watts, W., Johnson, J. *Diesel Aerosol Sampling Methodology – CRC E-43*, 8/19/2002, Coordinating Research Council, http://www.crcao.com/reports/recentstudies00-02/UMN%20Final%20E-43%20Report.pdf

Kittelson, D.B., J. Johnson, W. Watts, Q. Wei, M. Drayton, D. Paulsen, Diesel Aerosol Sampling in the Atmosphere, Paper 2212, Society of Automotive Engineers, Warrendale, PA, **2000**.

Kittelson, D.B., M. Arnold, W.F. Watts, *Review of Diesel Particulate Matter Sampling Methods*, Final Report, University of Minnesota, Department of Mechanical Engineering, Center for Diesel Research, Minneapolis, MN, **1999**.

Maricq, M.M.; Chase, R.E.; Xu, N. A Comparison of Tailpipe, Dilution Tunnel, and Wind Tunnel Data in Measuring Motor Vehicle PM, *J. Air Waste & Man. Assoc.* 51 **2001** 1529-1537.

Shi, J.P.; Harrison, R.M. Investigation of Ultrafine Particle Formation during Diesel Exhaust Dilution. *Environ. Sci. Technol.* 33 **1999** 3730-3736.

APPENDIX 2:

EVALUATION OF 1047 NM PHOTOACOUSTIC INSTRUMENTS AND PHOTOELECTRIC AEROSOL SENSORS IN SOURCE-SAMPLING OF BLACK CARBON AEROSOL AND PARTICLE BOUND PAH'S FROM GASOLINE AND DIESEL POWERED VEHICLES

Evaluation of 1047 nm photoacoustic instruments and photoelectric aerosol sensors in source-sampling of black carbon aerosol and particle bound PAH's from gasoline and diesel powered vehicles.

by

W. P. Arnott, B. Zielinska, C. F. Rogers, and J. Sagebiel; Desert Research Institute, Reno Nevada

K. Kelly, D. Wagner, A. Sarofim, and J. Lighty; University of Utah, Salt Lake City UT.

G. Palmer, Hill Air Force Base, Ogden UT.

ABSTRACT

A series of measurements have been performed at Hill Air Force Base to evaluate instruments that provide continuous measurements of black carbon aerosol and particle bound PAH's emitted from military vehicles. During the first series, gasoline and diesel powered vehicles were operated at idle or fast idle, though they were placed under load on a dynamometer during the second series. Photoacoustic instruments were developed that operated at a wavelength of 1047 nm where gaseous interference is not a problem, though sensitivity to black carbon is good. Compact, efficient, solid-state lasers with direct electronic modulation capability are used in these instruments. Black carbon measurements are compared with samples collected on quartz fiber filters that were evaluated using the thermal optical reflectance method. A measure of total particle-bound PAH was provided by photoelectric aerosol sensors (PAS) and is evaluated against a sum of PAH mass concentrations obtained with a filter-denuder combination. The photoacoustic instrument (PA) withstood the vigors of the field environment quite well, and provided sensitive measurement of black carbon mass concentration that agrees acceptably with thermal optical reflectance measurements of elemental carbon. The PAS had to be operated with

a dilution system held at approximately 150 C for most of the source-sampling to prevent spurious behavior, thus perhaps compromising detection of lighter PAH's. PA and PAS measurements were found to have a high degree of correlation, perhaps suggesting that the PAS can respond to the polycyclic nature of the black carbon aerosol, and perhaps that the detected particle-bound PAH's are produced in proportion, and are adsorbed to, the black carbon aerosol.

Introduction

Quantification of black carbon aerosol is important for both health and for the Earth's radiation balance (Andreae 2001; Lighty, Veranth et al. 2001) so the accurate, rapid assessment of these aerosols is needed, both in direct analysis of source emissions as well as in cities or remote locations. Black carbon aerosol is produced by combustion of fossil fuels and biomass with regional emissions being of sufficient magnitude to cause disruptions of atmospheric heatings and possibly large scale perturbations of the Earth's hydrological cycles (Ramanathan and Crutzen 2003). Historical trends point towards increasing levels of BC production (Novakov, Ramanathan et al. 2003). It is unhealthy to breath the polycyclic aromatic hydrocarbons that may exist in the vapor phase, may be absorbed in liquid phase aerosol, or may be adsorbed to the surface of black carbon aerosol (Mader and Pankow 2002; Naumova, Eisenreich et al. 2002; Naumova, Offenberg et al. 2003; Pankow 2003; Zielinska, Sagebiel et al. 2003). PAHs as a group are reasonably anticipated to be carcinogenic (NTP 2003), and a few individual PAHs, such as benz[a]anthracene and benzo[a]pyrene, are probably carcinogenic (IARC 2003). Diesel exhaust has also been linked with allergic inflammation (Nel, Diaz-Sanchez et al. 1998). This paper provides an assessment of real time instruments for measurement of BC and particle-bound PAH's for use in sampling combustion sources.

Methods for quantifying black carbon mass concentration can be divided into two categories; those that do and do not require a filter substrate. Examples of filter-based techniques include both thermal and optical methods, and both laboratory and real-time instruments exist for each. Thermal methods start with the collection of aerosol on a filter, followed by measurement of the carbon atoms evolved when the filter is heated, with elemental carbon being defined as the carbon mass observed in some temperature range. Filter-based optical methods measure the optical attenuation across a filter as aerosol are deposited, and exploit the observation that most particulate light absorption in the atmosphere is due to thusly defined black carbon aerosol. Accurate mass flow meters are vital for quantifying the volume of air sampled to obtain the observed aerosol accumulation on a filter. Filter methods have limitations with respect to dynamic range, lack of a common definition of elemental carbon, and scattering aerosol interferences in the black carbon measurement (Horvath 1997). Photoacoustic instruments also are used to measure BC and they overcome deficiencies of the filter-based sampling methods.

The photoelectric aerosol sensor (PAS) utilizes an ultraviolet lamp to ionize particles containing PAH's. The charged particles are collected on a filter and the charge is measured with an electrometer. The PAS signal was originally correlated to seventeen individual PAHs from several sources, with a universal conversion factor of 1-3 ng m^{-3} $femtoamp^{-1}$ (Wilson and Chuang 1991; Wilson and Barbour 1994; EPA 1997). Because PAH's are such a complex mix of vapor and particle-phase compounds, the PAS responds differently to each type of source, and the sensitivity varies in comparison to extractive methods (Agnesod, Maria et al. 1996). Furthermore, independent evaluations of the PAS are limited, and investigators report widely varying conversion factors (EPA 1997; Chuang, Callahan et al. 1999; Chetwittayachan,

Shimazaki et al. 2002). A chronicle is provided in this paper of the efforts employed to successfully use the PAS in source sampling, as well as a comparison of results from the PAS as compared to with measurements from a filter and denuder sampler followed by extraction and laboratory quantification of individual PAH's. Excellent correlation is found between BC and PAS measurements raising the issue, does the PAS respond to the polycyclic nature of the black carbon aerosol? This question takes on particular relevance since the laboratory extractions of PAH's showed only a weak correlation with BC (Zielinska, Sagebiel et al. 2003). The tubing inlet for the had to be heated to approximately 150 C to remove offending species, and, in the process, may have also greatly affected the gas to particle phase partition.

Photoacoustic Measurements of Aerosol Light Absorption and the Definition of Black Carbon

Photoacoustic instruments have been used in source sampling of black carbon aerosol. Sample air is pulled continuously through an acoustical resonator and is illuminated by laser light that is periodically modulated at the acoustical resonance frequency. Light absorption is manifested in particle heating and this heat transfers rapidly to the surrounding air, inducing pressure fluctuations that are picked up with a microphone on the resonator. Microphones have a very large dynamic range (at least 6 orders of magnitude), so black carbon measurements can be made over a large dynamic range with these instruments. The advancement that has been very important for the continued success of these instruments is the ability to measure very low levels of light absorption. Incidently, aerosol light absorption occurs throughout the entire particle volume for combustion particles, so black carbon aerosol mass concentration is found to vary in direct proportion with light absorption. Vehicle manufactures pursued these methods in the 1970's and 1980's using bulky Argon Ion lasers and dye lasers (Terhune and Anderson 1977;

Japar and Killinger 1979; Japar and Szkarlat 1981; Japar and Szkarlat 1981; Japar, Szkarlat et al. 1984; Roessler 1984), and a resurgence of interest has emerged in research laboratories that coincides with technological developments in compact, efficient laser sources (Petzold and Niessner 1994; Petzold and Niessner 1995; Arnott, Moosmüller et al. 1999; Moosmüller, Arnott et al. 2001).

The photoacoustic instrument developed for this work operates at a convenient wavelength of 1047 nm where gaseous interference is not a problem and where a laser source is available that allows for direct electronic modulation of the power at the resonator frequency. Figure 1 shows calculated light absorption for a standard atmosphere containing only gases, for it is gaseous interference that could potentially limit black carbon particle detection. Figure 1a shows that a number of micro-windows are available where relative minima of gaseous absorption occur. Figure 1b shows details around a commonly used wavelength of 532 nm. The chief interfering gas at this wavelength is NO_2, giving rise for a need to denude this common combustion gas for practical applications (Adams, Japar et al. 1986). Figure 1c shows that the laser wavelength of 1047 nm is ideal because of the relatively broad range over which gaseous interference is a minimum. NO_2 is not an interferent at 1047 nm, but can be useful in cross-calibrating instruments (Arnott, Moosmüller et al. 2000).

The acoustical resonator, shown schematically in Fig. 2, was designed for compactness, ease of reproducibility in manufacture, and robustness with respect to use of the instrument in very noisy, dirty sampling environments. . The instrument comprises two identical coupling sections, and a third resonator section. These parts are manufactured out of aluminum. The coupling sections allow the laser beam to enter the instrument through windows well separated from the resonator section. The sample inlets and outlets are followed by cavities that are tuned

to reduce the coupling of noise into the resonator section. The resonator section has a horizontal tube that is 1/2 of an acoustic wavelength long, and two vertical tubes that are 1/4 of an acoustic wavelength long. In previous designs (Arnott, Moosmüller et al. 1999), the vertical tubes were at an angle of 45 degrees to the horizontal instead of 90 degrees as they are now, and the tubes were formed from pipe rather than machined with precision. The 90 degrees angles allow for symmetry when deciding where the holes in the resonator are placed to allow for laser beam and sample air passage. The piezoelectric transducer is used as a sound source to occasionally scan the resonator resonance frequency and quality factor for use in calibrating the instrument from an acoustical perspective. The microphone and piezoelectric transducer sit at pressure antinodes of the acoustic standing wave, and the holes in the resonator are at pressure nodes. The instrument is bolted together in three parts for easy disassembly in case it needs to be cleaned. The laser beam passes through the windows and the holes in the resonator section. The laser beam pumps the acoustic wave through light absorption, and the transfer of the associated heat to the surrounding air, in the resonator section.

The truth of the matter is that the photoacoustic instrument measures the aerosol light absorption coefficient (Arnott, Moosmüller et al. 1999; Arnott, Moosmüller et al. 2000), and then a quantity defined as black carbon (BC) is computed from the absorption coefficient. The 'elemental' carbon (EC) part of the exhaust absorbs light at 1047 nm much more strongly than any other common particulate aerosol in exhaust and in the atmosphere so that it is reasonable to associate elemental carbon with aerosol light absorption. Why is it reasonable to associate aerosol light absorption with a black carbon mass concentration (BC)? Because aerosol light absorption occurs throughout the entire particle volume, giving rise to a direct proportionality between the absorption measurement and the aerosol mass. It is perhaps inevitable to speculate

that the aerosol complex refractive index could vary with combustion source [(Dalzell and Sarofim 1969) (Fuller, Malm et al. 1999), so that the black carbon measured values could be different for particles actually having the same numbers of carbon atoms in them. And it is possible to postulate that aerosol coatings or adsorbents, or particle morphology, could also give rise to different absorption coefficients than one would observe for uncoated particles.

Experiences to date have shown that for an emission source such as a late model diesel that is rich in EC, the Improve protocol method of quantifying EC (Chow, Watson et al. 1993) correlates well with the aeorsol light absorption measurement at 1047 nm. Figure 3 shows comparisons of aerosol light absorption at 1047 nm with EC and organic carbon (OC) from data acquired on quartz fiber filters and analyzed by the thermal optical reflectance method, Improve protocol. The vehicles were operated at idle or advanced idle with no load (Rogers, Sagebiel et al. 2003). Note the good correlation EC with BC (Fig. 3a), and the relatively poor correlation of OC with BC (Fig. 3b). The offset between EC and BC measurements is negligible, but is substantial between BC and OC. The lack of offset in the EC case indicates that the photoacoustic instrument has a negligible response to the various exhaust gases. The EC to total carbon ratio ranged from 0.1 to 0.4, and yet no systematic influence was seen on the correlation of BC with EC, addressing at least in a cursory manner the issues of particle coatings and refractive index variations. The photoacoustic instrument used for this work in 1999 was not actually the one shown schematically in Fig. 2, but was a previous prototype that was modified to allow use with the 1047 nm laser (Arnott, Moosmüller et al. 1999). The data in Fig. 3a) gave the impetus to accept the 1047 nm laser operation as ideal, and to move forward with the improved resonator design shown in Fig. 2. The prototype resonator was operated at both its fundamental acoustic frequency of 500 Hz, and in exploration of the noise reduction potential at

the next available harmonic at 1500 Hz, even though the resonator coupling efficiency at the higher frequency is only 1/3 of its value at 500 Hz. A significant reduction in effects of ambient noise were noted in the 1500 Hz operation, and so the resonator design shown in Fig. 3 was made with dimensions essentially 1/3 those of the prototype so that it operates in its fundamental mode of 1500 Hz.

From this point forward, the following relationship was used to obtain black carbon concentration from the aerosol light absorption measurement at 1047 nm:

$$BC\ (\mu g\ m^{-3}) = 5\ (m^2\ g^{-1})\ B_{abs}\ (Mm^{-1})\ [\text{measured at 1047 nm}]\ . \quad (1)$$

Most of the consequential data in Fig. 3 represents diesel emissions. EC from diesels provide a relatively unambiguous measurement from the various protocols and methods that have been developed though ambient and wood smoke samples have substantial differences (Watson, Chow et al. 1994; Chow, Watson et al. 2001). For these reasons it is good to use diesel emissions as a starting point to establish essentially an EC standard, and to use the BC measurement by the photoacoustic method as a standard for other types of sources.

BC and EC measurements for gasoline and diesel vehicles used in ground support at Hill Air Force Base were obtained in 2000 (Kelly, Wagner et al. 2003), and are shown in Fig. 4. The EC fraction ranged from 2.5% to 35% of the total carbon in these measurements, and the vehicle engine load ranged from idle to 93%. The photoacoustic instrument used in these measurements is the one shown schematically in Fig. 2. This time the EC measurements were made on the aluminum substrates used in a Moudi sequential analyzer. TOR analysis for these substates simply skips the pyrolysis correction stage and moves directly from OC4 to EC1. Most EC from diesel sources is contained in the EC2 phase (Watson, Chow et al. 1994) so the pyrolysis correction is not so important to the data shown in Fig. 4. It should be noted that the EC from

Moudi analysis correlated well with that obtained in by the quartz filter analysis for the data shown in Fig. 3; however, the quartz filter sampler had a leak in the 2000 SERDP experiment.

The Photoelectric Aerosol Sensor

The photoelectric aerosol sensor 2000 (PAS2000 EcoChem Messtechnik GmbH) qualitatively measures the concentration of particle-bound polycyclic aromatic hydrocarbons (pPAHs). Figure 5 shows a schematic of the PAS, and additional instrument details can be found in (EPA 1997) and (Burtscher 1992) and in (Burtscher and Siegmann 1994). Briefly, the PAS uses a KrCl excimer lamp operating at 222 nm as a photoionization source; the photon energy of the lamp is chosen so that gas-phase molecules are negligibly ionized. Samples flow continuously into the eximer-lamp ionization region, where particle-bound PAH molecules are ionized and lose an electron. The positively charged particles collect on a filter where charge is measured with an electrometer. The charge is integrated over time to give the photoelectric current (in femto- or picoamps), and this current should be proportional to the PAH loading on particles.

During the course of this study, temperature and exhaust concentration were identified as important factors governing the response and reproducibility of PAS readings. Other studies found little effect from temperature or humidity (EPA, 1997; Dubowsky et al., 1999; Lee et al., 1999); however, these studies focused on indoor air, ambient samples, or cigarette smoke and thus lower pPAH concentrations. For sampling exhaust from vehicles or aircraft, a PAS inlet temperature of at least 120 C produced more stable results than lower inlet temperatures. Even with dilution, it is possible that vehicles and aircraft contain enough vapor-phase hydrocarbons and water vapor in their exhaust to condense inside the PAS and produce erratic results, as illustrated for example in Fig. 6 data from the 1999 SERDP project (Rogers, Sagebiel et al.

2003). In addition, exposing the PAS directly to undiluted exhaust caused spurious negative signals. In order to maintain stable PAS readings during this study, the PAS inlet was heated to a constant temperature 150 C; the exhaust was diluted with dry, particle-free air; and the PAS response was generally maintained in the femtoamp range.

Figure 7 shows the times series of emissions from a FA18a jet aircraft obtained with the PAS and PA. The aircraft was in for repairs at the Navy base on North Island, San Diego CA, and an eductor system was used to dilute the exhaust with a dilution ratio of about 1:15. The aircraft was brought from idle to 80% of full power. Exhaust emissions become more diluted by ambient air as the aircraft power setting increases. Note that the PAS curve is everywhere positive, and at times, matches the form of the BC curve quite well. Of course it is not expected necessarily that the PAS and BC curves should be in 1:1 correspondence, as the PAH emission rate may be different than that of the BC. Also note that Fig. 7 shows that the photoacoustic instrument can provide useful data even in a very loud environment.

Figure 8 shows measurements of emissions from gasoline and diesel vehicles from SERDP 2000 (Kelly, Wagner et al. 2003). Two PAS instruments were used, with one behind the DRI dilution system (described in (Rogers, Sagebiel et al. 2003), and one behind the so-called Matter dilution system (Hueglin, Scherrer et al. 1997). The Matter dilution system samples directly from the tail pipe. Note that in both cases, Figs. 8a) and 8b), the correlation of PAS signals with BC measurements is quite high, perhaps suggesting that PAH production is correlated highly with BC production, and/or that the PAS responds directly to BC. It could also be that the need to operate the PAS with an inlet at 150 C favors PAH's being in the vapor phase.

However, extractive measurements of PAH's do not show a strong correlation of black carbon with the ratio of particle to gas phase concentrations of pyrene and fluoranthene for the

vehicles whose emission is reported in Fig. 8 (Zielinska, Sagebiel et al. 2003). The so-called Seigmann sum of particle-bound PAH's are shown in Figs. 8c and 8d against BC and the PAS, respectively. Note in Fig. 8c) that the data tends to clump into two super data points, and the wide spread of values at the low end, likely due to the uncertainly in the PAH measurement as well as due to the variations of emissions from different sources. The substantial offset is perhaps suggestive that the particle bound PAH's are not exclusively associated with BC. Note that the slope of the linear curve fit implies around 1.25 ng of particle-bound PAH produced per 1 ug of BC. A ratio of around 1 (and for gasoline vehicles, 3) ng particle-bound PAH per ug BC can be calculated from the tunnel study data reported in (Miguel, Kirchstetter et al. 1998).

The PAS versus extractive PAH measurements are shown in Fig. 8d. The data clumping is not as severe as in Fig. 8c), and the correlation is modest. The slope of the curve, 0.11 ng m^{-3} / femtoamp is consistent with values found in an ambient study in Italy where traffic and meteorological inversions contributed to the observed levels of air pollutants. Some fraction of the pPAH is absorbed into the organic carbon particulate in the exhaust, particularly the lower molecular weight higher vapor pressure molecules; not all pPAH is adsorbed to the surface of elemental carbon aerosol (Allen, Sarofim et al. 1997). Much of the organic carbon fraction may be volatized by the use of the 150 C inlet on the PAS necessary to avoid negative signals such as those shown in Fig. 6. These negative signals may be due to charge separation occurring during evaporation of relatively volatile aerosol from the PAS filter, just as happens with water droplets in the atmosphere (Dong and Hallett 1992). PPAH's adsorbed or absorbed in a film thicker than a single molecular level would very likely have their charge separation from the UV lamp quenched so as not to contribute to the PAS signal anyway (Burtscher and Siegmann 1994). From the outstanding correlation of PAS and BC measurements as shown in Figs. 8a and 8b, it is

to be concluded that the PAS responds to pPAH's that are produced in combustion at the same rate as BC, or that a good portion of the PAS response can be to the BC itself.

Acknowledgments

This research was supported by the Strategic Environmental Research and Development Program, Project CP-1106. We thank Bob Armstrong of HAFB for his assistance with the vehicles; John Walker of DRI for his assistance with some mechanical aspects of the photoacoustic instrument design; and Hans Moosmüller of DRI for conversations concerning the choice of laser wavelength to use for the photoacoustic instrument. James B. Griffin, Jacob D. McDonald, and Dana Overacker contributed to the conduct of the first SERDP experiment in 1999, and thus to the laying of the groundwork for what was to follow in subsequent experiments.

FIGURES

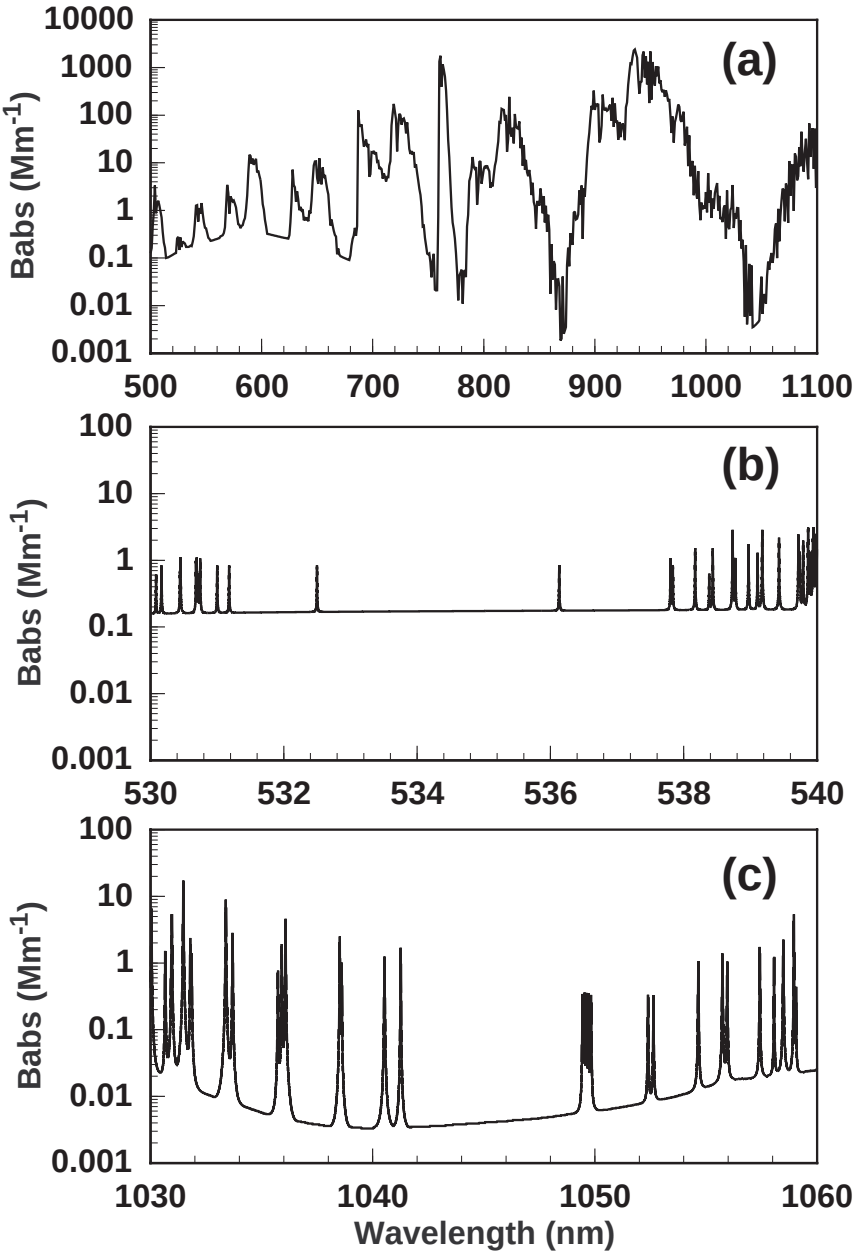

Figure 1. Calculation of light absorption by gases in a standard atmosphere for most of the visible and near IR spectrum (a), and near wavelengths where convenient laser sources are available at 532 nm (b), and 1047 nm (c). Note that gaseous interference is especially low at 1047 nm. The main interfering gas at 532 nm is NO_2, a common gas produced in combustion.

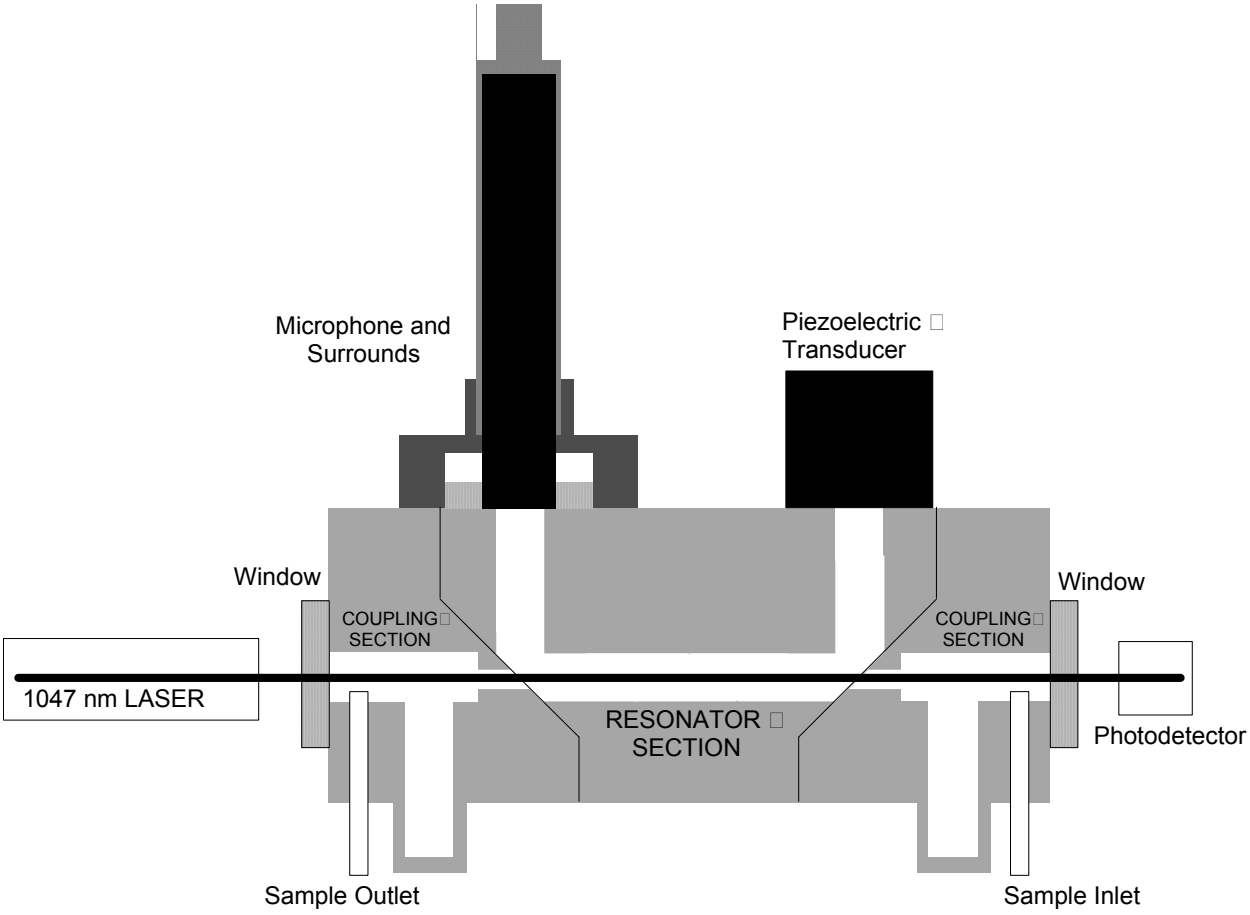

Figure 2. Schematic representation of the new acoustical resonator used in the photoacoustic instrument.

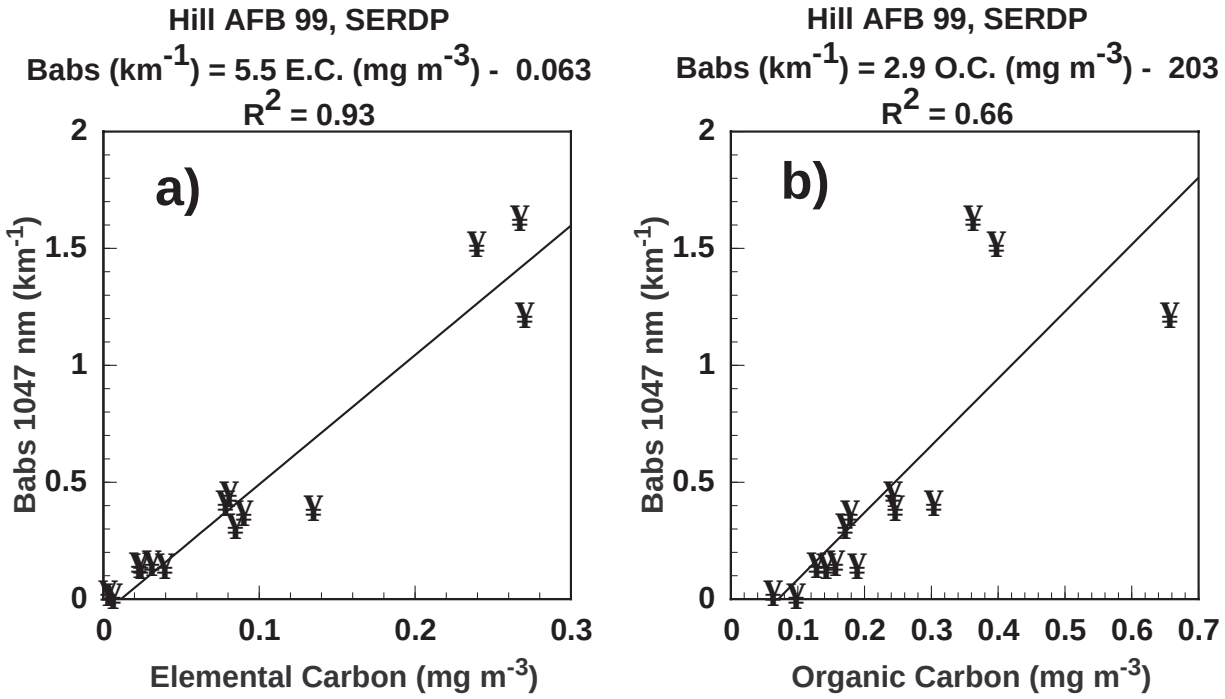

Figure 3. Aerosol light absorption measurements for gasoline and diesel vehicles at Hill Air Force Base. Comparison with elemental and organic carbon measurements are shown in a) and b) respectively. The two left most data points on each figure are from gasoline vehicles. Vehicles were either idling or were elevated idling, and were not under any other load.

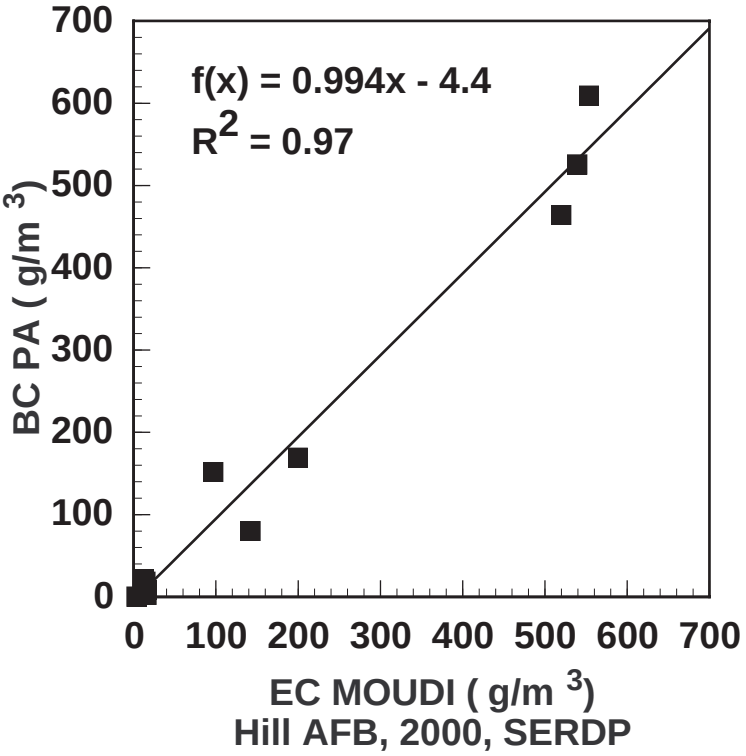

Figure 4. Black carbon and elemental carbon measurements for gasoline and diesel vehicles operated under load. The gasoline vehicles were particularly clean, and provided the left most data points. These measurements were made using the photoacoustic instrument shown schematically in Fig. 2.

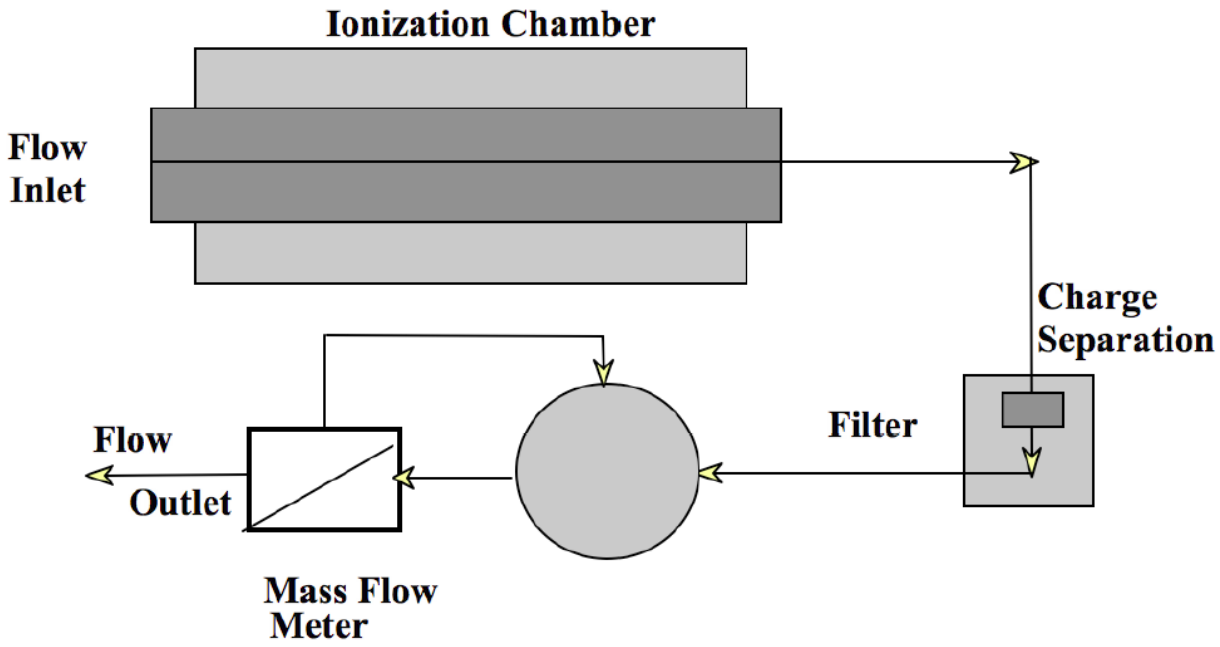

Figure 5. Schematic of the photoelectric aerosol sensor (PAS).

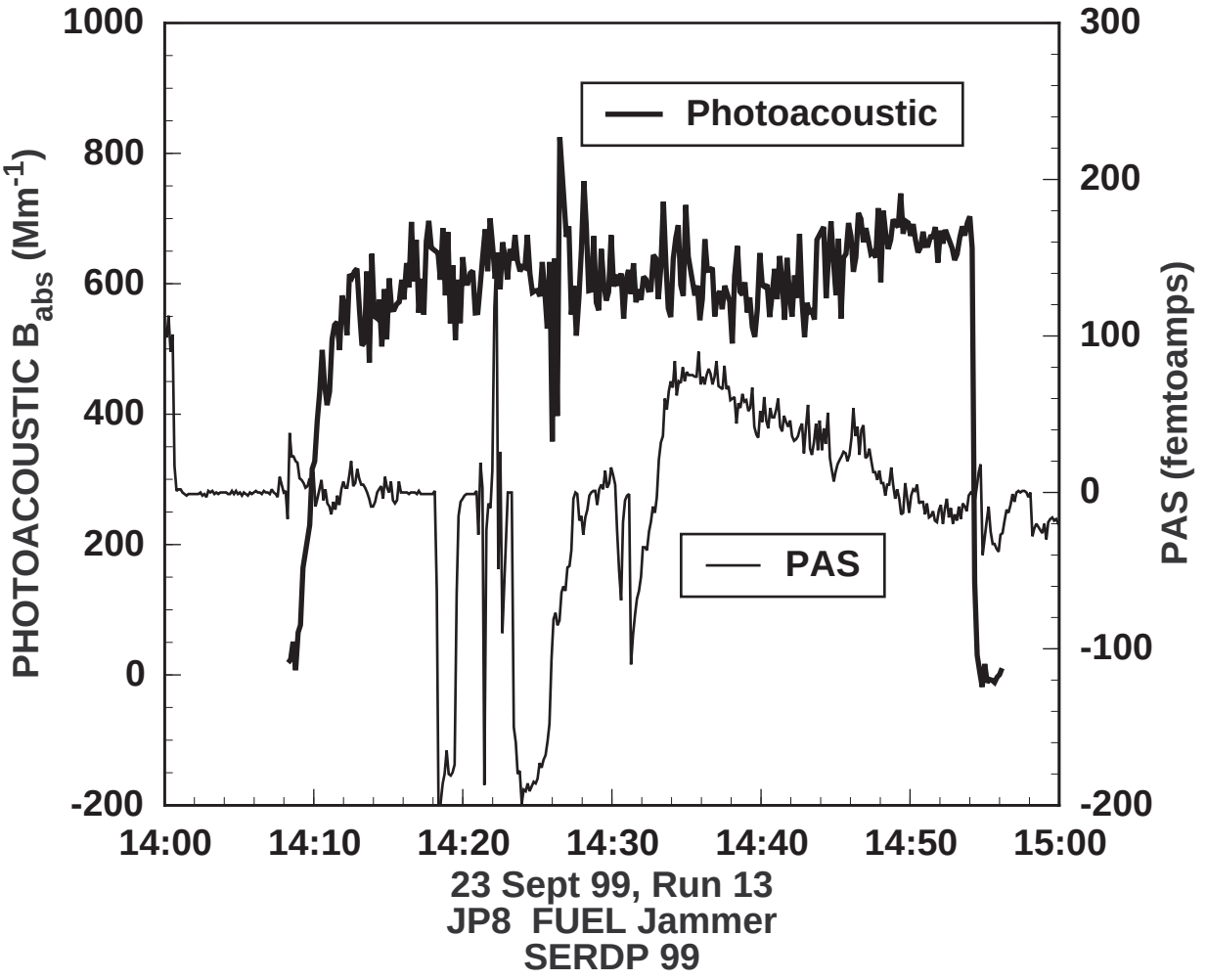

Figure 6. Time series showing aerosol light absorption on the left axis and photoelectric aerosol sensor current on the right axis, for a 'Jammer' vehicle operated on JP8 fuel. Note the substantial periods when the PAS signal is negative, and the perhaps unexpected decay of the PAS signal around time 14:40. This is a typical series for the PAS before the instrument was thoroughly cleaned, and before the PAS inlet was heated to 150 C.

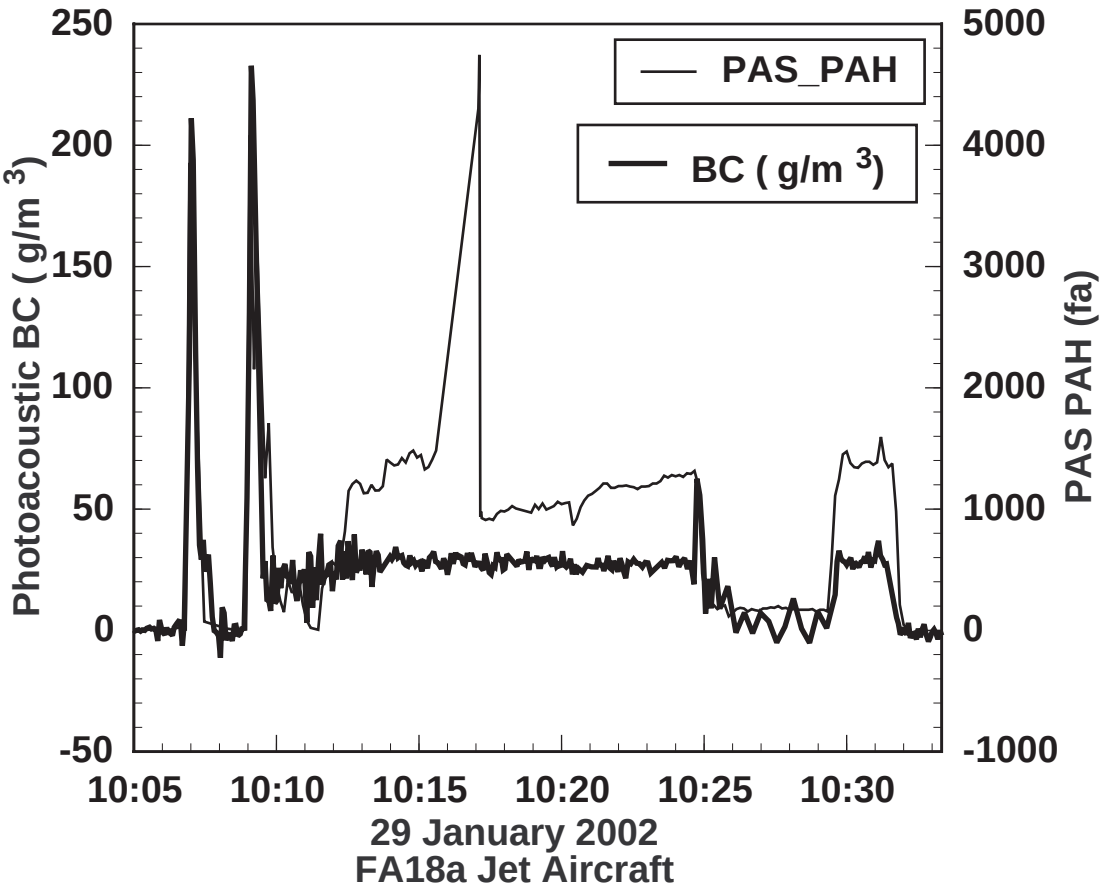

Figure 7. Time series for photoacoustic black carbon and photoelectric aerosol sensor measurements from a tethered FA18a jet aircraft under variable load. Curves nearly overlap after crank-up, between 10:05 and 10:10. The time interval 10:25 – 10:30 had the greatest load (80% full power) and lowest emission concentrations, as the aircraft was pulling in more dilution air at this time. Data is from SERDP 2002.

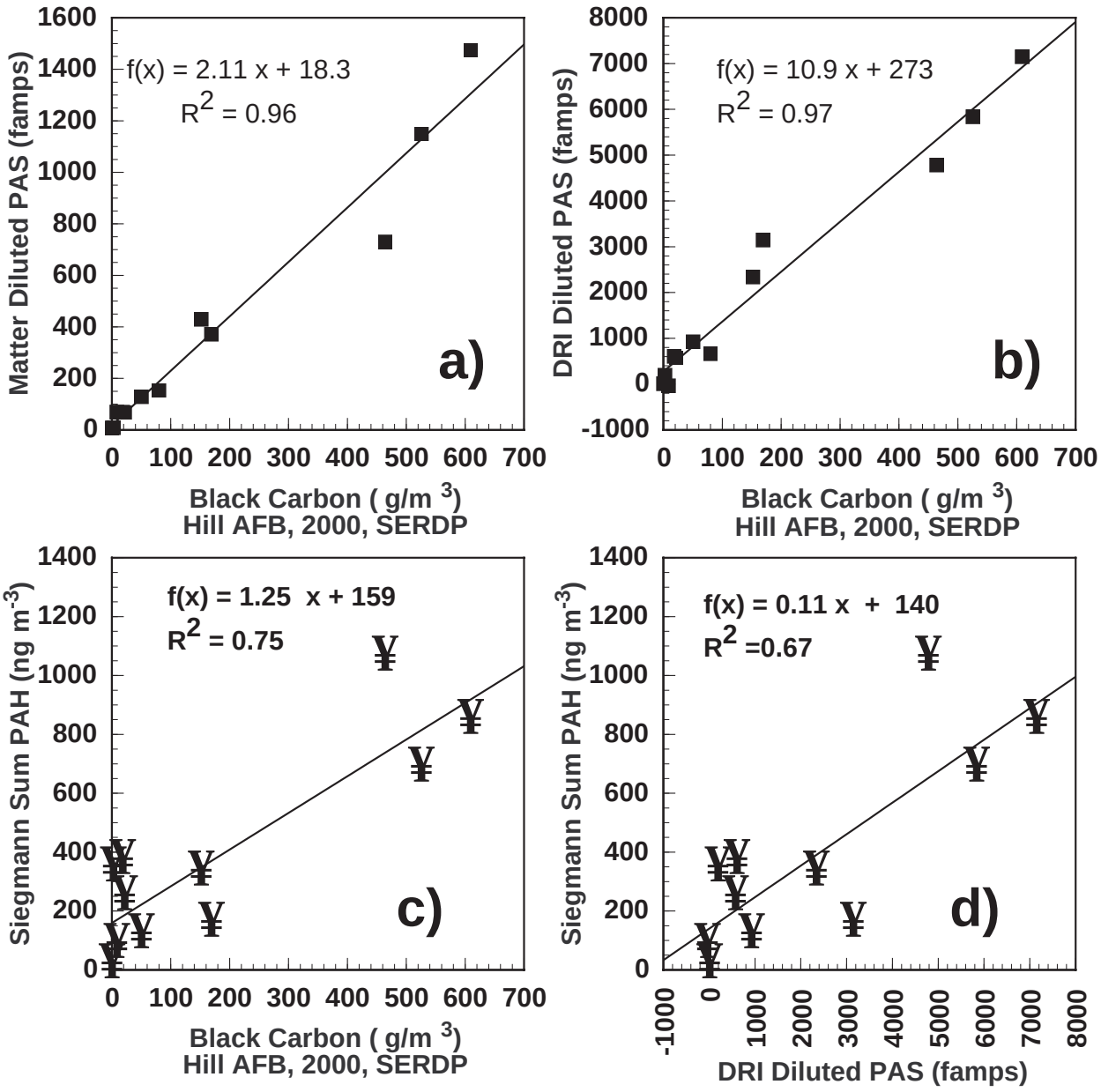

Figure 8. Scatter plot of black carbon and PAS measurements of emissions from gasoline and diesel vehicles during SERDP 2000. In a), PAS sampled behind the so-called Matter dilution system, and in b), a second PAS sampled behind the DRI dilution tunnel. In both cases the BC measurements were obtained behind the DRI dilution tunnel. Note the high degree of correlation of PAS and BC data. Extractive PAH's are shown in c) and d) against BC and the PAS. Linear regressions in c) and d) are subject to substantial data clumping around the lowest and highest values, and to the uncertainty in the PAH measurements. Particle-bound PAH blanks were around 30 ng m^{-3}, and can be viewed as one measure of the uncertainty in the PAH measurement.

References

Adams, K. M., S. M. Japar and W. R. Pierson (1986). "Development of a MnO_2-Coated, Cylindrical Denuder for Removing NO_2 from Atmospheric Samples." Atmospheric Environment **20**(6): 1211-1215.

Agnesod, G., R. D. Maria, M. Fontana and M. Zublena (1996). "Determination of PAH in airborne particulate: Comparison between off-line sampling techniques and an automatic analyser based on a photoelectric aerosol sensor." The Science of the total environment **189-190**: 443-449.

Allen, J. O., A. F. Sarofim and K. A. Smith (1997). "A critical evaluation of two proposed atmospheric partitioning mechanisms, adsorption and absorption, using atmospheric data for polycyclic aromatic hydrocarbons." Journal of Aerosol Science **28**: S335-S336.

Andreae, M. O. (2001). "The dark side of aerosols." Nature **409**: 671-672.

Arnott, W. P., H. Moosmüller, C. F. Rogers, T. Jin and R. Bruch (1999). "Photoacoustic spectrometer for measuring light absorption by aerosols: Instrument description." Atmospheric Environment **33**: 2845-2852.

Arnott, W. P., H. Moosmüller and J. W. Walker (2000). "Nitrogen dioxide and kerosene-flame soot calibration of photoacoustic instruments for measurement of light absorption by aerosols." Review of Scientific Instruments **71**(7): 4545-4552.

Burtscher, H. (1992). "Measurement and characteristics of combustion aerosols with special consideration of photoelectric charging and charging by flame ions." J. Aerosol Science **23**(6): 549-595.

Burtscher, H. and H. C. Siegmann (1994). "Monitoring PAH-Emissions from combustion processes by photoelectric charging." Combustion Science and Technology **101**: 327-332.

Chetwittayachan, T., D. Shimazaki and K. Yamamoto (2002). "A comparison of temporal variation of particle-bound polycyclic aromatic hydrocarbons (pPAHs) concentration in different urban environments: Tokyo, Japan, and Bangkok, Thailand." Atmospheric Environment **36**: 2027-2037.

Chow, J., J. Watson, D. Crow, D. Lowenthal and T. Merrifield (2001). "Comparison of IMPROVE and NIOSH Carbon Measurements." Aerosol Science and Technology **34**(1): 23-34.

Chow, J. C., J. G. Watson, L. C. Pritchett, W. R. Pierson, C. A. Frazier and R. G. Purcell (1993). "The DRI thermal/optical reflectance carbon analysis system: Description, evaluation and applications in U.S. air quality studies." Atmospheric Environment **27A**: 1185-1201.

Chuang, J. C., P. J. Callahan, C. W. Lyu and N. K. Wilson (1999). "Polycyclic aromatic hydrocarbon exposures of children in low-income families." J. Exposure Analysis and Environ. Epid. **2**: 85-98.

Dalzell, W. H. and A. F. Sarofim (1969). "Optical constants of soot and their application to heat flux calculations." Journal of Heat Transfer: 100-104.

Dong, Y. and J. Hallett (1992). "Charge Separation by Ice and Water Drops During Growth and Evaporation." Journal of geophysical research **97**(D18): 20,361.

EPA (1997). Field and Laboratory Analyses of a Real-Time PAH Analyzer, EPA Office of Research and Development.

Fuller, K. A., W. C. Malm and S. M. Kreidenweis (1999). "Effects of mixing on extinction by carbonaceous particles." Journal of geophysical research **104**(D13): 15941-15954.
Horvath, H. (1997). "Systematic deviations of light absorption measurements by filter transmission methods." Journal of Aerosol Science **28**: S55-S56.
Hueglin, C., L. Scherrer and H. Burtscher (1997). "An accurate, continuously adjustable dilution system (1:10 to 1:10^4) for submicron aerosols." Journal of aerosol science **28**(6): 1049-1055.
IARC (2003). International Agency for Research on Cancer.
Japar, S. M. and D. K. Killinger (1979). "Photoacoustic and absorption spectrum of airborne carbon particulate using a tunable dye laser." Chemical Physics Letters **66**: 207-209.
Japar, S. M. and A. C. Szkarlat (1981). "Measurement of Diesel Vehicle Exhaust Particulate Using Photoacoustic Spectroscopy." Combustion Science and Technology **24**: 215-219.
Japar, S. M. and A. C. Szkarlat (1981). Real-time measurements of diesel vehicle exhaust particulate using photoacoustic spectroscopy and total light extinction. Fuels and Lubricants Meeting, Tulsa OK, SAE.
Japar, S. M., A. C. Szkarlat and W. R. Pierson (1984). "The determination of the optical properties of airborne particle emissions from diesel vehicles." The Science of the Total Environment **36**: 121-130.
Kelly, K. E., D. A. Wagner, J. S. Lighty, A. F. Sarofim, C. F. Rogers, J. Sagebiel, B. Zielinska, W. P. Arnotl and G. Palmer (2003). "Characterization of Exhaust Particles from Military Vehicles Fueled with Diesel, Gasoline, and JP-8." Journal of the Air & Waste Management Association **53**(3): 273-282.
Lighty, J. S., J. M. Veranth and A. F. Sarofim (2001). "Combustion aerosols: Factors governing their size and composition and implications to human health." Journal of Air and Waste Management Association **50**: 1565-1618.
Mader, B. T. and J. F. Pankow (2002). "Study of the Effects of Particle-Phase Carbon on the Gas/Particle Partitioning of Semivolatile Organic Compounds in the Atmosphere Using Controlled Field Experiments." Environmental science & technology **36**(23): 11.
Miguel, A. H., T. W. Kirchstetter, R. A. Harley and S. V. Hering (1998). "On-Road Emissions of Particulate Polycyclic Aromatic Hydrocarbons and Black Carbon from Gasoline and Diesel Vehicles." Environmental science & technology **32**(4): 6.
Moosmüller, H., W. P. Arnott, C. F. Rogers, J. L. Bowen, J. A. Gillies, W. R. Pierson, J. F. Collins, T. D. Durbin and J. M. Norbeck (2001). "Time resolved characterization of particulate emission: 2. Instruments for elemental and organic carbon measurements." Environmental Science & technology **35**: 1935-1942.
Naumova, Y. Y., S. J. Eisenreich, B. J. Turpin, C. P. Weisel, M. T. Morandi, S. D. Colome, L. A. Totten, T. H. Stock, A. M. Winer, S. Alimokhtari, J. Kwon, D. Shendell, J. Jones, S. Maberti and S. J. Wall (2002). "Polycyclic Aromatic Hydrocarbons in the Indoor and Outdoor Air of Three Cities in the U S." Environmental science & technology **36**(12): 8.
Naumova, Y. Y., J. H. Offenberg, S. J. Eisenreich, Q. Meng, A. Polidori, B. J. Turpin, C. P. Weisel, M. T. Morandi, S. D. Colome, T. H. Stock, A. M. Winer, S. Alimokhtari, J. Kwon, S. Maberti, D. Shendell, J. Jones and C. Farrar (2003). "Gas/particle distribution of polycyclic aromatic hydrocarbons in coupled outdoor/indoor atmospheres." Atmospheric environment **37**(5): 18.
Nel, A. E., D. Diaz-Sanchez, D. Ng, T. Hiura and A. Saxon (1998). "Updates on cells and cytokines - Enhancement of allergic inflammation by the interaction between diesel

exhaust particles and the immune system." The journal of allergy and clinical immunology : official organ of American Academy of Allergy **102**(4 1): 539-554.
Novakov, T., V. Ramanathan, J. E. Hansen, T. W. Kirchstetter, M. Sato, J. E. Sinton and J. A. Sathaye (2003). "Large historical changes of fossil-fuel black carbon aerosols." Geophysical Research Letters **30**: doi:10.1029/2002GL016345.
NTP (2003). 10th Report on Carcinogen, National Toxicology Program. U.S. Department of Health and Human Services, National Toxicology program.
Pankow, J. F. (2003). "Gas/particle partitioning of neutral and ionizing compounds to single and multi-phase aerosol particles 1 Unified modeling framework." Atmospheric environment **37**(24): 12.
Petzold, A. and R. Niessner (1994). The Photoacoustic Soot Sensor for Black Carbon Monitoring. Fifth International Conference on Carbonaceous Particles in the Atmosphere, Berkeley, CA.
Petzold, A. and R. Niessner (1995). "Novel Design of a Resonant Photoacoustic Spectrophone for Elemental Carbon Mass Monitoring." Applied Physics Letters **66**(10): 1285-1287.
Ramanathan, V. and P. J. Crutzen (2003). "New Directions: Atmospheric Brown 'Clouds'." Atmospheric Environment **37**: 4033-4035.
Roessler, D. M. (1984). "Photoacoustic Insights on Diesel Exhaust Particles." Applied Optics **23**(8): 1148-1155.
Rogers, C. F., J. C. Sagebiel, B. Zielinska, W. P. Arnott, E. M. Fujita, J. D. McDonald, J. B. Griffin, K. Kelly, D. Overacker, D. Wagner, J. S. Lighty, A. Sarofim and G. Palmer (2003). "Characterization of Submicron Exhaust Particles from Engines Operating Without Load on Diesel and JP-8 Fuels." Aerosol Science & Technology **37**(4): 355-368.
Terhune, R. W. and J. E. Anderson (1977). "Spectrophone Measurements of the Absorption of Visible Light by Aerosols in the Atmosphere." Optics Letters **1**(2): 70-72.
Watson, J. G., J. C. Chow, D. H. Lowenthal and L. C. Pritchett (1994). "Differences in the carbon composition of source profiles for diesel- and gasoline-powered vehicles." Atmospheric environment **28**(15): 2493-2505.
Wilson, N. K. and R. K. Barbour (1994). "Evaluation of a real-time monitor for fine particle-bound PAH in air, Polycyclic Aromatic Compound." Polycyclic Aromatic Compounds **5**: 167-174.
Wilson, N. K. and J. C. Chuang (1991). "Sampling polycyclic aromatic hydrocarbons and related semivolatile organic compounds in indoor air." Indoor Air **4**: 512-513.
Zielinska, B., J. Sagebiel, W. P. Arnott, C. F. Rogers, K. E. Kelly, D. A. Wagner, J. S. Lighty, A. F. Sarofim and G. Palmer (2003). "Phase and size distribution of polycyclic aromatic hydrocarbons in diesel and gasoline vehicle emissions." environmental Science & technology **submitted in 2003**.

APPENDIX 3:

PHASE AND SIZE DISTRIBUTION OF POLYCYCLIC AROMATIC HYDROCARBONS IN DIESEL AND GASOLINE VEHICLE EMISSIONS

Phase and Size Distribution of Polycyclic Aromatic Hydrocarbons in Diesel and Gasoline Vehicle Emissions

B. Zielinska[1*], J. Sagebiel[1], W. P. Arnott[1], C.F. Rogers[1], K.E. Kelly[2], D.A. Wagner[2], J. S. Lighty[2], A.F. Sarofim[2], and G. Palmer[3]

[1] *Desert Research Institute, Division of Atmospheric Sciences, University and Community College System of Nevada, 2215 Raggio Parkway, Reno, NV 89512*
[2]*Department of Chemical and Fuels Engineering, University of Utah, Kennecott Research Center, 100 S., 1495 E., Salt Lake City, UT 84112*
[3]*Hill Air Force Base, Ogden, UT*

Abstract

Emission measurements were made for aircraft ground support equipment (AGE) vehicles at Hill Air Force Base (HAFB, Ogden, UT) as part of a Strategic Environmental Research and Development Program, using chassis dynamometers. The exhaust from the tested vehicle was passed to a dilution tunnel where it was diluted 30 to 40 times, and collected using Micro-Orifice Uniform Deposit Impactor (MOUDI), a XAD-coated annular denuder, and a filter followed by a solid adsorbent. MOUDI substrates were analyzed for mass and for organic (OC) and elemental (EC) carbon, by the thermal/optical reflectance (TOR) method and for polycyclic aromatic hydrocarbons (PAH) by GC/MS. The denuder and filter/solid adsorbent samples were analyzed for PAH. Overall, there is more mass and higher EC contribution when the vehicle is run under higher load in comparison with the low load. Older vehicles generally show more mass and EC emissions than newer vehicles, and there is a shift toward smaller particle sizes for the low load, which is most pronounced for newer vehicles. PAH are present predominantly on the sub-micron particles collected on MOUDI stages 0.18-0.32 μm, 0.32-0.56 μm and 0.1-0.18 μm. For the low-load runs, the distribution of PAH seems to be shifted towards smaller size particles. The gas-particle phase distribution of semi-volatile PAH depends also on the engine loading. For idle, not only two- three-ring PAH are retained on the denuder segment, but also less volatile 4-ring PAH are retained at the 80 –90% range, which implies that they are present predominantly in the gas phase. In contrast, for engines under high loads a much larger portion of 3 and 4-ring PAH are partitioned to the particle phase.

Introduction

Polycyclic aromatic hydrocarbons (PAH) constitute a broad family of compounds that are sometimes described as semi-volatile organic compounds (SVOC). This term refers to the fact that PAH are distributed between gas and particle phases. The factor of ~10^7 in the range of their vapor pressures is reflected in the fact that, at equilibrium at ambient temperature, two-ring naphthalene exists almost entirely in the gas phase, whereas benzo[*a*]pyrene (B[*a*]P), other five-ring PAHs, and higher-ring PAHs are predominantly adsorbed on particles. The intermediate three- and four-ring PAHs are distributed between the two phases. However, the gaseous concentrations of these intermediate

PAHs can be significantly reduced by their adsorption and absorption on various types of surfaces. Because of this phenomenon, the amount and type of particulate matter play an important role, together with temperature, in the vapor-particle partitioning of semi-volatile organic compounds[1,2,3,4]. Thus, the phase distribution of the PAH in the atmosphere is determined by the liquid phase (or sub-cooled liquid phase) vapor pressure of the individual species, by the amount and chemical nature of the particulate matter present (adsorption onto the aerosol surface and absorption into the aerosol organic matter), and by the temperature.

Diesel and gasoline-powered engines emit significant amounts of PAH distributed between the gas- and particle phases. However, the distribution of these PAH in the diluted exhaust in relation to the engine work cycle (i.e. running under different loads or at idle) is not well characterized. Since the amount and chemical nature of particulate matter (PM) produced by the given engine changes according to the work cycle, is the PAH phase and particle size distribution also cycle dependant? Are PAH emitted by spark-ignition vehicles phase and particle size distributed at the same way as those emitted by diesel? This paper attempts to evaluate these questions.

Experimental

Sample collection. The emission measurements were obtained for a variety of military vehicles at Hill Air Force Base (HAFB, Ogden, UT) in November 2000, as part of a Strategic Environmental Research and Development Program, SERDP [5,6]. The selection of aircraft ground support equipment (AGE) vehicles is shown in Table 1, along with fuel type.

AGE vehicles, with exception of the Jammer were tested using chassis dynamometers under pre-determined load. It was not possible to operate the Jammer on a dynamometer; therefore, it was only tested under idle conditions. The experimental conditions are presented in Table 2. The exhaust from the tested vehicle was passed to the DRI dilution tunnel based on the design of [7]. The inlet to the dilution sampler was a 3.2m long line heated to 150°C. The sample stream was diluted by air that had passed through a HEPA filter, desiccant and activated carbon beds. The dilution ratios for each run are shown in the third to last column of Table 2. The diluted sample was allowed to equilibrate in the residence chamber for approximately 80 seconds before being passed to the aerosol characterization instruments. The temperature and the relative humidity in the dilution sampler ranged from 18°C to 33°C and from approximately 5% to 31%, respectively, depending on engine and ambient conditions. The dilution sampler flow supplied four sampling trains, two of which (No. 1 and 2) were fitted with Bendix-Unico 240 cyclones [8], which provide a 50% cut-point of 2.5 micrometers aerodynamic diameter at a volumetric flow rate of 113 liters/minute (LPM). The remaining two sampling trains (No. 3 and 4) did not contain size-classifying devices. Sampling train No. 1 and 2 supplied the DRI fine particulate/semi volatile organic compound sampler (FP/SVOC) and an annular denuder (both described below), respectively. A Micro-Orifice Uniform Deposit Impactor (MOUDI) was connected to sampling train #4.

Sampling Methods. The semi-volatile polycyclic aromatic hydrocarbons (PAH) were collected using a sorbent-coated annual denuder [9]. The denuder sampler, purchased from the University Research Glassware Corporation (URG, Chapel Hill, NC), consisted of

three stages; the first stage was an 8-channel denuder section (52 mm OD, 600 mm length) coated with polystyrene-divinylbenzene resin XAD-4, which strips the gas-phase species from the airstream before collection of the particles on a second stage, consisting of a 47 mm Teflon-impregnated glass fiber (TIGF, T60X20) filter. The third stage consisted of polyurethane foam plugs (1" diameter) in combination with the 5 g of adsorbent resin XAD-4 (PUF/XAD/PUF "sandwich" cartridge) that were placed downstream of the filter to assess "blow off" or volatilization loss of semi-volatile PAH from the particles. The denuder XAD coating was performed by Dr. Lara Gundel of the University of California, Berkeley. In parallel, a medium-volume DRI fine particulate/semi volatile organic compound (FP/SVOC) sampler, using 90 mm TIGF (T60X40) filters backed by the PUF/XAD/PUF "sandwich" cartridge (10 g of XAD-4 resin between two 2" PUF plugs) was employed. The flow was set at approximately 90 L/min for the denuder and at 100 L/min for the FP/SVOC sampler.

Prior to sampling, the XAD-4 resin was cleaned by Soxhlet extraction with methanol followed by dichloromethane (CH_2Cl_2), each for 48 hours. The cleaned resin was then dried in a vacuum oven heated at 40 ºC and stored in sealed glass containers in a clean freezer. The PUF plugs were cleaned by Soxhlet extraction with acetone followed by extraction with 10% diethyl ether in hexane, as described in U.S. EPA Method TO-13. Prior to sampling, XAD-4 resin and PUF plugs were loaded into the glass sampling cartridges. The TIGF filters were cleaned by sonication in methanol for 10 minutes (twice), followed by two more 10-minute sonications in CH_2Cl_2. The filters are then dried, placed in clean aluminum foil, and labeled. Each batch of precleaned XAD-4 resin and ~10% of precleaned PUF plugs and TIGF filters was checked for purity by solvent extraction and GC/MS analysis of the extracts. The sampling flow rates were checked before and after sampling. After sampling, the filters were placed in clean aluminum foil and the PUF/XAD/PUF sandwich cartridges were also wrapped in aluminum foil and stored at ice temperature until transported to a laboratory freezer.

Micro-Orifice Uniform Deposit Impactor (MOUDI). A MOUDI sampler was used in this sampling campaign; it was fitted with aluminum media for thermal/optical reflectance (TOR) carbon analyses. The MOUDI is an inertial cascade impactor with multiple nozzles. At each stage, jets of particle-laden air are impinged upon an impaction plate and particles larger than the cut size of each stage are collected on the impaction plates. Smaller particles with less inertia follow the air streamlines and proceed onto the next stage. The nozzles of each succeeding stage are smaller than the prior stage, giving a higher velocity through the nozzles, and a smaller particle size cut. The airflow continues through a series of eight impactor stages until the smallest particles are removed by the after-filter. In the configuration we used, the top stage (which would nominally be 5.6 μm) was greased with high vacuum grease to remove any larger particles and prevent particle bouncing. The stages at 3.2, 1.8, 1.00, 0.53, 0.32, 0.18, and 0.096, 0.049 μm were used in the normal manner, with the after-filter collecting particles smaller than 0.049 μm. The MOUDI operated at a flow rate of 30 LPM.

Analysis Methods. The SVOCs collected on each denuder-filter-PUF/XAD/PUF sampling train were extracted separately with high purity, HPLC grade solvents. The denuder portion was extracted with cyclohexane immediately following the sample collection. Approximately 200 ml of cyclohexane was poured into the denuder section, which had been capped at one end. The other end was capped and the denuder manually inverted about 10 times. The solvent was drained and the procedure repeated two more times, using n-hexane for the last extraction. The PUF/XAD plugs were microwave-extracted with 10% diethyl ether in hexane [10] and the filters were microwave-extracted with dichloromethane. Prior to extraction, the following deuterated internal standards were added to each PUF, filter, and XAD sorbent: naphthalene-d_8, acenaphthylene-d_8, phenanthrene-d_{10}, anthracene-d_{10}, chrysene-d_{12}, fluoranthene-d_{10}, pyrene-d_{10}, benz[a]anthracene-d_{12}, benzo[e]pyrene-d_{12}, benzo[a]pyrene-d_{12}, benzo[k]fluoranthene-d_{12} and benzo[ghi]perylene-d_{12}. The extracts were concentrated by rotary evaporation at 20 ºC under gentle vacuum to ~1 ml and filtered through 0.20 μm Anatop (Whatman International, Ltd.), rinsing the sample flask twice with 1 ml CH_2Cl_2 each time. Approximately 50 μl of acetonitrile was added to the sample and CH_2Cl_2 was evaporated under a gentle stream of nitrogen. The final volume was adjusted to 1 ml with acetonitrile. The sample was then analyzed by electron impact (EI) GC/MS technique, using an Ion Trap Varian Saturn 2000, operating in the selected ion storage (SIS) mode. Injections (1 μl) were made in the splitless mode onto a 30 m x 0.25 mm ID CPSil 8 fused-silica capillary column (Varian, Inc.). Identification and quantification of the SVOC was made by SIS, monitoring the molecular ion of each SVOC and deuterated SVOC. Calibration curves for the GC/MS/SIS quantification were made for the molecular ion peaks of the SVOC using the corresponding deuterated species (or the deuterated species most closely matched in volatility and retention characteristics) as internal standards. NIST SRM 1647 (certified PAH), with the addition of deuterated internal standards and authentic standards of compounds not present in the SRM, were used to make calibration solutions.

All aluminum MOUDI substrates were analyzed for mass and for organic (OC) and elemental (EC) carbon, by thermal/optical reflectance (TOR) method, as described previously [11]. The TOR analysis used ¼ of an aluminum substrate and no correction for pyrolysis was applied to these samples. The remaining ¾ of selected MOUDI samples were spiked with deuterated PAH standards, extracted by sonication with dichloromethane (repeated 3 times), concentrated to 25 μl and analyzed for PAH, as described above.

All data discussed below are not corrected for dilution. The phase and size distribution of PAH discussed in this paper relates to the diluted exhaust and may not be valid for tailpipe conditions. Therefore, the correction for dilution might be potentially misleading.

Results and Discussion

MOUDI Mass and Carbon Data. With the exception of the quartz after-filter, all OC/EC data were obtained from aluminum foil by the TOR method [11]. However, due to the reflective nature of aluminum foil, it was not possible to apply the pyrolysis correction

for these samples. Thus, the concentrations of EC might be slightly overestimated. Although MOUDI EC data correlate very well with black carbon data obtained by the continuous photoacustic method (W. Arnott, unpublished results) for the same runs (slope = 0.99 and $r^2 = 0.972$) there is an significant difference between BC and EC concentrations for the runs with low mass emissions, as shown later.

Figure 1 shows the distribution of mass, organic carbon x 1.2 (to account for hydrogen mass) and elemental carbon between individual MOUDI stages for the system blank and for the diluted exhaust from the AGS vehicles, run under different conditions (see Table 2 for the run description). Although the system blank sample (Figure 1A) shows some mass, the distribution of mass between different MOUDI stages is different than for the exhaust samples. For the system blank the majority of mass is found on the 1.0 – 1.8 and 1.8 – 3.2 um stages, indicating that some accumulation mode particles are desorbing from the dilution tunnel walls. The gasoline vehicle diluted exhaust from a run under high (53%) load (Figure 1B) shows very different mass distribution, with the majority of mass collected on 0.32-0.53; 0.18-0.32; 0.05-0.1 and <0.05 um stages. The mass is composed mostly of organic carbon, with very little elemental carbon present.

For the two diesel vehicles tested on the dynamometer, 1996 Dodge Bobtail and 1986 Jeep Bobtail, there is overall more mass and higher EC contribution when the vehicle is run under higher load (Figure 1C and 1E) in comparison with the low load (Figure 1D and 1F). However, the older vehicle shows in general more mass and EC emissions than the newer vehicle (EC constitutes 35% and 26% of TC for the Jeep tested under high and low load, respectively, as compared with 11% and 3% for Dodge). Also, there is a shift toward smaller particle sizes for the low load, which is the most pronounced for the newer vehicle, 1996 Dodge Bobtail. Figures 1G and 1F show the distribution of mass and OC/EC for the two vehicles running under idle conditions, a 1992 Jammer and 1996 Dodge Bobtail, respectively. The Jammer exhaust contains more mass than the Dodge Bobtail, but the emissions from both vehicles is mostly of OC.

The quartz after filters (<0.056 um) contain significant amount of mass for all runs. However, since the mass was obtained from the gravimetric analysis of quartz filters, there are two factors that can make these measurements inaccurate: 1) the quartz filter is prone to a positive sampling artifact, i.e. adsorption of gaseous organic compounds on the filter during sampling; 2) some particle bouncing could have occurred during sampling. Since the main constituent of the after filter mass is organic carbon, with very little of elemental carbon, this supports the first assumption.

Table 3 shows the distribution of the particle mass and OC/EC between individual MOUDI stages for runs selected for PAH analysis in the diluted vehicle exhaust. Since two Dodge Bobtail runs under 27% load were replicates, they were combined in order to obtain sufficient mass for these analyses.

MOUDI PAH Data. Figure 2 A, B and C show the distribution of PAH between the MOUDI stages collected from the diluted Dodge Bobtail exhaust run under high load (95, 81, 54, 27%) and Figure 2D, E and F - under constant low load (27%). Although it is generally assumed [12] that the aluminum foil has very low affinity for gaseous organic

compounds and thus is not prone to positive sampling artifacts, it is clear from this figure that the gas-phase PAH (Figure 2A and D) are present in measurable amounts in all stages. Naphthalene, methyl- and dimethyl- naphthalenes are present in very high concentrations in spark-ignition and diesel vehicle exhaust, and are even few orders of magnitude higher than particle-associated four and five ring PAH. These gas-phase PAH are distributed randomly between all stages, which indicates their non-specific adsorption, most likely on the particles collected on the various MOUDI stages (i.e. positive sampling artifact). The particle-associated semi-volatile PAH (Figure 2B and E) and non-volatile 4 through 6-ring PAH (Figure 2C and F) are present predominantly on the sub-micron particles collected on MOUDI stages 0.18-0.32 μm, 0.32-0.56 μm and 0.1-0.18 μm (see Table 4 for the explanation of mnemonics). For the low-load runs (27%), the distribution of PAH seems to be shifted towards smaller size particles, which is consistent with mass and OC distribution. In addition, the concentrations of PAH are much lower in low-load runs.

The system blanks showed very low PAH concentrations, distributed randomly between all stages, in contrast to the diesel runs, as shown in Figure 3.

Denuder PAH Data. Figure 4 shows the percentage of PAH present on the denuder portion (covered with XAD resin) of the annual denuder for 1996 Doge Bobtail run under idle (Figure 4A), low load (27%, Figure 4B) and high load (Figure 4C) conditions, in relation to total PAH present on denuder+filter+PUF/XAD/PUF cartridge. The PAH are shown according to their elution order from a non-polar capillary column (CPSil 8, 5% phenylmethylsilicone), which separates PAH according to their volatility. It can be seen from this figure that the gas-particle phase distribution for these diesel runs depends on the engine loading. For idle (Figure 4A), the more volatile two-three-ring PAH, from naphthalene to dimethylphenanthrenes, are retained on the denuder portion, and the less volatile 4-ring PAH, such as fluoranthene and pyrene, are retained by the denuder at the 80 –90% range. These results imply that they are present predominantly in the gas phase. In contrast, for engines under high load (Figure 4C) a much larger portion of 3 and 4-ring PAH is partitioned to the particle phase. The low-load results (27%, Figure 4B) are clearly situated between these two extremes. The non-volatile 5 – ring PAH, such as benzo(b+j+k)fluoranthene, BaP, BeP, or benzo(g,h,i)perylene are present predominantly on the filter for all runs.

The most volatile and most abundant PAH (naphthalene and methyl-naphthalenes) shows the significant break through the denuder (approximately 20% and 10%, respectively), as Figure 4 shows. The flow rate through our denuder was calculated based on Possanzini model [13] to be optimal for phenanthrene (99.5% efficiency) at 92 L/min. Thus, PAH more volatile than phenanthrene might experience a break through the denuder with this flow rate. However, the lower flow rate could have resulted in a particle loss to the denuder walls and evaporative losses of more volatile PAH from particles. The diffusional losses depend on the particle residence time and are important for smaller particles (dp <0.01 um). As it can be seen from Figure 2C and 4F, the higher molecular weight (mw) PAH (from BaA to coronene) are present in significant amounts on small particles (0.05-0.1 um MOUDI cut-off stage), especially for a low load run (27%). Consequently, some diffusional particle losses might have occurred for low load or idle

runs and, as it can be seen in Figure 4, the gas-phase concentrations of some higher mw PAH, such as BeP or benzo(g,h,i)perylene are higher than expected.

Evaporative losses are important for higher volatility compounds that can evaporate from particles during their residence time in the denuder, as surrounding gases are removed and the equilibrium is disturbed [14]. Thus, the transit time through the sorbent-coated section should be short enough to limit evaporation of semi-volatile PAH from particles (≤ 0.3 sec recommended). For 92 L/min flow rate and 5.2 cm x 60 cm 8-channel denuder used in this work, the transit time was approximately 0.3 sec.

The mechanism of gas/particle (G/P) partitioning of SVOC, such as PAH, includes adsorption onto the aerosol surface and absorption into the aerosol organic matter layer [2,3,15,16]. Several investigators have suggested that G/P partitioning is primarily absorptive in nature and can be described by the gas-liquid interaction processes under many conditions [2,3,17,18,19]. However, it has been recently argued that adsorption onto aerosol soot carbon dominates G/P partitioning of PAH and that absorption may account for less than 10% of total PAH in the particulate phase [20]. Since our dynamometer measurements include several vehicles and test cycles that produced different amount of soot and organic carbon fractions, it was interesting to compare the G/P partitioning of PAH for these runs.

Table 5 lists OC*1.2, EC and black carbon (BC, obtained by the photoacustic method) concentrations in the diluted exhaust of all vehicle's runs listed in Table 2. Also, the ratio of particle to gas phase concentrations (Cp/Cg) for fluoranthene and pyrene are listed. Cg values are obtained from the XAD coated denuder section, whereas Cp represents the sum of filter and PUF/XAD/PUF concentrations. As mentioned before, EC and BC are highly correlated for these runs. However, since no correction for pyrolysis was applied to the TOR method (due to the reflective nature of aluminum foil), the EC values might be slightly overestimated, especially for the runs with low EC content and high OC content. Thus, the BC values reflect probably more correctly the emissions soot content than EC values.

Figure 5 shows the relationship between Cp/Cg and BC and Cp/Cg and OC*1.2 for fluoranthene and pyrene in all runs. It is obvious that no correlation exists between these parameters. However, if the runs are sorted according to the BC content in emissions, it can be seen (Figure 6, lower graphs) that the good correlations exist between Cp/Cg and BC for runs with higher BC contents (i.e all 1986 Jeep Bobtail and 1992 Jammer runs) and between Cp/Cg and OC*1.2 for all runs with low BC content (i.e.1996 Dodge Bobtail and 1993 Ford F350 gasoline runs). The slope of the trend line, which represents a gas-particle partition coefficient, is higher for the Cp/Cg and OC*1.2 relationship than for Cp/Cg and BC relationship, thus implying that the gas-particle phase distribution of these PAH is influenced more by the organic layer than BC content. However, both mechanisms, i.e. adsorptive to BC (if present in sufficient amount) and absorptive to OC, are responsible for the G/P partitioning of PAH under these conditions.

The exhaust from all vehicles tested on the dynamometer was diluted 30 to 40 times and allowed to equilibrate for approximately 80 sec prior to collection (see Table 2). It has been shown [21] that under warm conditions (as used in this study, see Table 2), the equilibrium between gas- and particle phase PAH is reached very quickly, on the order of several seconds.

Comparison of Denuder and FP/SVOC Sampler. Figure 7 A, B, C, D shows the comparison of samples collected with the denuder and with the DRI FP/SVOC sampler for 1996 Dodge Bobtail idle and high load runs. The PUF/XAD/PUF extract from the FP/SVOC sampler is compared with the denuder extract (Fig 7 B and D) and filter extract from FP/SVOC sampler is compared with denuder filter extract plus the extract from the PUF/XAD/PUF cartridge following the filter (Fig 7 A and C). The most volatile 2-ring PAH are shown on the figure inserts. Their concentrations are approximately an order of magnitude higher than the concentrations of the most abundant 3-ring PAH, and they show approximately 10 to 20% breakthrough the denuder. For semi-volatile 2- 4 rings PAH, the sampling system consisting of a TIGF filter followed by a PUF/XAD/PUF cartridge (FP/SVOC sampler), showed lower concentrations on the filter and higher concentrations on the PUF/XAD/PUF cartridge in comparison with the denuder sampler, which indicates blow-off semi-volatile PAH from the filter (negative sampling artifact) for the FP/SVOC system. The exceptions are combined methyl- and dimethyl-phenanthrene isomers, for which the concentrations are generally higher for the denuder samples. The reason for this phenomenon is not clear – it may indicate breakthrough the PUF/XAD/PUF cartridge of FP/SVOC sampler, or the presence of some interfering compounds on the XAD-coated denuder section of the annular denuder.

Figure 8 shows the same comparison for the gasoline-powered 1993 Ford F-350 run under high (53%) load (Figure 8 A and B) and under variable (from 53% to 11%) load (Figure 8 C and D). This vehicle shows generally low PM emission rates when compared with diesel vehicles tested (see Figure 1) and the total PM concentrations for high load run was approximately 4 times lower than for low load run. Figure 8 shows that the concentrations of the gas-phase 2-ring PAH for these two runs are comparable (or higher) than the diesel vehicle shown in Figure 7, but the concentrations of 3-ring PAH are lower. In addition, the concentration of 5-ring PAH and coronene are higher for gasoline vehicle, especially for high load. This is consistent with the previous reports [22]. Again, for semi-volatile 2- 4 rings PAH, the sampling system consisting of a TIGF filter followed by a PUF/XAD/PUF cartridge (FP/SVOC sampler) showed lower concentrations on the filter and higher concentrations on the PUF/XAD/PUF cartridge in comparison with the denuder sampler, which indicates blow-off semi-volatile PAH from the filter (negative sampling artifact) for the FP/SVOC system. For diluted gasoline and diluted diesel exhaust, no evidence of positive filter artifact was observed. This indicates that the Teflon coated glass-fiber filters are less susceptible to gas-phase adsorption of volatile organic compounds than glass fiber filters.

In summary, for both diesel and gasoline vehicles there is more mass and higher EC contribution when the vehicle is run under higher load in comparison with the low load. However, the gasoline vehicle shows predominantly OC emissions, with very little EC present. The older diesel vehicles generally show more mass and EC emissions than

newer vehicles, and there is a mass shift toward smaller particle sizes for the low load, which is most pronounced for newer vehicles. The particle-associated semi-volatile PAH and non-volatile 4 through 6-ring PAH are present predominantly on the sub-micron particles collected on MOUDI stages 0.18-0.32 μm, 0.32-0.56 μm and 0.1-0.18 μm. For the low-load diesel vehicle runs, the distribution of PAH seems to be shifted towards smaller size particles. The gas-particle phase distribution of semi-volatile PAH depends also on the engine loading. For idle, the more volatile two- three-ring PAH, from naphthalene to dimethylphenanthrenes are retained on the denuder portion, but also less volatile 4-ring PAH, such as fluoranthene and pyrene are retained by the denuder at the 80 –90% range, which implies that they are present predominantly in the gas phase. In contrast, for engines under high loads a much larger portion of 3 and 4-ring PAH are partitioned to the particle phase.

Particle bound PAH tends to be associated with OC through the process of absorption when the EC content is small. Even when the EC fraction is larger and PAH's are adsorbed to the EC surface, an appreciable fraction of particle-bound PAH is associated with OC. These are the conclusions of direct source sampling with diluted, scrubbed air. Further dilution and trasformation may occur in the atmosphere to adjust this picture of the gas- and particle-phase distribution.

Acknowledgements

This research was supported by Strategic Environmental Research and Development Program (SERDP) Project CP-1106, Characterization of Particulate Emission: Size Characterization and Chemical Speciation. We thank Mr. Bob Armstrong of Hill Air Force Base for his assistance.

References

(1) Ligocki, M. P.; Pankow, J. F. *Environ.Sci.Technol.* **1989**, *23*, 75-83.
(2) Pankow, J. F. *Atmos.Environ.* **1994**, *28*, 185-188.
(3) Pankow, J. F. *Atmos.Environ.* **1994**, *28*, 189-194.
(4) Odum, J. R.; Hoffman, T.; Bowman, F. A.; Collins, D.; Flagan, R. C.; Seinfeld, J. H. *Environ.Sci.Technol.* **1996**, *30*, 2580-2585.
(5) Rogers, C. F.; Sagebiel, J. C.; Zielinska, B.; Arnott, W. P.; Fujita, E. M.; McDonald, J. D.; Griffin, J. B.; Kelly, K.; Overacker, D.; Wagner, D.; Lighty, J. S.; Sarofim, A.; Palmer, G. *Aerosol Sci.Technol.* **2003**, *37*, 355-368.
(6) Kelly, V. R.; Lovett, G. M.; Weathers, K. C.; Likens, G. E. *Atmos.Environ.* **2002**, *36*, 1569-1575.
(7) Hildemann, L. M.; Cass, G. R.; Markowski, G. R. *Aerosol Sci.Technol.* **1989**, *10*, 193-204.
(8) Chan, T.; Lippmann, M. *Environ.Sci.Technol.* **1977**, *11*, 377-386.
(9) Gundel, L. A.; Stevens, R. K.; Daisey, J. M.; Lee, V. C.; Mahanama, K. R. R.; Cancel-Velez, H. G. *Atmos.Environ.* **1995**, *29*, 1719-1733.
(10) Autho, 1998.
(11) Chow, J. C.; Watson, J. G.; Pritchett, L. C.; Pierson, W. R.; Frazier, C. A.; Purcell, R. G. *Atmos.Environ.* **1993**, *27A*, 1185-1201.

(12) Offenberg, J. H.; Baker, J. E. *Atmos.Environ.* **2002**, *36*, 1205-1220.
(13) Possanzini, M.; Febo, A.; Liberti, A. *Atmos.Environ.* **1983**, *17*, 2605-2610.
(14) Kamens, R. M.; Coe, D. L. *Environ.Sci.Technol.* **1997**, *31*, 1830-1833.
(15) Pankow, J. F. *Atmos.Environ.* **1987**, *21*, 2275-2283.
(16) Jang, M.; Kamens, R. M.; Leach, K. B.; Strommen, M. R. *Environ.Sci.Technol.* **1997**, *31*, 2805-2811.
(17) McDow, S. R.; Sun, Q. R.; Vartiainen, M.; Hong, Y. S.; Yao, Y. L.; Fister, T.; Yao, R. Q.; Kamens, R. M. *Environ.Sci.Technol.* **1994**, *28*, 2147-2153.
(18) Kamens, R. M.; Odum, J. R.; Fan, Z. H. *Environ.Sci.Technol.* **1995**, *29*, 43-50.
(19) Jang, M.; Kamens, R. M. *Environ.Sci.Technol.* **1998**, *32*, 1237-1243.
(20) Dachs, J.; Eisenreich, S. J. *Environ.Sci.Technol.* **2000**, *34*, 3690-3697.
(21) Kamens, R. M.; Jang, M.; Chien, C. J.; Leach, K. *Environ.Sci.Technol.* **1999**, *33*, 1430-1438.
(22) Miguel, A. H.; Kirchstetter, T. W.; Harley, R. A.; Hering, S. V. *Environ.Sci.Technol.* **1998**, *32*, 450-455.

Table 1. Aircraft ground support equipment tested in the HAFB experiment

Vehicle Type	Fuel Type	Engine Manufacturer	Engine Displacement	Exhaust Treatment
1993 Ford F-350	Gasoline	Ford	5.8 liter	catalytic converter
1996 Dodge Bobtail	Diesel	Cummins	5.9 liter	none
1986 Jeep Bobtail	Diesel	Nissan	4.4 liter	none
1992 Jammer	JP-8 aviation fuel	HATZ	1.27 liter	none

"Bobtail" vehicles tow aircraft, and "Jammers" lift munitions into aircraft.

Table 2. Vehicle and dilution conditions for HAFB tests.

Run (min)	AGE	Engine speed (rpm)	Engine Load (% /kW)	Torque (N m)	Dilution ratio	RH (%)	Tem (°C)
60	Ford F350	2450	53/72	224	1:34.2	2-31	22-24
60	Ford F350	2450	53, 43,32, 21,11/ 72,58,43,28,14	224,179,134,90, 45	1:37.6	13-32	20-26
60	Dodge Bobtail	700	idle	idle	1:33.5	11-13	27-28
60	Dodge Bobtail	1500	95, 81,54, 27/ 96,72,48,24	759, 616, 411, 206	1:31.7	15-21	24-26
60	Dodge Bobtail	1500	27/24	206	1:30.3	18-22	22-24
60	Dodge Bobtail	1500	27/24	206	1:30.4	23-29	18-22
45	Jeep Bobtail	1700	23/24	411	1:31.8	23-31	19-24
20	Jeep Bobtail	1700	23/24	411	1:31.8	10-22	24-26
20	Jeep Bobtail	1700	23, 9/24, 9	411,164	1:31.1	9-16	26-28
20	Jeep Bobtail	1700*	93,*, 23/ 87,*, 48	1640, *, 822	1:42.0	8-20	24-27
30	Jammer	2500	idle	idle	1:32.1	14-29	16-26
30	Jammer	2500	idle	idle	1:31.3	2-14	27-33

* acceleration during the middle of the test;
RH: relative humidity

Table 3. MOUDI mass, organic mass (OC*1.2) and EC data (ug/m3).

Stage No.	Cut-off (um)	Blank			Dodge Bobtail, High			Dodge Bobtail, Low			Dodge Bobtail, Low*			Jeep Bobtail, Low			Jeep Bobtail, High		
		Mass	OC	EC	Mass	OC	EC	Mass	OC	EC	Mass	OC	EC	Mass	OC	EC	Mass	OC	EC
1	3.2	0.7	4.6	0.4	6.7	3.5	1.2	61.4	31.8	0.5	7.0	4.7	0.2	21.0	11.2	3.4	32.8	21.3	8.1
2	1.8	65.4	26.6	1.9	21.8	8.8	2.4	3.5	4.5	0.2	3.5	3.4	0.1	738.4	274.8	12.0	84.9	44.0	27.2
3	1	104.7	35.3	3.4	7.3	5.6	1.5	1.8	3.3	0.1	3.5	3.9	0.2	36.3	25.6	11.1	271.9	154.8	109.9
4	0.56	5.8	5.2	0.5	20.1	14.1	3.1	4.1	4.6	0.2	4.1	3.6	0.2	291.9	149.1	45.4	345.2	225.6	141.9
5	0.32	0.0	4.7	1.0	315.3	241.5	25.9	28.7	9.5	0.4	5.8	6.3	0.4	469.4	313.7	144.4	798.4	523.0	303.8
6	0.18	0.7	3.2	0.1	736.1	541.5	75.3	127.5	122.1	6.1	158.4	151.3	6.4	1194.5	911.5	278.6	1955.6	1177.7	655.3
7	0.1	0.0	2.4	0.0	309.2	227.0	21.9	132.2	91.5	1.9	142.0	156.3	2.9	173.6	155.0	33.4	152.4	100.7	47.4
8	0.056	0.0	2.6	0.0	82.0	64.8	3.6	88.3	90.3	1.1	101.7	82.7	1.6	47.7	44.4	3.6	30.9	25.0	4.8
AF		53.8	45.9	2.4	83.2	91.8	7.1	142.1	63.9	1.5	47.9	84.2	2.2	158.4	123.0	7.3	129.2	217.3	11.0

*Duplicate run

Table 4. The list of PAH and their mnemonics

Mnemonic	PAH
naphth	Naphthalene
mnaph	Methylnaphthalenes (2 isomers)
biphen	Biphenyl
dmenaph	Dimethylnaphthalene (6 isomers)
mebiph	Methylbiphenyls (3 isomers)
tmenaph	Trimethylnaphthalenes (12 isomers)
acnapy	Acenaphthylene
acnape	Acenaphthene
fluore	Fluorene
phenan	Phenanthrene
meflu	Methylfluorenes (3 isomers)
xanone	Xanthone
acquone	Acenaphthenequinone
mephen	Methylphenanthrene (5 isomers)
anrquone	Anthraquinone
dmephen	Dimethylphenanthrene (7 isomers)
anthra	Anthracene
fluora	Fluoranthene
pyrene	Pyrene
bntiop	Benzonaphthothiophene
mefl/py	MePyrene/MeFluoranthene (6 isomers)
bzcphen	Benzo(c)phenanthrene
baanth	Benz(a)anthracene
chrysn	Chrysene
bzantone	Benzanthrone
baa7_12	Benz(a)anthracene-7,12-dione
chry56m	5+6-methylchrysene
bbjkfl	Benzo(b+j+k)fluoranthe
bepyrn	BeP
peryle	Perylene
bapyrn	BaP
incdpy	Indeno[123-cd]pyrene
bghipe	Benzo(ghi)perylene
dbanth	Dibenz(ah+ac)anthracene
corone	Coronene

Table 5. Mass, EC, BC, OC*1.2 and Cp/Cg data for fluoranthene and pyrene

VEHICLE	Load, %	Mass (ug/m3)	EC (ug/m3)	BC (ug/m3)	OCx1.2 (ug/m3)	Fluoran-thene	Pyrene
Ford F-350	53	218.4	15.7	2.5	69.8	0.27	0.59
Ford F-351	53,43,32, 21,11	40.2	3.5	0.25	54.7	0.02	0.08
Dodge Bobtail	Idle	168.3	16.5	8.5	144.8	0.05	0.07
Dodge Bobtail	95,81,54, 27	1581.6	142.0	79.88	1198.6	1.43	1.95
Dodge Bobtail	27	589.6	12.0	21.67	421.5	0.19	0.41
Dodge Bobtail	27	474.0	14.3	18.39	496.3	0.24	0.53
Jeep Bobtail	23	1686.9	519.8	464.06	1027.0	0.31	0.39
Jeep Bobtail	23	2622.1	553.5	609.21	1604.7	0.38	0.59
Jeep Bobtail	23,9	3131.2	539.2	525.59	2008.3	0.38	0.47
Jeep Bobtail	93,23	3801.2	1309.5	na	2489.5	0.57	1.37
Jammer	Idle	881.7	199.5	169.19	633.6	0.13	0.18
Jammer	Idle	1702.4	96.7	151.79	1154.9	0.11	0.16
Jammer	Idle	na	na	50.24	na	0.08	0.09

List of Figures

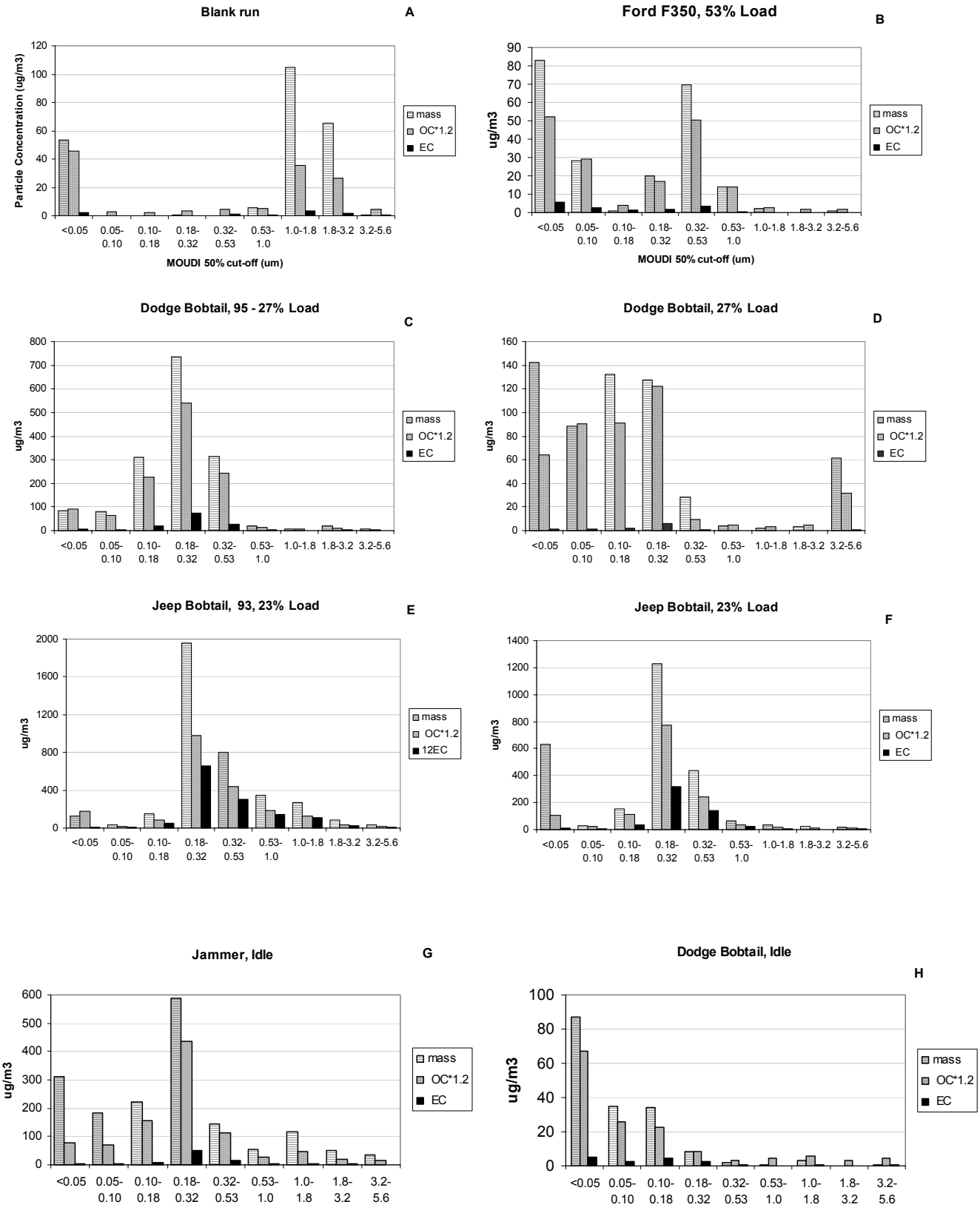
Blank run
A
Particle Concentration (ug/m3)
MOUDI 50% cut-off (um)
Ford F350, 53% Load
B
ug/m3
MOUDI 50% cut-off (um)
Dodge Bobtail, 95 - 27% Load
C
ug/m3
Dodge Bobtail, 27% Load
D
ug/m3
Jeep Bobtail, 93, 23% Load
E
ug/m3
12EC
Jeep Bobtail, 23% Load
F
ug/m3
Jammer, Idle
G
ug/m3
Dodge Bobtail, Idle
H
ug/m3
mass
OC*1.2
EC
<0.05
0.05-0.10
0.10-0.18
0.18-0.32
0.32-0.53
0.53-1.0
1.0-1.8
1.8-3.2
3.2-5.6

Figure 1

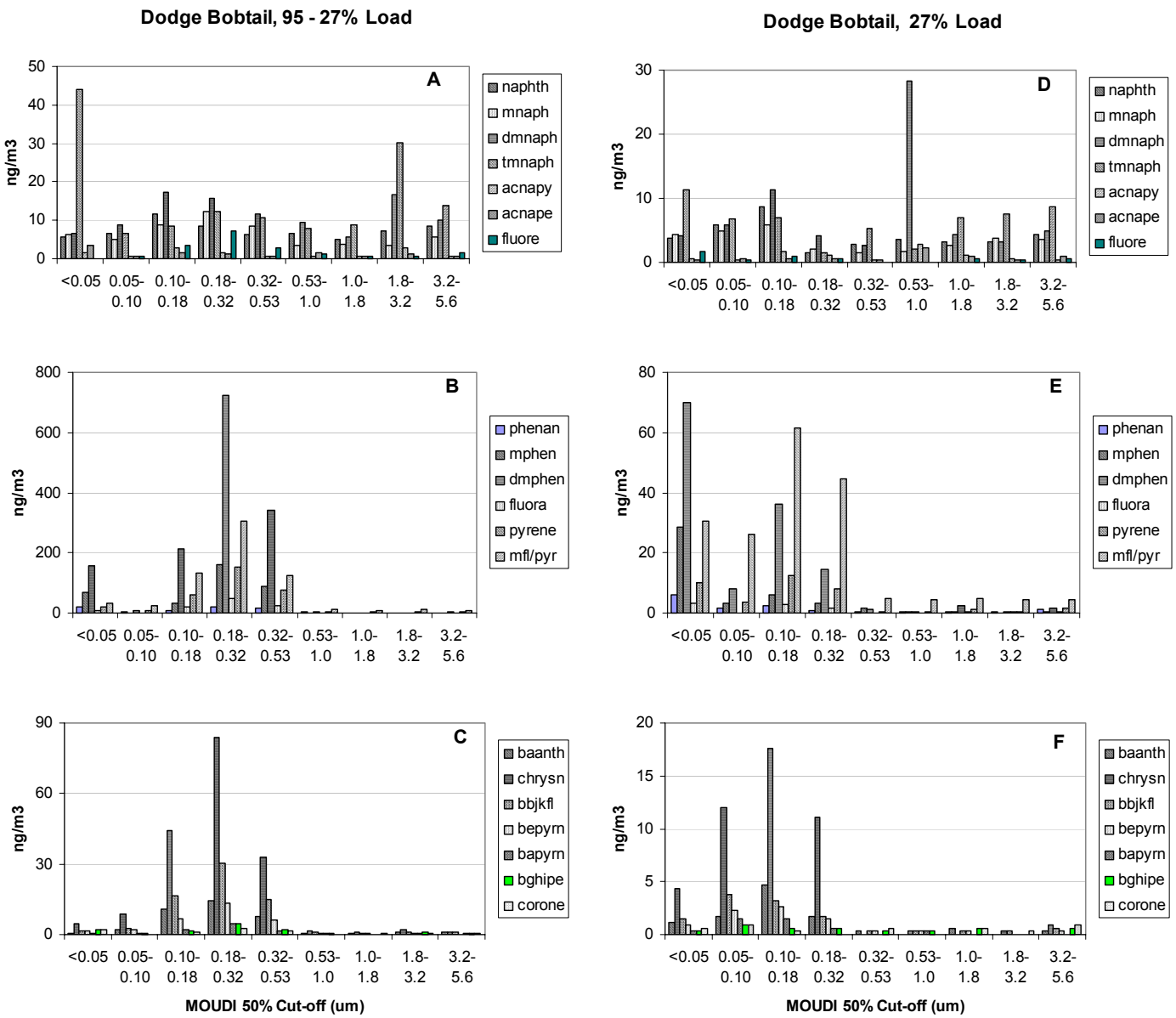
Dodge Bobtail, 95 - 27% Load
Dodge Bobtail, 27% Load
A
B
C
D
E
F
ng/m3
naphth
mnaph
dmnaph
tmnaph
acnapy
acnape
fluore
phenan
mphen
dmphen
fluora
pyrene
mfl/pyr
baanth
chrysn
bbjkfl
bepyrn
bapyrn
bghipe
corone
<0.05
0.05-0.10
0.10-0.18
0.18-0.32
0.32-0.53
0.53-1.0
1.0-1.8
1.8-3.2
3.2-5.6
MOUDI 50% Cut-off (um)

Figure 2

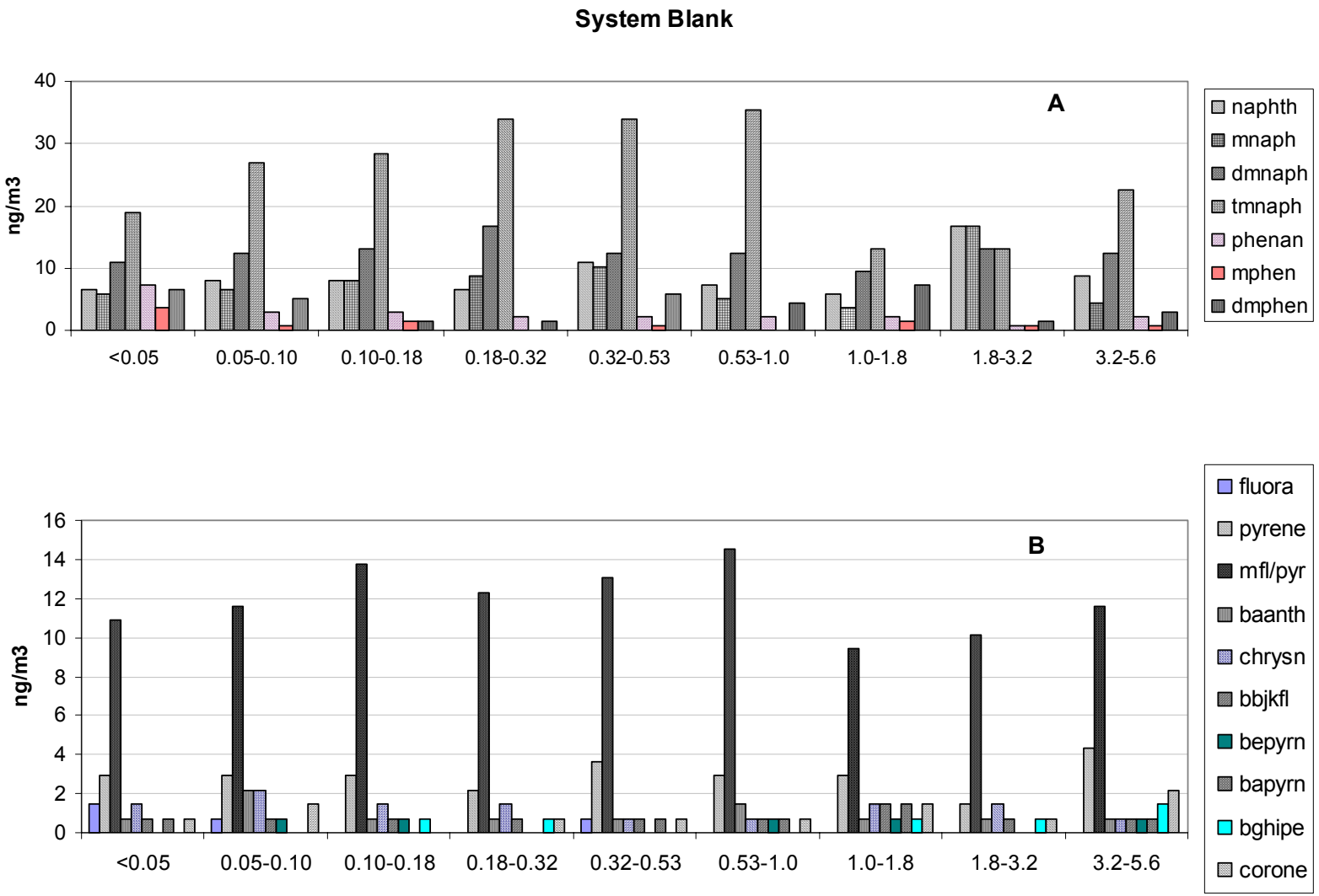
System Blank
A
ng/m3
40
30
20
10
0
<0.05
0.05-0.10
0.10-0.18
0.18-0.32
0.32-0.53
0.53-1.0
1.0-1.8
1.8-3.2
3.2-5.6
naphth
mnaph
dmnaph
tmnaph
phenan
mphen
dmphen
B
ng/m3
16
14
12
10
8
6
4
2
0
<0.05
0.05-0.10
0.10-0.18
0.18-0.32
0.32-0.53
0.53-1.0
1.0-1.8
1.8-3.2
3.2-5.6
fluora
pyrene
mfl/pyr
baanth
chrysn
bbjkfl
bepyrn
bapyrn
bghipe
corone

Figure 3

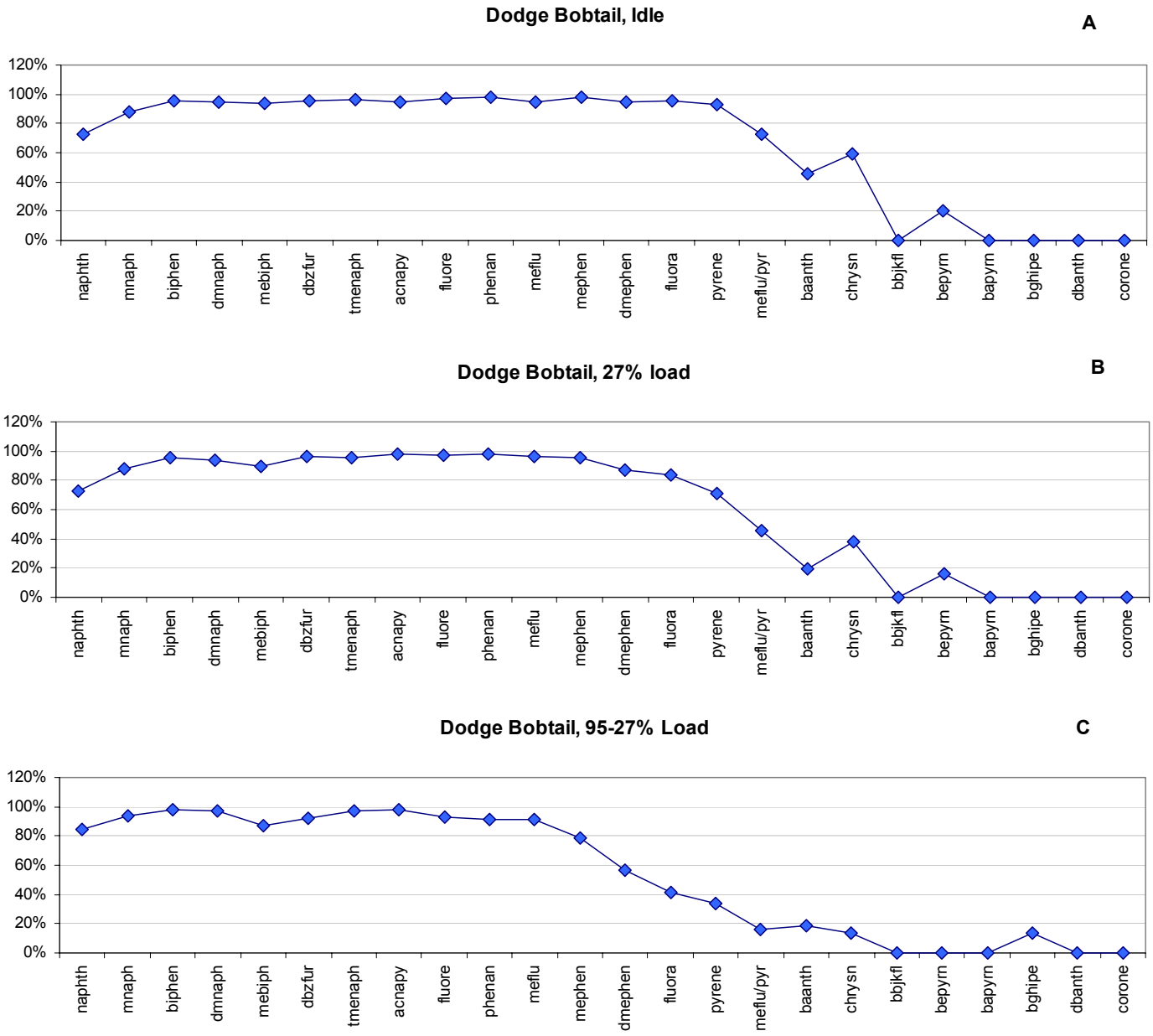
Dodge Bobtail, Idle
A
120%
100%
80%
60%
40%
20%
0%
naphth
mnaph
biphen
dmnaph
mebiph
dbzfur
tmenaph
acnapy
fluore
phenan
meflu
mephen
dmephen
fluora
pyrene
meflu/pyr
baanth
chrysn
bbjkfl
bepyrn
bapyrn
bghipe
dbanth
corone
Dodge Bobtail, 27% load
B
120%
100%
80%
60%
40%
20%
0%
naphth
mnaph
biphen
dmnaph
mebiph
dbzfur
tmenaph
acnapy
fluore
phenan
meflu
mephen
dmephen
fluora
pyrene
meflu/pyr
baanth
chrysn
bbjkfl
bepyrn
bapyrn
bghipe
dbanth
corone
Dodge Bobtail, 95-27% Load
C
120%
100%
80%
60%
40%
20%
0%
naphth
mnaph
biphen
dmnaph
mebiph
dbzfur
tmenaph
acnapy
fluore
phenan
meflu
mephen
dmephen
fluora
pyrene
meflu/pyr
baanth
chrysn
bbjkfl
bepyrn
bapyrn
bghipe
dbanth
corone

Figure 4

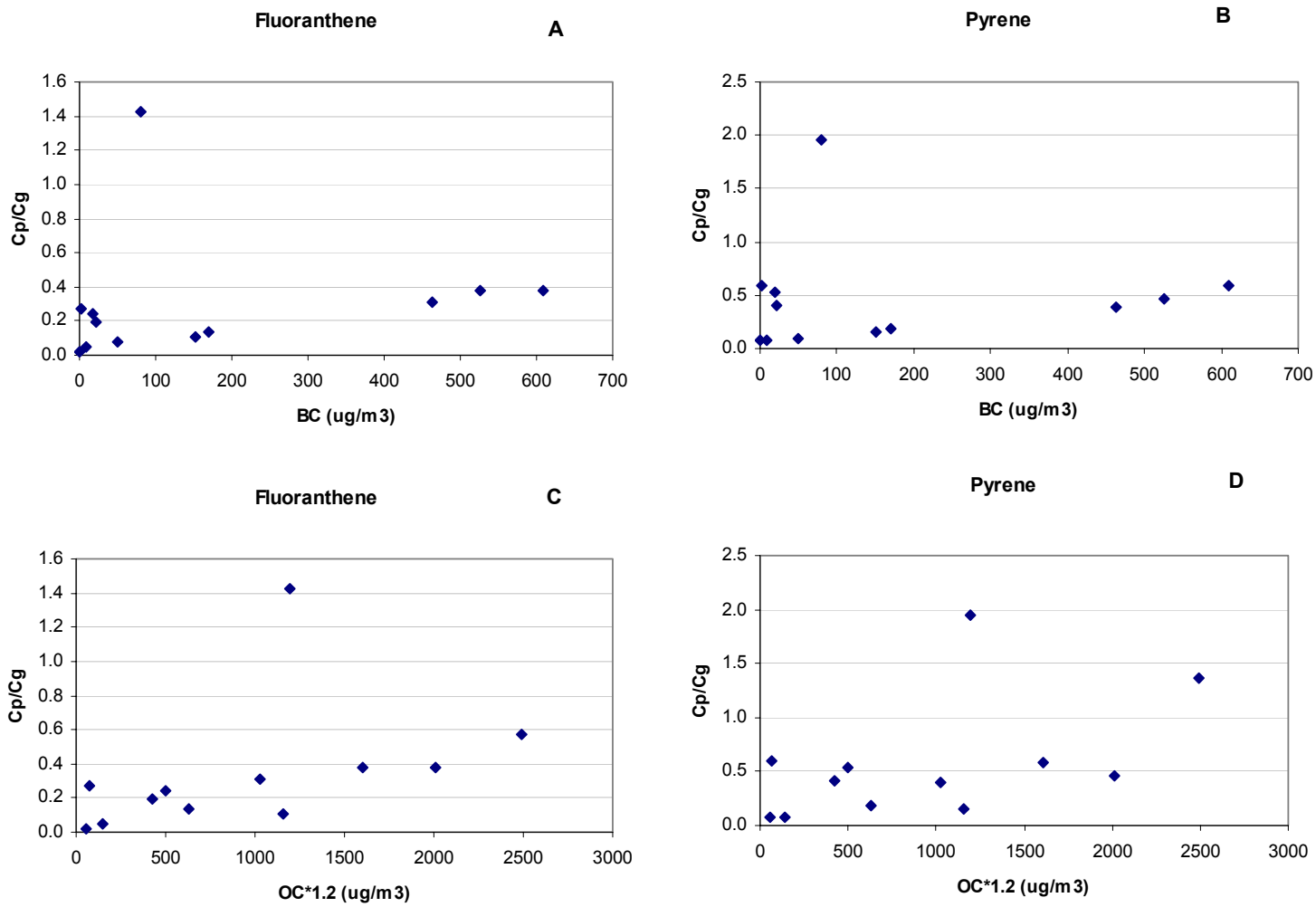
Fluoranthene
A
Cp/Cg
BC (ug/m3)
Pyrene
B
Cp/Cg
BC (ug/m3)
Fluoranthene
C
Cp/Cg
OC*1.2 (ug/m3)
Pyrene
D
Cp/Cg
OC*1.2 (ug/m3)

Figure 5

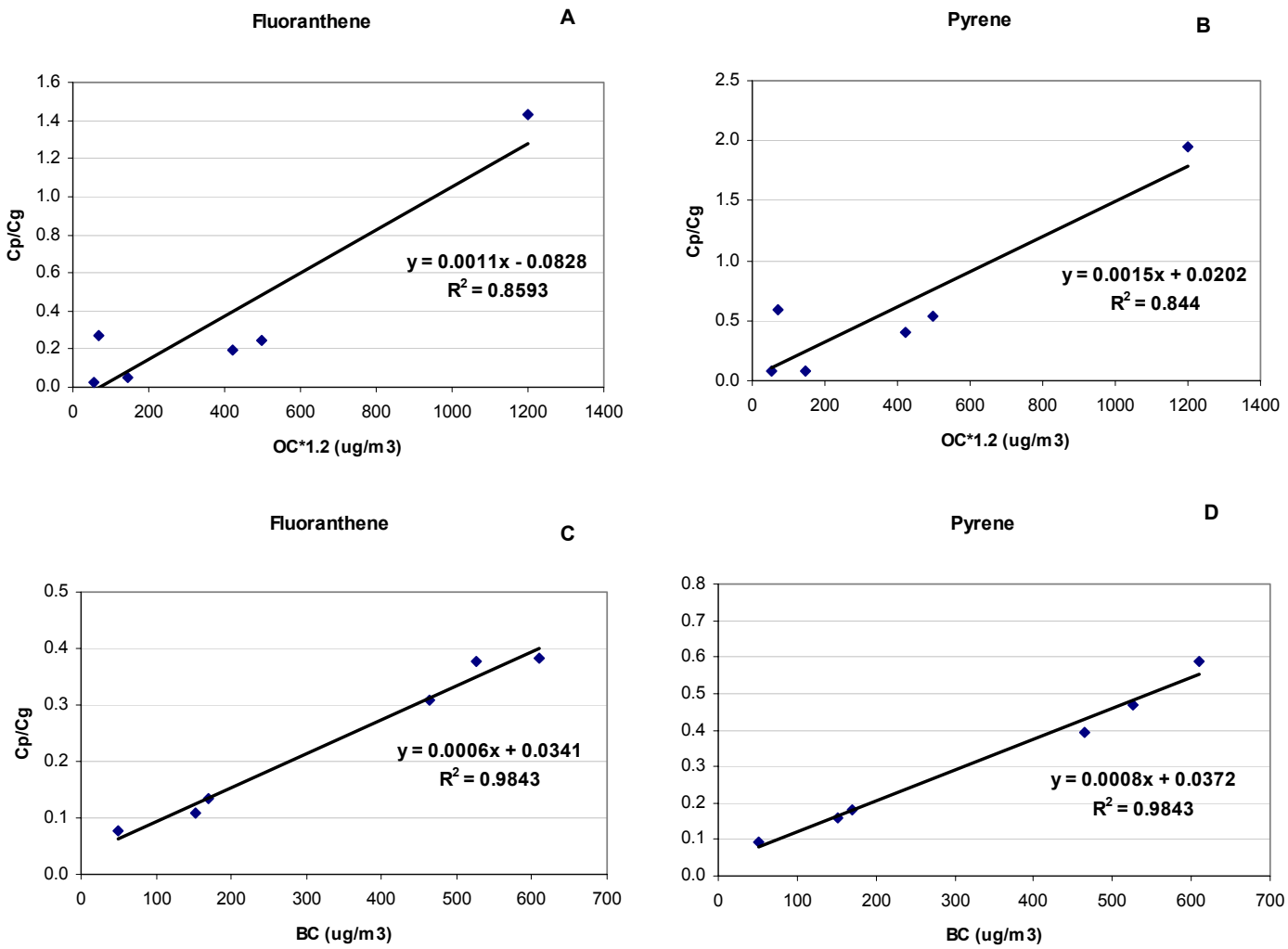
Fluoranthene
A
Cp/Cg
y = 0.0011x - 0.0828
R2 = 0.8593
OC*1.2 (ug/m3)
Pyrene
B
Cp/Cg
y = 0.0015x + 0.0202
R2 = 0.844
OC*1.2 (ug/m3)
Fluoranthene
C
Cp/Cg
y = 0.0006x + 0.0341
R2 = 0.9843
BC (ug/m3)
Pyrene
D
y = 0.0008x + 0.0372
R2 = 0.9843
BC (ug/m3)

Figure6

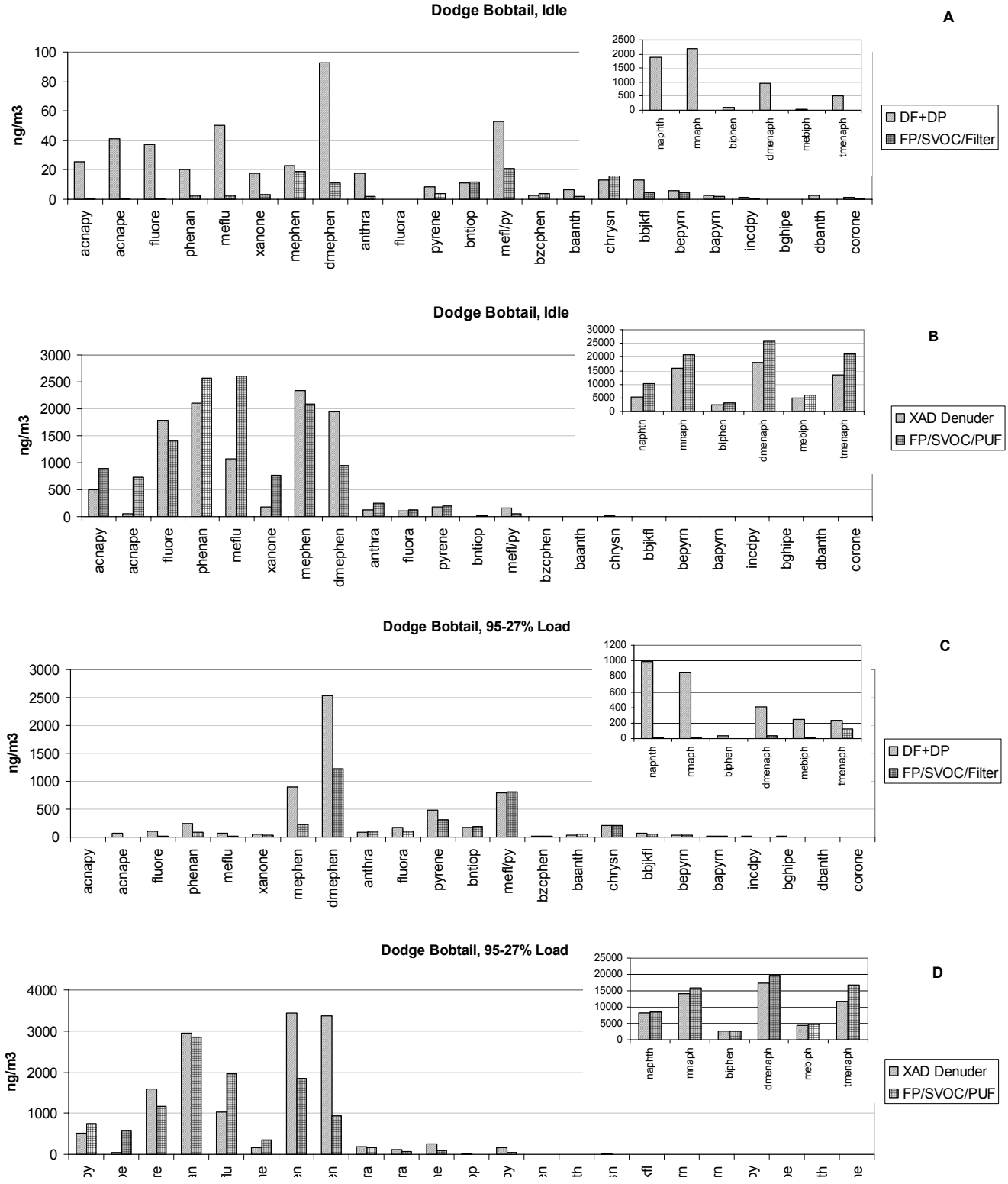
Dodge Bobtail, Idle
A
ng/m3
DF+DP
FP/SVOC/Filter
acnapy
acnape
fluore
phenan
meflu
xanone
mephen
dmephen
anthra
fluora
pyrene
bntiop
mefl/py
bzcphen
baanth
chrysn
bbjkfl
bepyrn
bapyrn
incdpy
bghipe
dbanth
corone
naphth
mnaph
biphen
dmenaph
mebiph
tmenaph
Dodge Bobtail, Idle
B
ng/m3
XAD Denuder
FP/SVOC/PUF
Dodge Bobtail, 95-27% Load
C
ng/m3
DF+DP
FP/SVOC/Filter
Dodge Bobtail, 95-27% Load
D
ng/m3
XAD Denuder
FP/SVOC/PUF

Figure 7

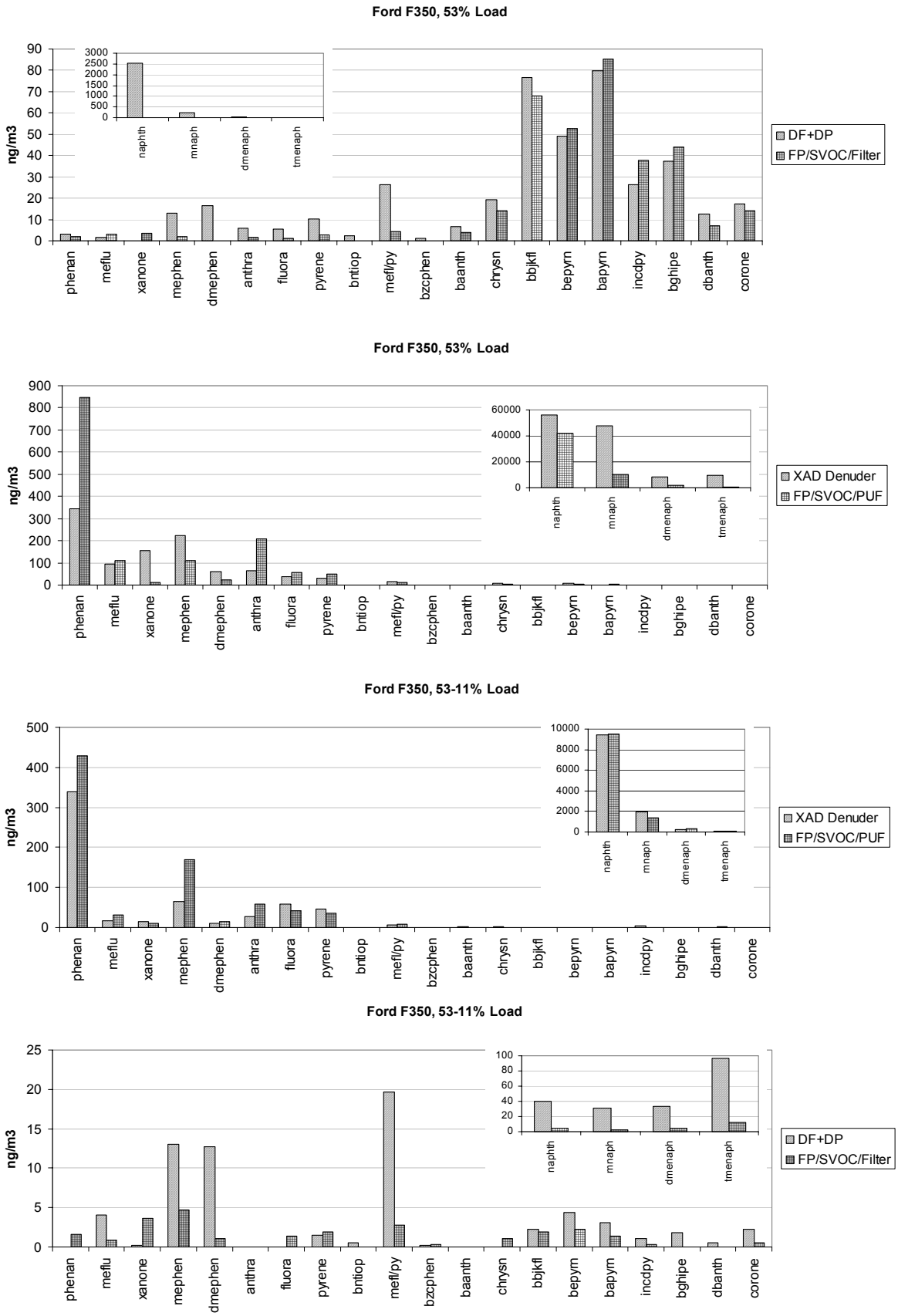
Ford F350, 53% Load
ng/m3
DF+DP
FP/SVOC/Filter
naphth
mnaph
dmenaph
tmenaph
phenan
meflu
xanone
mephen
dmephen
anthra
fluora
pyrene
bntiop
mefl/py
bzcphen
baanth
chrysn
bbjkfl
bepyrn
bapyrn
incdpy
bghipe
dbanth
corone
Ford F350, 53% Load
ng/m3
XAD Denuder
FP/SVOC/PUF
Ford F350, 53-11% Load
ng/m3
XAD Denuder
FP/SVOC/PUF
Ford F350, 53-11% Load
ng/m3
DF+DP
FP/SVOC/Filter

Figure 8

APPENDIX 4:

NORTH ISLAND PAH RESULTS

North Island PAH Results

This Appendix shows the PAH concentrations in the diluted engine exhausts, obtained by the denuder sampling method. Table A4-1 shows the list of PAH quantified for this study and the explanation of their mnemonics. Table A4-2 shows the concentrations of PAH for run 1 through 6 (see Table 4-2 and Section 4 for the description of individual runs). Run 4 was a dynamic blank, i.e. the ambient air was sampled from the discharge chamber, without an engine present. Run # 7 was a field blank of the denuder, collected after the last run. If the average sampling volume (4.5 m^3) is assumed for the field blank, the PAH concentrations are low in comparison with the dynamic blank and the actual runs.

Table A4-2 shows the concentration of the PAH in the gas phase (Cg), in the particle phase (Cp) and the percentage of each PAH present in the gas phase in relation to the total concentration. Cg is equal to the PAH concentrations obtained from the XAD coated denuder section (denuder) and Cp is the sum of the concentration on a filter plus concentration on a PUF/XAD/PUF cartridge (blow-off the filter). For most volatile PAH, i.e. naphthalene, methylnaphthalenes and dimethylnaphthalenes, the concentration on the PUF/XAD/PUF cartridge reflect the breakthrough the denuder section rather than the blow-off the filter, since the flow rate was optimized to assure 99% collection efficiency of phenanthrene (Zielinska et al., 2003).

Figure A4-1 shows the percentage of more abundant PAH present in the gas phase. For simplicity, methyl-PAH isomers are summed together (i.e. methylnaphthalenes, dimethylnaphthalenes, etc). The phase distribution of semi-volatile PAH is in general consistent with those reported previously by Zielinska et al.(2003), with exception of run 7, helicopter engine. This engine emitted very high amount of PAH and the denuder sampler was clearly overloaded. PAH from naphthalene to phenanthrene show significant breakthrough the XAD coated denuder section. PAH with lower vapor pressure than phenanthrene are present in higher percentage in the gas phase in comparison with run 1, 2, 3, and 5. This could be real, since the helicopter engine showed high PM emission rates with significant amount of organic and elemental carbon (Zielinska et al., 2003).

Table A4-2 shows the concentrations of PAH in the diluted engine exhaust collected on seven MOUDI stages (1.8, 1, 0.53, 0.32, 0.18, 0.096 and 0.049 micron) and quartz after filter (AF) for run 2, 3, 5, and 6. Figure X-2 shows this data graphically. For simplicity, methyl-PAH isomers are summed together. The particle-associated PAH concentrations for runs 2, 3, and 5 are very low, thus highly uncertain. However, as it can be seen from Figure A4-2, the semi-volatile and particle associated PAH are mostly present on lower MOUDI stages (0.18 micron and smaller). This is clearly the case for run 6, for which the concentrations of PAH are significantly higher. This is consistent with the previous observations (Zielinska et al., 2003).

Table A4-1. PAH quantified for this study and their mnemonics

Name	Compound	Name	Compound
NAPHTH	Naphthalene	M_1PHT	1-methylphenanthrene
MNAPH2	2-methylnaphthalene	M_9ANT	9-methylanthracene
MNAPH1	1-methylnaphthalene	ANTHRON	Anthrone
BIPHEN	Biphenyl	ANRQUONE	Anthraquinone
ENAP12	1+2ethylnaphthalene	DM36PH	3,6-dimethylphenanthrene
DMN267	2,6+2,7-dimethylnaphthalene	A_DMPH	A-dimethylphenanthrene
DM1367	1,3+1,6+1,7dimethylnaphth	B_DMPH	B-dimethylphenanthrene
D14523	1,4+1,5+2,3-dimethylnaphth	C_DMPH	C-dimethylphenanthrene
DMN12	1,2-dimethylnaphthalene	DM17PH	1,7-dimethylphenanthrene
M_2BPH	2-Methylbiphenyl	D_DMPH	D-dimethylphenanthrene
M_3BPH	3-Methylbiphenyl	E_DMPH	E-dimethylphenanthrene
M_4BPH	4-Methylbiphenyl	FLUORA	Fluoranthene
DBZFN	Dibenzofuran	PYRENE	Pyrene
ATMNAP	A-trimethylnaphthalene	ANTAL9	9-Anthraaldehyde
EM_12N	1-ethyl-2-methylnaphthalene	RETENE	Retene
BTMNAP	B-trimethylnaphthalene	BNTIOP	Benzonaphthothiophene
CTMNAP	C-trimethylnaphthalene	C1MFLPY	1-MeFl+C-MeFl/Py
EM_21N	2-ethyl-1-methylnaphthalene	BMPYFL	B-MePy/MeFl
ETMNAP	E-trimethylnaphthalene	CMPYFL	C-MePy/MeFl
FTMNAP	F-trimethylnaphthalene	DMPYFL	D-MePy/MeFl
TMI235N	2,3,5+I-trimethylnaphthalene	M_4PYR	4-methylpyrene
TM245N	2,4,5-trimethylnaphthalene	M_1PYR	1-methylpyrene
JTMNAP	J-trimethylnaphthalene	BZCPHEN	Benzo(c)phenanthrene
TM145N	1,4,5-trimethylnaphthalene	BAANTH	Benz(a)anthracene
ACNAPY	Acenaphthylene	CHRYSN	Chrysene
ACNAPE	Acenaphthene	M_7BAA	7-methylbenz(a)anthracene
FLUORE	Fluorene	BZANTONE	Benzanthrone
PHENAN	Phenanthrene	BAA7_12	Benz(a)anthracene-7,12-dione
ANTHRA	Anthracene	CHRY56M	5+6-methylchrysene
A_MFLU	A-methylfluorene	BBJKFL	Benzo(b+j+k)fluoranthene
M_1FLU	1-methylfluorene	BEPYRN	BeP
B_MFLU	B-methylfluorene	BAPYRN	BaP
FL9ONE	9-fluorenone	PERYLE	Perylene
XANONE	Xanthone	M_7BPY	7-methylbenzo(a)pyrene
PNAPONE	Perinaphthenone	INCDPY	Indeno[123-cd]pyrene
A_MPHT	A-methylphenanthrene	DBANTH	Dibenzo(ah+ac)anthracene
M_2PHT	2-methylphenanthrene	BGHIPE	Benzo(ghi)perylene
B_MPHT	B-methylphenanthrene	CORONE	Coronene
C_MPHT	C-methylphenanthrene		

*u after the compound name means uncertainty

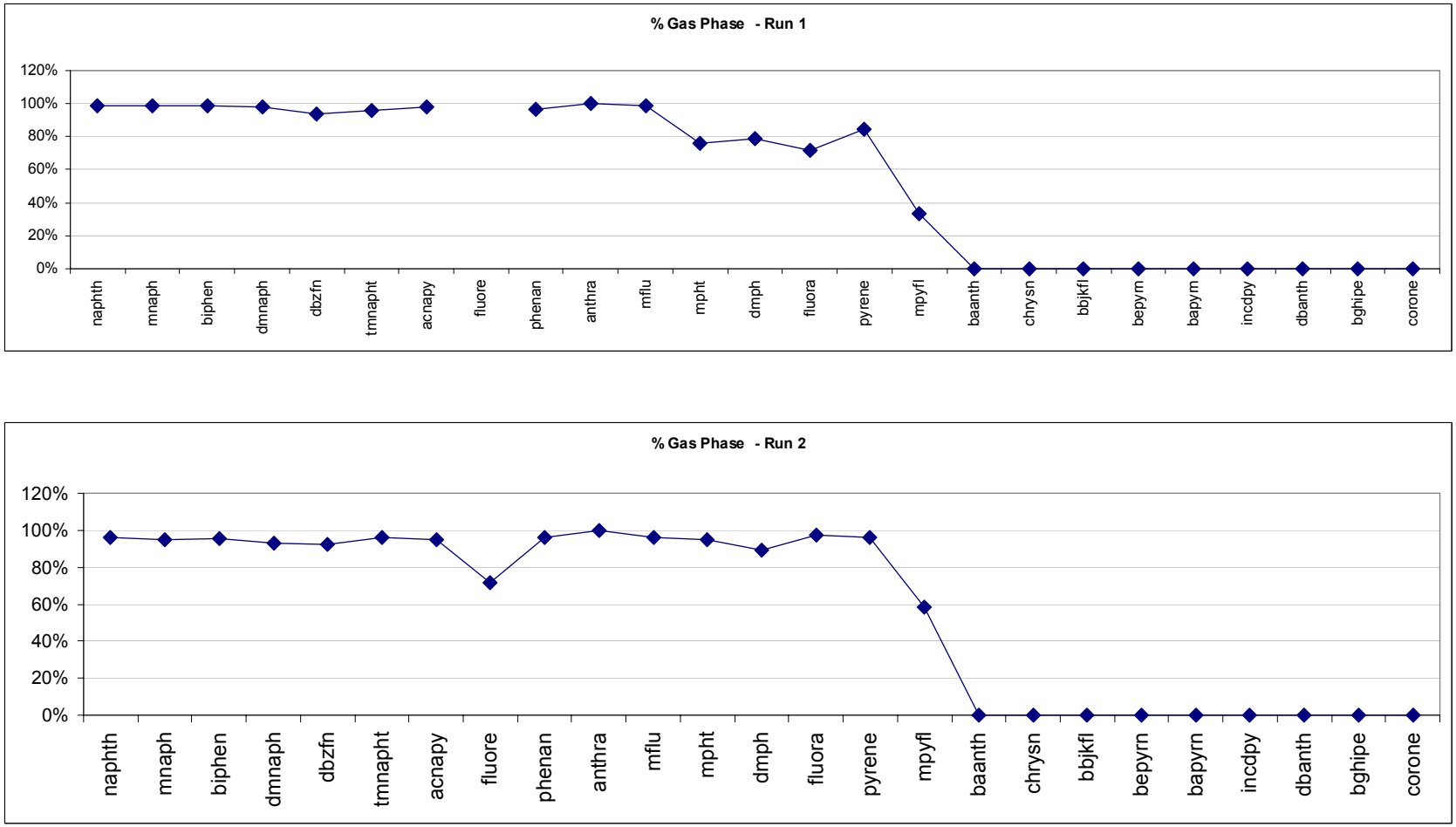

Figure A4-1. Percentage of selected PAHs in the gas phase. Note the MW of compounds increases from left to right.

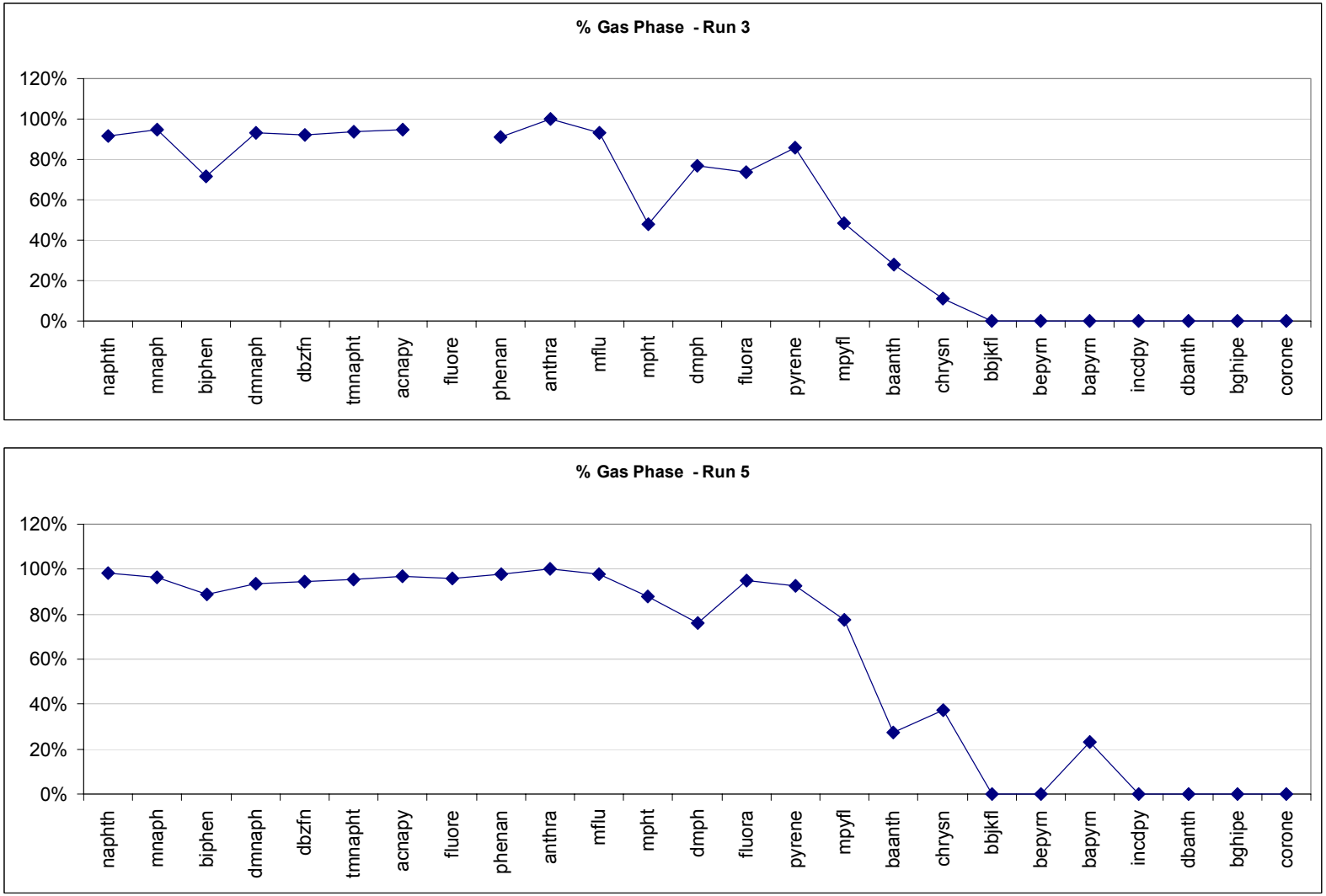

Figure A4-1. Percentage of selected PAHs in the gas phase. Note the MW of compounds increases from left to right.

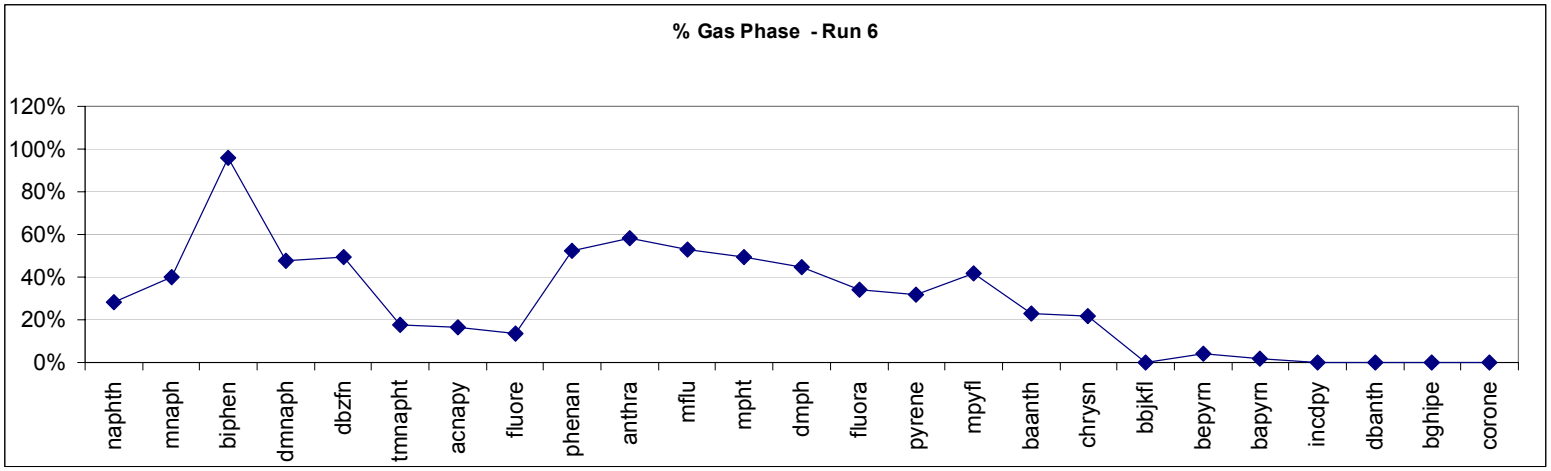

Figure A4-1. Percentage of selected PAHs in the gas phase. Note the MW of compounds increases from left to right.

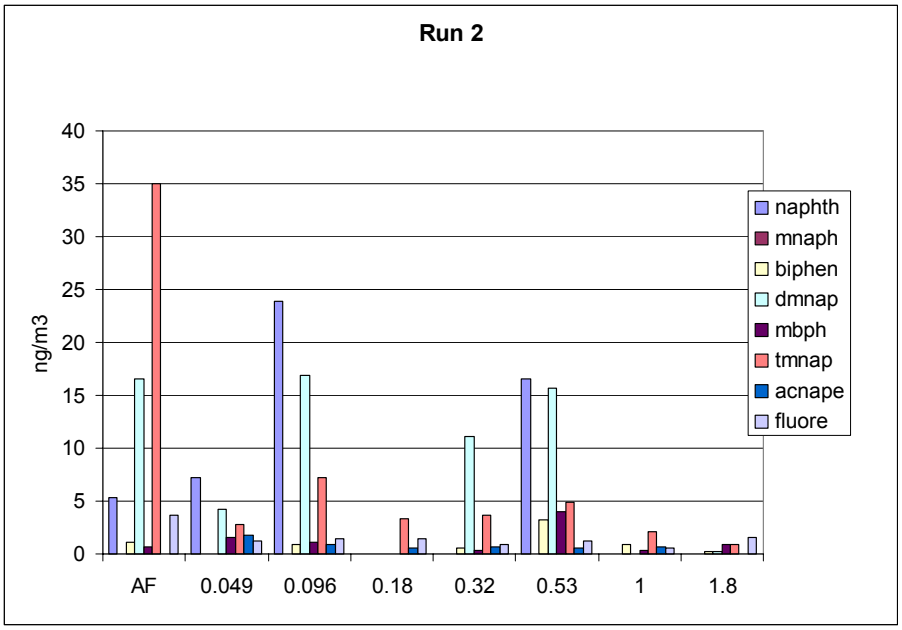

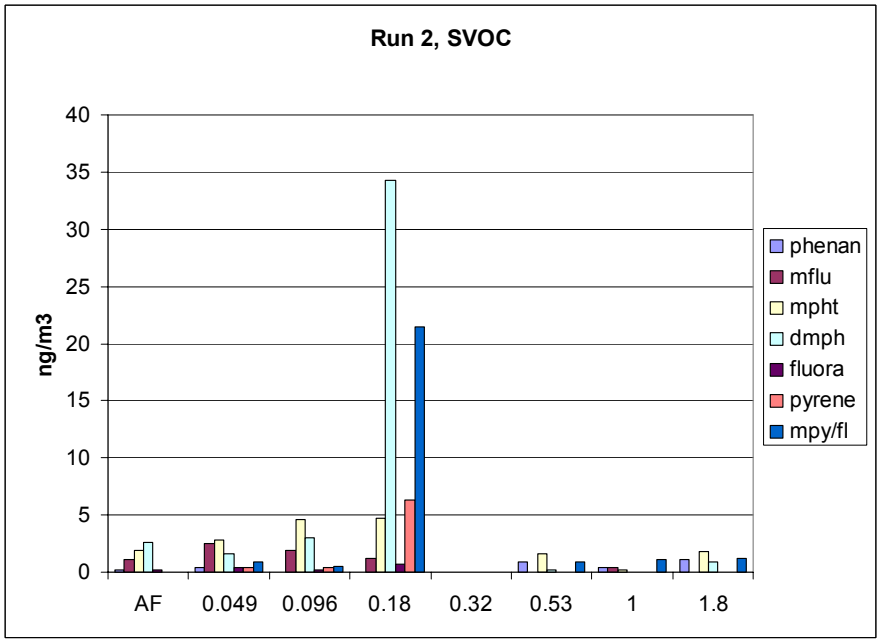

Figure A4-2. MOUDI PAH results.

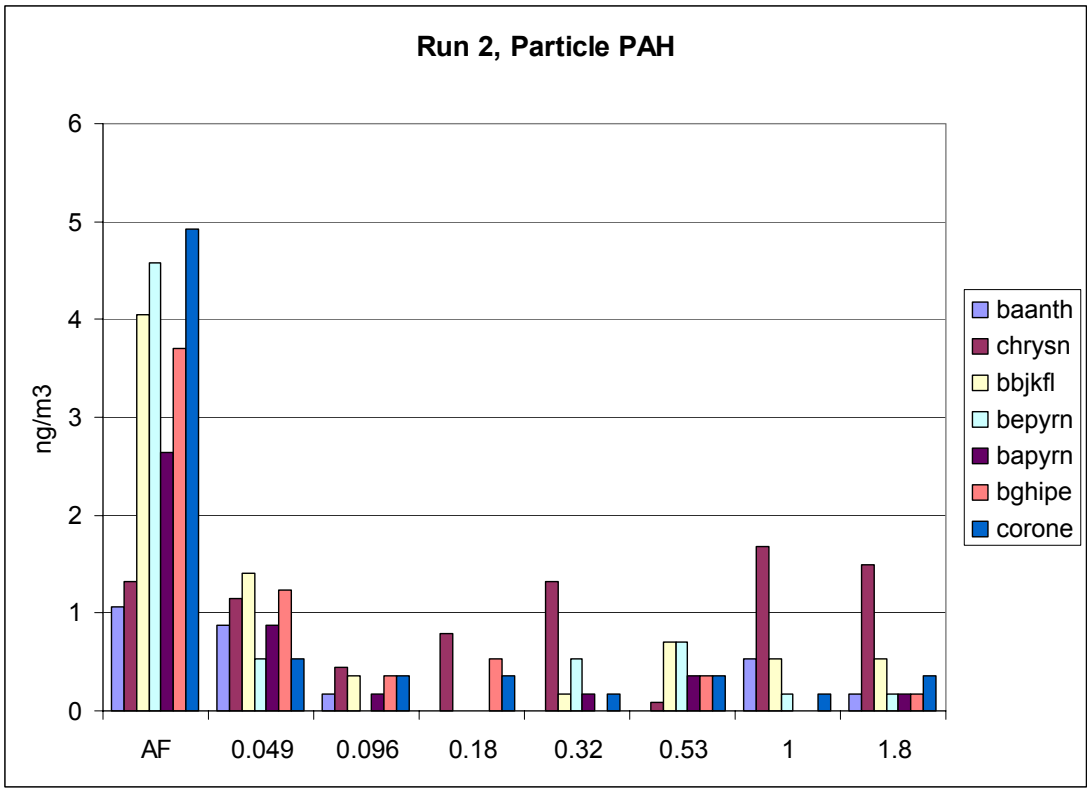

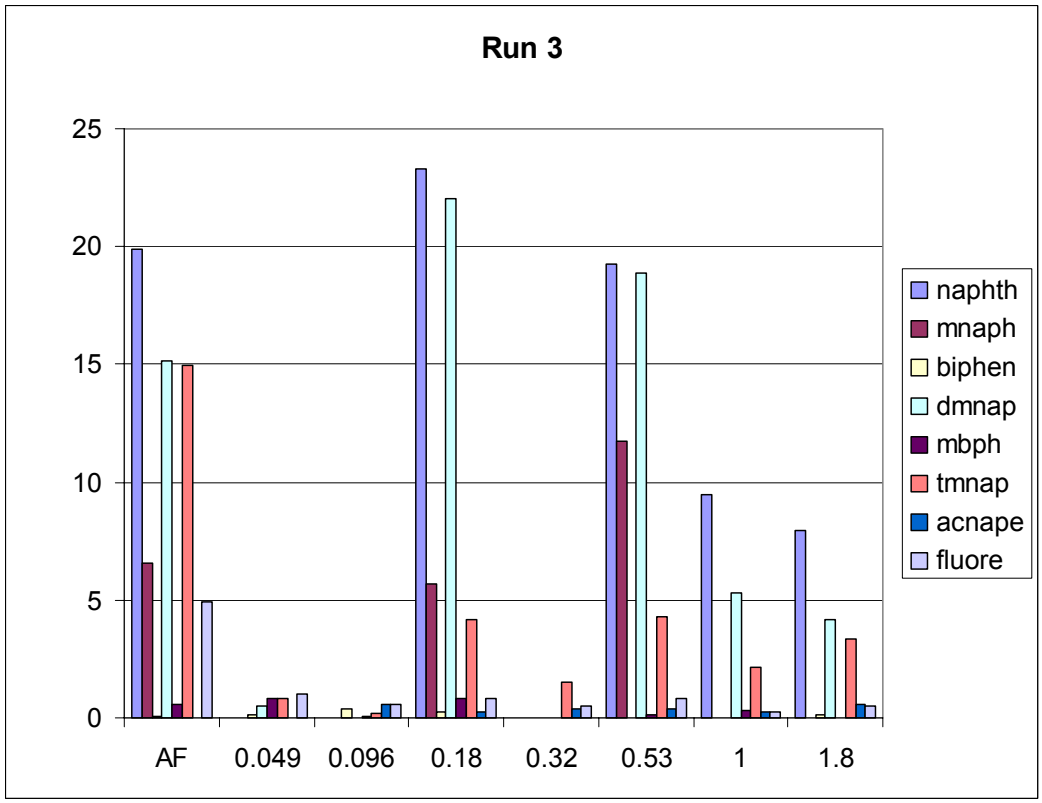

Figure A4-2. MOUDI PAH results.

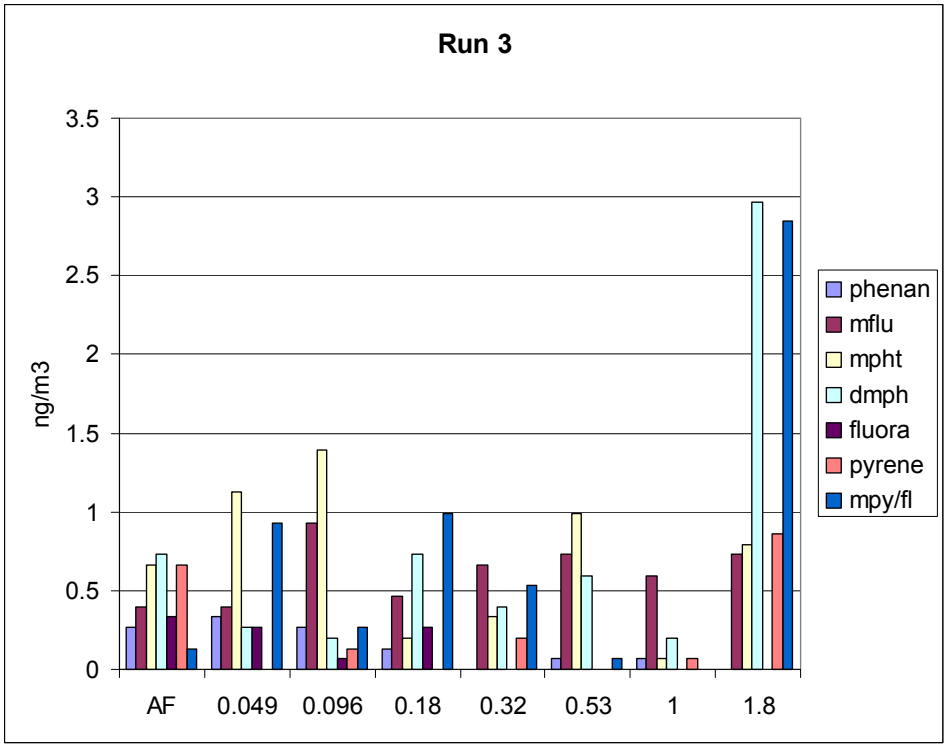

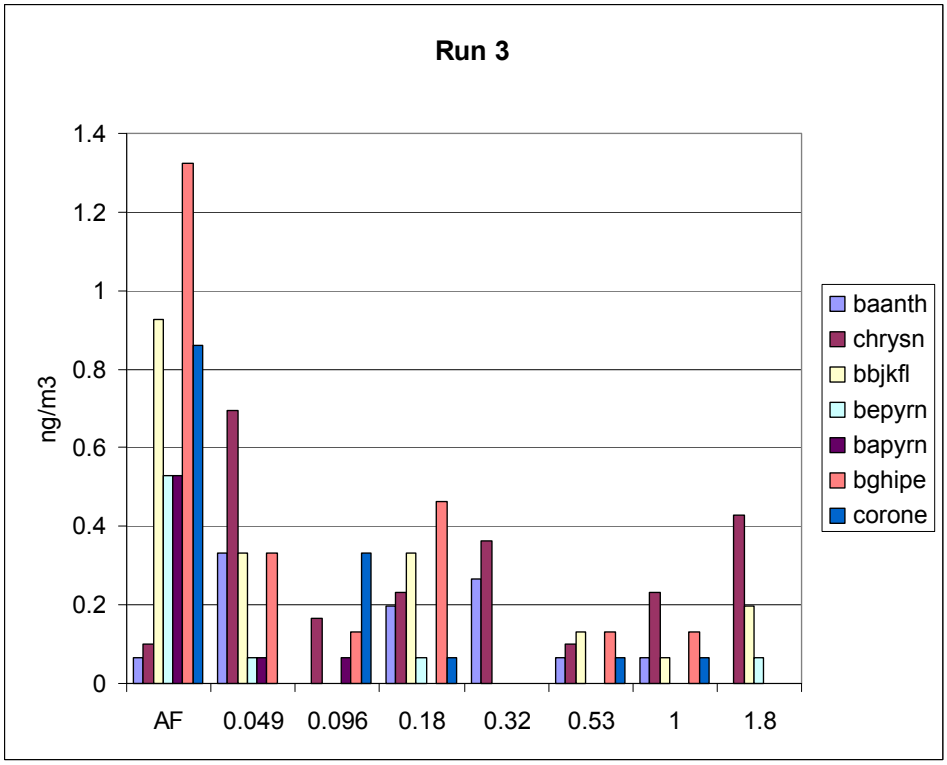

Figure A4-2. MOUDI PAH results.

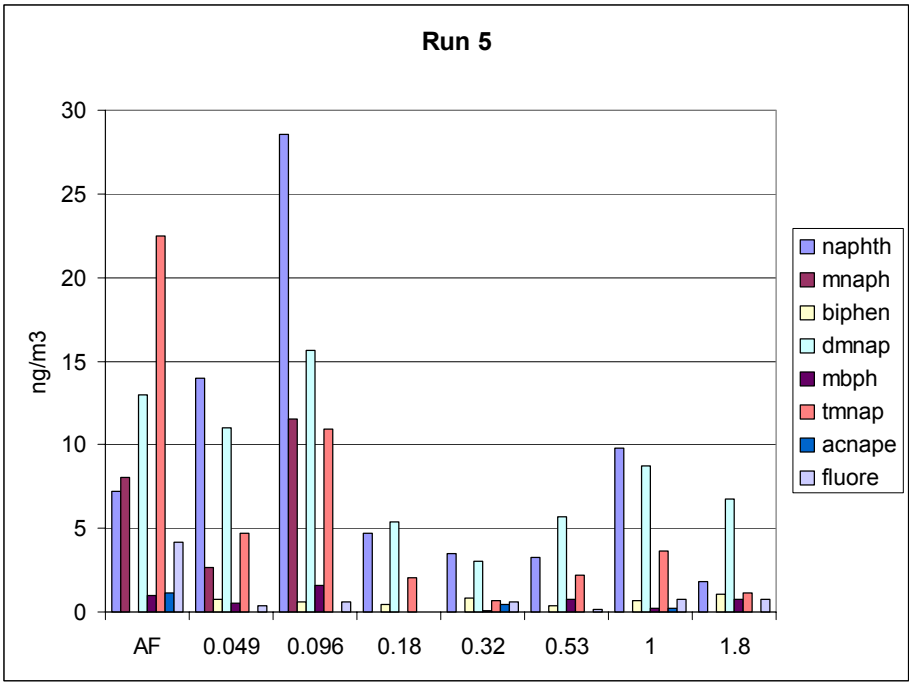

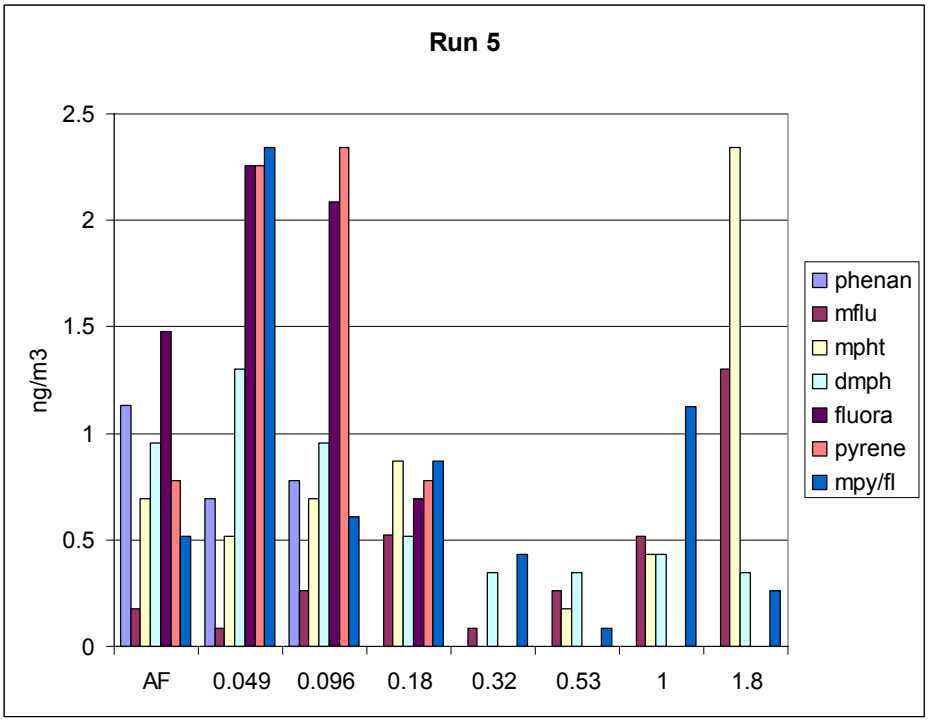

Figure A4-2. MOUDI PAH results.

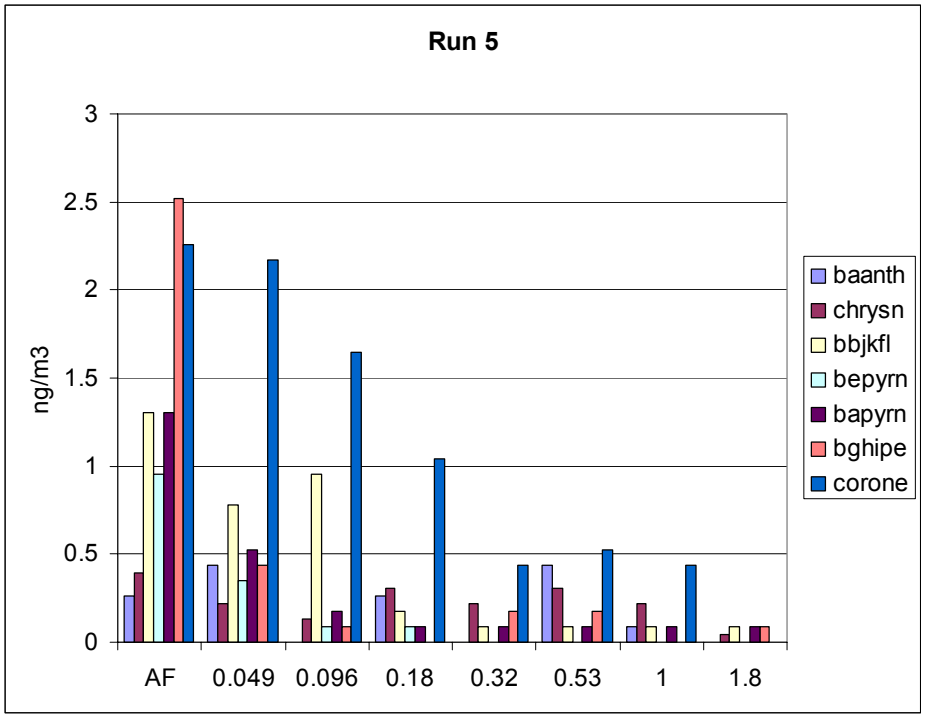

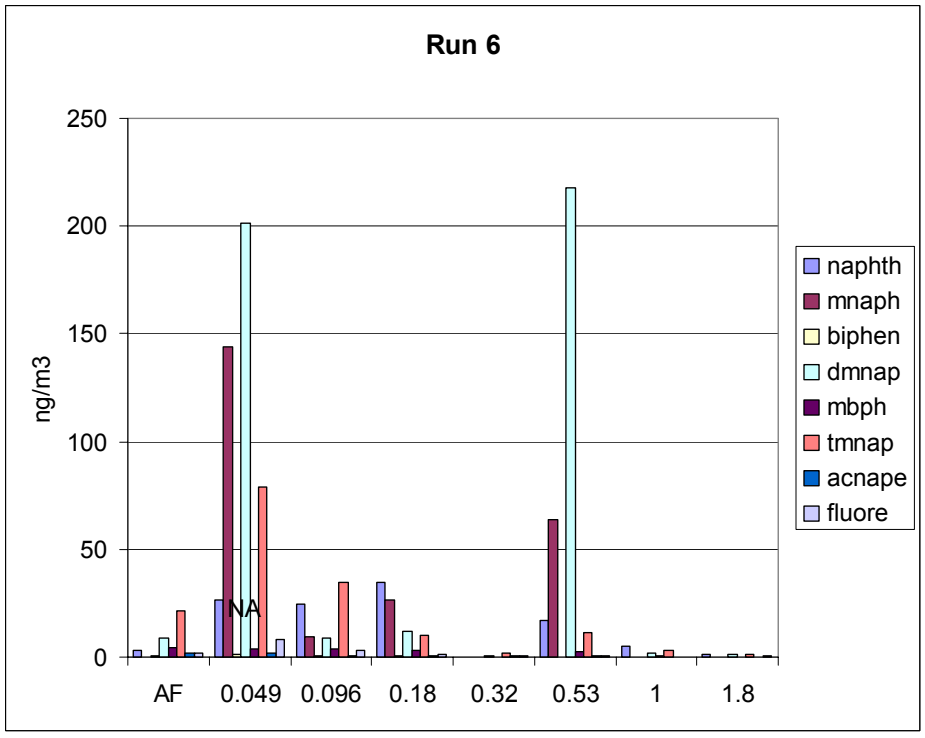

Figure A4-2. MOUDI PAH results.

APPENDIX 5:

EVALUATION OF DIESEL SOOT FILTERS

This article will be published shortly in the Journal of the Air & Waste Management Association.

APPENDIX 6:

SUMMARY OF EMISSION FACTORS

Emission Factor Summary														
						MOUDI	TEOM	MOUDI	MOUDI	SMPS	PAS**	Gundel vapor	Gundel	Napthalene
Source	Tested	Year	Type	Fuel	Engine load	PM* (g/kg)	PM (g/kg)	EC (g/kg)	OC (g/kg)	(#/kg)	pPAH (mg/kg	PAH (mg/kg)	PM (mg/kg)	(mg/kg)
Chevy S-10	1999		AGE	gasoline	idle	3.15				7.08E+13		17.6	14.9	7.7
F-350	2000	1993	F350	gasoline	53%	0.104	0.0845	0.00746	0.0277	7.15E+13	0.0042	122	1.51	24.6
F-350	2000	1993	F350	gasoline	variable	0.017	0.0181	0.00204	0.0263		0.00624	5.89	0.228	4.13
F-350	1999		AGE	gasoline	idle	0.115		0.0347	0.0411	3.43E+14		38.6	1.21	22.7
Dodge Bobtail	2000	1996	Dodge Bob	Diesel	idle, 700 rpm	0.578	1.3	0.0565	0.414	3.24E+15	0.901	31.4	2.72	2.36
Dodge Bobtail	2000	1996	Dodge Bob	Diesel	variable		18.9							
Dodge Bobtail	2000	1996	Dodge Bob	Diesel	27%		4.45							
Dodge Bobtail	1999	1996	AGE	Diesel	idle	1.23		0.162	0.337	3.82E+15		369	18	29
Jeep Bobtail	2000	1986	Jeep Bob	Diesel	23%	2.58		0.641	1.31	9.37E+14	5.5	37.7	4.19	8.11
Jeep Bobtail	2000	1986	Jeep Bob	Diesel	23%,9%	3.45		0.595	1.84		5.4	23.1	3.62	3.83
Jeep Bobtail	2000	1986	Jeep Bob	Diesel	variable	3.69		1.27	2.02		7.03	36.4	2.61	7
Bobtail	1999	1990	AGE	Diesel	idle	4.63		1.92	4.58	4.81E+15		970	588	51
Coleman	1999	1997	AGE	Diesel	idle	0.783		0.158	0.347	3.77E+15		419	14.2	39
Jammer	1999		Jammer	JP8	idle	352		31.2	193.3	3.85E+17		23600	23700	2600
Jammer	2000	1992	Jammer	JP8	idle	3.43		0.13	1.99	1.49E+15	3.88	53.0	4.84	9.1
TF-34	2001	variable	Aircraft	JP5	variable	1.50-154		0.07-8.29	0.46-33.2		0.044-3.05	42.8-223	3.76-15.1	8.36-43.7
T-700	2001	unknown	Helicopter	JP5	variable	0.32		0.18	0.07		0.77	23.4	40.9	1.68
*PM is PM1.8														
pPAH: particle-bound PAH concentration														
** PAS: assuming 1 ftA/ng PAH														
Emission factors were estimated using the method described in Kirchstetter et al., 2001														
All individual PAHs are vapor phase														

Emission Factor Summary											
						Benz[a]anthracene	benzo[b,j,k]fluoranthene	benzo[a]pyrene	chyrsene	indeno[1,2,3-cd]pyrene	
Source	**Tested**	**Year**	**Type**	**Fuel**	**Engine load**	**(ug/kg)**	**(ug/kg)**	**(ug/kg)**	**(ug/kg)**	**(ug/kg)**	
Chevy S-10	1999		AGE	gasoline	idle	24.8	0	24.8	0.656	1.66	
F-350	2000	1993	F350	gasoline	53%	0.256	0	0	2.64	0	
F-350	2000	1993	F350	gasoline	variable	1.04	0	0	0.883	1.85	
F-350	1999		AGE	gasoline	idle	4.69	3.74	1.18	5.42	3.7	
Dodge Bobtail	2000	1996	Dodge Bob	Diesel	idle, 700 rpm	3.02	0	0	8.59	0	
Dodge Bobtail	2000	1996	Dodge Bob	Diesel	variable						
Dodge Bobtail	2000	1996	Dodge Bob	Diesel	27%						
Dodge Bobtail	1999	1996	AGE	Diesel	idle	10.9	0	5.63	40.1	2.82	
Jeep Bobtail	2000	1986	Jeep Bob	Diesel	23%	5.04	0	0	2.67	2.95	
Jeep Bobtail	2000	1986	Jeep Bob	Diesel	23%,9%	12	0	0	34.7	1.97	
Jeep Bobtail	2000	1986	Jeep Bob	Diesel	variable	15.7	0	0	24.4	4.77	
Bobtail	1999	1990	AGE	Diesel	idle	64.7	54.4	20.8	103	27.7	
Coleman	1999	1997	AGE	Diesel	idle	2.17	1.85	5.38	41.7	5.12	
Jammer	1999		Jammer	JP8	idle	2642	3208	189	5239	8490	
Jammer	2000	1992	Jammer	JP8	idle	6.92	0	0	1.22	1.49	
TF-34	2001	variable	Aircraft	JP5	variable	0-3.22	0	0	0-3.22	0	
T-700	2001	unknown	Helicopter	JP5	variable	0.989	0	0	0.206	4.12	
*PM is PM1.8											
pPAH: particle-bound PAH concentration											
** PAS: assuming 1 ftA/ng PAH											
Emission factors were estimated using the method described in Kirchstetter et											
All individual PAHs are vapor phase											